University of Ioannina
School of Health and Science
Department of Biological Applications and Technology
Laboratory of Biotechnology

Natural polymers systems as carriers for bioactive compounds

Doctoral Thesis

Evdokia Vassiliadi
Biologist

Ioannina 2024

Assignment date of the Three-member Advisory Committee: 22/06/2018

Assignment date of the Seven Member Examination Committee:12/06/2024

Three-member Advisory Committee: Dr

Haralambos Stamatis
Professor, Department of Biological Applications and Technology

Dr. Petros Katapodis
Assistant Professor, Department of Biological Applications and Technology

Dr Aristotelis Xenakis
Research Director, Institute of Chemical Biology, National Hellenic Research Foundation

Seven-member Examination Committee

1. Dr. Haralambos Stamatis	Professor, Department of Biological Applications and Technology, Ioannina
2. Dr. Aristotelis Xenakis	Research Director, National Hellenic Research Foundation, Athens
3. Dr. Petros Katapodis	Assistant Professor, Department of Biological Applications and Technology, Ioannina
4. Dr. Nektaria Barkoula	Professor, Department of Materials Engineering, Ioannina
5. Dr. Anna Koukkou	Assistant Professor, Department of Chemistry, Ioannina
6. Dr. Vassiliki Papadimitriou	Senior Researcher, National Hellenic Research Foundation, Athens
7. Dr. Ioannis Simos	Assistant Professor, Faculty of Medicine, Ioannina

Publications

Parts of the present thesis have been published in international peer-review scientific journals.

(The publications can be found in section Publications)

Publication 1	Vassiliadi, E., Mitsou, E., Avramiotis, S., Chochos, C.L., Pirolt, F., Medebach, M., Glatter, O., Xenakis, A. and Zoumpanioti, M., (2020). Structural study of (Hydroxypropyl) methyl cellulose microemulsion-based gels used for biocompatible encapsulations. Nanomaterials,10(11), 2204.
Publication 2	Vassiliadi, E., Aridas, A., Schmitt, V., Xenakis, A. and Zoumpanioti, M., (2022). (Hydroxypropyl)methyl cellulose-chitosan film as a matrix for lipase immobilization: Operational and morphological study. Molecular Catalysis, 522, 112252
Publication 3	Vassiliadi, E., Tsirigotis-Maniecka, M., Symons, H. E., Gobbo, P., Nallet, F., Xenakis, A., & Zoumpanioti, M. (2022). (Hydroxypropyl) methyl Cellulose-Chitosan Film as a Matrix for Lipase Immobilization—Part II: Structural Studies. Gels, 8(9), 595.

Conferences

Parts of present thesis results have been presented at the below conferences.

17th Conference of the International Association of Colloid and Interface Scientists 2022
HPMC And Chitosan Film for The Immobilization of Lipase from *Mucor Miehei*: Operational, Structural and Morphological Study. Evdokia Vassiliadi, Anastasios Aridas, Marta Tsirigotis-Maniecka, Véronique Schmitt, Maria Zoumpanioti and Aristotelis Xenakis, oral presentation, 26-30 June 2022, Australia

11th International Colloids Conference 2022
A novel functional film for immobilization of lipase. Structural and biocatalytical study. Evdokia Vassiliadi, Marta Tsirigotis-Maniecka, Anastasios Aridas, Veronique Schmitt, Maria Zoumpanioti, Aristotelis Xenakis, oral presentation, 12-15 June 2022, Portugal

Greek Lipid Forum 2021:
Lipase immobilization on chitosan matrix for the synthesis of fatty acid esters

Evdokia Vassiliadi, Aristotelis Xenakis, Maria Zoumpanioti, oral presentation, 18 October 2021, online

European Colloid and Interface Society 2021:
HPMC and chitosan film as an enzyme carrier, Evdokia Vassiliadi, Aristotelis Xenakis, Maria Zoumpanioti, poster presentation, 5-10 September, Greece

Euro Fed Lipid Congress 2021

Lipase Entrapped in Film Gels from Natural Polymers for the Synthesis of Fatty Acid Ester, Evdokia Vassiliadi, Maria Zoumpanioti, Aristotelis Xenakis, poster presentation, 18 – 21 October 2021, online congress

Okinawa Colloids 2019:
Microemulsion based organogels as lipase carriers: A structure and efficacy study, oral presentation, Maria Zoumpanioti, Evdokia Vassiliadi, Christos Chochos, Spyridon Avramiotis and Aristotelis Xenakis, oral presentation, 5-8 November, Japan

Euro Fed Lipid Congress 2019:
Encapsulation of bioactive compounds in Chitosan hydrogels. Maria Zoumpanioti, Aristotelis Xenakis and Evdokia Vassiliadi, oral presentation, 20-23 October 2019, Spain

European Student Colloid Conference 2019:
Chitosan hydrogels: A novel matrix for encapsulation of bioactive compounds. Evdokia Vassiliadi, Aristotelis Xenakis and Maria Zoumpanioti, oral Presentation, 18-22 June 2019, Bulgaria

European Colloid and Interface Society 2018:
Lipase encapsulation in cellulose derivative: structure and function, Maria Zoumpanioti, Evdokia Vassiliadi, Christos Chochos, Spyridon Avramiotis and Aristotelis Xenakis, oral presentation, 2-7 September 2018, Slovenia

Acknowledgments

It is indeed wonderful to have the chance to express your gratitude to all those people that surrounded you throughout this journey.

Firstly, I would like to express my deepest appreciation to my supervisor Dr. Aris Xenakis, who was a mentor and a leader that always showed me the way of finding solutions. I'm extremely grateful to have been part of his team. As the years past, starting as an undergraduate and now completing my student journey, it has been a pleasure not only working in his group but also exploring Greece and France, singing, discovering wonderful wine and food and of course science by his side.

I could not thank enough Prof. Haris Stamatis, who was the first one to introduce me to Dr. Xenakis group, and gave me the opportunity to be part the collaboration between the two labs. He also gave me the chance and trusted me to start this long-distance scientific relationship with him, giving me the freedom of thought and action. In addition, many thanks to Assistant Prof. Petros Katapodis, who was also one of the Professors in the University of Ioannina that encouraged me to start my journey into the world of Biotechnology.

My scientific journey would not have been possible without the support and nurturing of Dr. Maria Zoumpanioti. I could not thank enough my personal guru, that was a torch for my scientific path. It was always wonderful having a clean view to all my vague thoughts, as well as a helping handle even in the smallest details.

There has been found that there are three types of support throughout the PhD life, emotional, academic and instrumental. I was truly lucky to receive all three kinds of support from my lovely friend and colleague Dr. Evgenia Mitsou, without whom I couldn't have discovered the fun of being curious and the beauty of being hamble.

I couldn't thank enough Dr Maria Chatzidaki, who was always there to provide the -out of the box- thinking that was enlightening. She has been a great role model and an even greater friend with her multitasking skills and her generosity outbursting in every opportunity.

Of course, I would like to thank Dr Vassiliki Papadimitriou for her valuable advice. Particularly helpful to me during this time were Dr. Sotiria Demisli, Dr. Ioanna Theohari, Konstantina Matskou, and Eleni Galani, who I had great pleasure working aside as PhD students all together.

My PhD journey would not be complete if I had not been to Centre de Recherche Paul Pascal, where Dr. Veronique Schmitt allowed me to gain experience and broaden my study with her help. Alongside, Dr. Frédéric Nallet, with his vivid speeches showed me why passion makes a good scientist.

Furthermore, I would like to thank Dr. Pierangelo Gobbo for his enlightening contribution of my scientific publications alongside with Dr. Henry E. Symons.

Special thank you to Dr. Marta Tsirigotis-Maniecka who not only helped me scientifically but taught me that science does not have a specific timetable and schedule.

I'm extremely grateful to have met and work with Dr. Spyros Avramiotis that guided me scientifically and, unquestionably, melodically. He was the common sense in my unlogic thoughts and my stress relief through his wonderful piano notes.

I cannot conclude this journey without mentioning my dad Agis and sister Natassa that were always there for me even if I sounded as a lunatic at some points. Also, I couldn't have managed to get it all together without my partner Angelos who never stopped believing in me and making me laugh in my hardest moments. Of course, I want to thank all my friends Artemi, Chrysanthi, Vasso, Haris, Dimitris, Nikos who were my biology buddies with wonderful ideas and actual thoughtfulness.

I'd like to acknowledge the assistance of all my scientific committee for their guidance and useful advice.

Praised be doubt! I advise you to greet
cheerfully and with respect the man
who tests your word like a bad penny

Bertolt Brecht

Contents

Abbreviation

AFM	Atomic Force Microscopy
A_N	hyperfine splitting constant
AOT	Sodium bis(2-ethylhexyl)sulfosuccinate
CL	cathodoluminescence
CS	CHITOSAN
DMS	doxyl methyl stearate
DSA	doxyl stearic acids
EBSD	electron backscatter diffraction
EPR	Electron Paramagnetic Resonance
FESEM	field emission scanning electron microscope
FID	flame ionization detector
FTIR	Fourier transform infrared
GC	Gas Chromatography
HPMC	(Hydroxypropyl)methyl cellulose
MBGS	Microemulsion Based Gels
p-NPB	4-Nitrophenyl butyrate
q	scattering wave vectors
S	order parameter
SAXS	Small Angle X-ray Scattering
SEM	Scanning Electron Microscopy
STEM	scanning transmission electron microscopy
TEMPO	2,2,6,6-tetramethylpiperidine-1-oxyl
τ_R	rotational correlation time
WDS	wavelength dispersive X-ray spectroscopy
w/o	water in oil

Abstract

Biocatalysis refers to the use of natural catalysts, called biocatalysts, to accelerate chemical reactions. One fascinating class of biocatalysts is derived from natural polymers, which can be a promising scaffold for enzymes. Natural polymers are abundant in nature and exhibit diverse properties that make them excellent candidates for biocatalysis. Biocatalysts offer several advantages over traditional chemical catalysts, including high selectivity, specificity, and efficiency, as well as biodegradability and compatibility with the environment. Polysaccharides, as natural polymers, contribute to the biocatalytic landscape. For example, cellulose, a polysaccharide found in plant cell walls, can be converted into a modified cellulose derivative such as (hydroxypropyl)methyl cellulose, which is water soluble. Chitosan, a derivative of chitin, is another natural polymer that exhibits biocompatible and biodegradable properties. Chitosan and its derivatives have been used as an enzyme carrier in various organic transformations due to their unique structure. These polymers serve as feedstocks for the formation of natural biocatalyst, when the enzyme is incorporated in the matrix. They have been applied in processes such as enzymatic synthesis and asymmetric catalysis, among others.

This study focuses on two main aspects. Firstly, the aim of the present study was to create an easily operative carrier for the immobilization of bioactive compounds, such as enzymes, and secondly to analyze these carriers structurally. Two main biopolymers, (hydroxypropyl)methyl cellulose and chitosan, were used to form the carriers and were studied with the immobilized enzyme. A structural study of (hydroxypropyl)methyl cellulose microemulsion-based gels, used for lipase immobilization, was conducted. The study delves into the characterization of the gels, focusing on their composition and morphology. Techniques such as EPR (Electro Paramagnetic Resonance) SEM (Scanning Electron Microscopy) and SAXS (Small Angle X-ray Scattering) were performed in order to explore the structural properties. This research contributes to understanding the excessive performance, investigated in previous studies, of (hydroxypropyl)methyl cellulose microemulsion-based gels as matrices for lipase immobilization.

Next, the use of (hydroxypropyl)methyl cellulose and chitosan film as a matrix for lipase immobilization was investigated. The combination of the two biopolymers was used to form films where the enzyme, lipase from *Mucor miehei*, was trapped and performed

as a biocatalyst for the model reaction of esterification, which was monitored with Gas Chromatography. Its morphology and composition were examined using AFM (Atomic force Microscopy), shedding light on its potential as an effective matrix for enzyme immobilization.

After optimizing the composition of the biocatalyst, the operational and morphological aspects of (hydroxypropyl)methyl cellulose-chitosan film for lipase immobilization, was investigated. The study explores the practical implications of using these films, including enzyme activity and stability, as well as the physical characteristics of the film. By investigating the operational and morphological aspects, with SEM, optical microscopy and profilometry measurements, FTIR (Fourier transform infrared) and SAXS several valuable insights were provided into the application of (hydroxypropyl)methyl cellulose-chitosan films as matrices for lipase immobilization.

In summary, this study focuses on (hydroxypropyl)methyl cellulose microemulsion-based gels and (hydroxypropyl)methyl cellulose-chitosan films as matrices for lipase immobilization, aiming to contribute to the understanding of the structural properties, operational characteristics, and potential applications of these matrices in various enzymatic processes.

Keywords: (hydroxypropyl)methyl cellulose; chitosan; biocatalysis; lipase; microemulsion based gels; film; esterification; EPR (Electron Paramagnetic Resonance); SAXS (Small Angle X-ray Scattering); FTIR (Fourier transform infrared); AFM (Atomic Force Microscopy),

Περίληψη

Η βιοκατάλυση αναφέρεται στη χρήση φυσικών καταλυτών, που ονομάζονται βιοκαταλύτες, για την επιτάχυνση των χημικών αντιδράσεων. Μια ενδιαφέρουσα κατηγορία βιοκαταλυτών προέρχεται από φυσικά πολυμερή, τα οποία μπορεί να διαμορφώσουν ένα πολλά υποσχόμενο ικρίωμα για ένζυμα. Τα φυσικά πολυμερή είναι άφθονα στη φύση και παρουσιάζουν ποικίλες ιδιότητες που τα καθιστούν εξαιρετικούς υποψηφίους για βιοκατάλυση. Οι βιοκαταλύτες προσφέρουν πολλά πλεονεκτήματα σε σχέση με τους παραδοσιακούς χημικούς καταλύτες, συμπεριλαμβανομένης της υψηλής επιλεκτικότητας, εξειδίκευσης και αποτελεσματικότητας, καθώς και βιοδιασπασιμότητας και συμβατότητας με το περιβάλλον. Οι πολυσακχαρίτες, ως φυσικά πολυμερή, συμβάλλουν στο πεδίο της βιοκατάλυσης. Για παράδειγμα, η κυτταρίνη, ένας πολυσακχαρίτης που βρίσκεται στα κυτταρικά τοιχώματα των φυτών, μπορεί να μετατραπεί σε ένα τροποποιημένο παράγωγό της, όπως η (υδροξυπροπυλ)μεθυλοκυτταρίνη, η οποία είναι υδατοδιαλυτή. Η χιτοζάνη, ένα παράγωγο της χιτίνης, είναι ένα άλλο φυσικό πολυμερές βιοσυμβατό και βιοδιασπώμενο. Η χιτοζάνη και τα παράγωγά της έχουν χρησιμοποιηθεί ως φορέας ακινητοποίησης ενζύμων σε διάφορους οργανικούς μετασχηματισμούς λόγω της μοναδικής δομής τους. Αυτά τα πολυμερή χρησιμεύουν ως πρώτες ύλες για το σχηματισμό φυσικού βιοκαταλύτη, όταν το ένζυμο ενσωματώνεται στη μήτρα. Έχουν βρει εφαρμογές σε διαδικασίες όπως η ενζυμική σύνθεση και η ασύμμετρη κατάλυση, μεταξύ άλλων.

Η παρούσα μελέτη εστιάζει σε δύο βασικές πτυχές. Πρώτον, στόχος της παρούσας μελέτης ήταν η δημιουργία ενός εύκολα λειτουργικού φορέα για την ακινητοποίηση βιοδραστικών ενώσεων, όπως τα ένζυμα, και δεύτερον η δομική ανάλυση αυτών των φορέων. Δύο κύρια βιοπολυμερή, η (υδροξυπροπυλ)μεθυλοκυτταρίνη και η χιτοζάνη, χρησιμοποιήθηκαν για τον σχηματισμό των φορέων και μελετήθηκαν παρουσία και απουσία του ακινητοποιημένου ενζύμου. Διεξήχθη μια δομική μελέτη πηκτωμάτων υδροξυπροπυλ)μεθυλοκυτταρίνης σε συνδιασμό με μικρογαλάκτωμα, που χρησιμοποιούνται για ακινητοποίηση λιπάσης. Η μελέτη εμβαθύνει στον χαρακτηρισμό των πηκτωμάτων, εστιάζοντας στη σύνθεση και τη μορφολογία τους. Εφαρμόστηκαν τεχνικές όπως EPR (Φασματοσκοπία Ηλεκτρονικού Παραμαγνητικού Συντονισμού) , SEM (Ηλεκτρονική μικροσκοπία σάρωσης) και SAXS (Σκέδαση ακτίνων Χ υπό μικρή γωνία) προκειμένου να διερευνηθεί η δομή τους. Αυτή η έρευνα συμβάλλει στην κατανόηση της εξαιρετικής απόδοσης, που

διερευνήθηκε σε προηγούμενες μελέτες, των πηκτωμάτων υδροξυπροπυλ)μεθυλοκυτταρίνης που συνδυάζονται με μικρογαλάκτωμα, ως φορέας για ακινητοποίηση λιπάσης.

Στη συνέχεια, διερευνήθηκε η χρήση (υδροξυπροπυλ)μεθυλοκυτταρίνης και χιτοζάνης σε φιλμ ως μήτρα για ακινητοποίηση λιπάσης. Ο συνδυασμός των δύο βιοπολυμερών χρησιμοποιήθηκε για το σχηματισμό μεμβρανών όπου το ένζυμο, η λιπάση από το *Mucor miehei*, ακινητοποιήθηκε και λειτούργησε ως βιοκαταλύτης για πρότυπη αντίδραση εστεροποίησης, η οποία παρατηρήθηκε μέσω αέριας χρωματογραφίας. Η μορφολογία και η σύνθεσή του εξετάστηκαν χρησιμοποιώντας AFM (Atomic Force Microscopy), ρίχνοντας φως στη δυνατότητά του ως αποτελεσματική μήτρα για την ακινητοποίηση των ενζύμων.

Μετά τη βελτιστοποίηση της σύνθεσης του βιοκαταλύτη, διερευνήθηκαν οι λειτουργικές και μορφολογικές πτυχές του φιλμ (υδροξυπροπυλ)μεθυλοκυτταρίνης-χιτοζάνης για ακινητοποίηση λιπάσης. Η μελέτη διερευνά τις πρακτικές συνέπειες της χρήσης αυτών των μεμβρανών, συμπεριλαμβανομένης της ενζυμικής δραστηριότητας και σταθερότητας, καθώς και τα φυσικά χαρακτηριστικά του φιλμ. Με τη διερεύνηση των λειτουργικών και μορφολογικών πτυχών, με FTIR (Φασματοσκοπία υπέρυθρου με μετασχηματισμό Fourier),SEM, οπτική μικροσκοπία, μετρήσεις προφιλομετρίας και SAXS δόθηκαν πολλές πολύτιμες γνώσεις σχετικά με την εφαρμογή μεμβρανών (υδροξυπροπυλο)μεθυλοκυτταρίνης-χιτοζάνης ως μήτρες για ακινητοποίηση λιπάσης.

Συνοπτικά, αυτή η μελέτη επικεντρώνεται σε πηκτώματα (υδροξυπροπυλ)μεθυλοκυτταρίνης με μικρογαλάκτωμα και μεμβράνες (υδροξυπροπυλ)μεθυλοκυτταρίνης-χιτοζάνης ως μήτρες για ακινητοποίηση λιπάσης, με στόχο να συμβάλει στην κατανόηση των δομικών ιδιοτήτων, των λειτουργικών χαρακτηριστικών και των πιθανών εφαρμογών αυτών των μέσων σε διάφορες ενζυμικές διεργασίες.

Λέξεις-κλειδιά: (υδροξυπροπυλ)μεθυλοκυτταρίνη, χιτοζάνη, βιοκατάλυση, λιπάση, πηκτώματα με βάση μικρογαλάκτωμα, φιλμ, εστεροποίηση, EPR (Ηλεκτροπαραμαγνητικός συντονισμός), SAXs (Σκέδαση ακτίνων Χ υπό μικρή γωνία), FTIR (υπέρυθρο μετασχηματισμό Fourier), AFM (Μικροσκοπία Ατομικής Δύναμης).

1. Introduction

Biocatalysis refers to the use of natural catalysts, such as enzymes, to facilitate chemical reactions. In biocatalysis, enzymes are used to catalyze various chemical transformations, ranging from simple hydrolysis reactions to more complex synthetic processes[1]. Enzymes can exhibit remarkable selectivity and efficiency, allowing for the production of specific target compounds with high yields and purity[2]. This makes biocatalysis an attractive alternative to traditional chemical methods, which often require harsh reaction conditions and generate unwanted by-products.

Biocatalysis has been applied in diverse fields such as pharmaceuticals[1], food[3] and beverage production[4], biofuels, and environmental remediation[5,6]. By harnessing the power of enzymes, biocatalysis offers several advantages, including milder reaction conditions, reduced energy consumption, and reduced environmental impact[2].

In order for enzymes to perform in optimum conditions and to be reused easily, without the need of specific techniques to wash and separate the substrates and products from the catalyst, several scaffolds have been introduced that incorporate the enzyme and create a biocatalyst that provide highly pure products[7–10]. These scaffolds are, gels[11–13] and solid particles[14–16]. Each category offers different advantages. Suitable support features involve the lack of interaction with enzymes, biodegradability, reasonability, and availability[2,17,18].

Natural polymers serve as excellent scaffolds for enzyme immobilization[19–22], offering numerous advantages in biocatalysis. These polymers, such as chitosan, cellulose, alginate, collagen and gelatin, possess inherent biocompatibility and biodegradability[22,23]. The nature of these polymers allows for better dispersion of enzymes within the scaffold, ensuring optimal accessibility to substrates[24]. Moreover, several natural polymers, such as chitosan, offer the advantage of mild and gentle immobilization conditions, preserving the enzymatic activity[11]. With their diverse properties natural polymer scaffolds hold great potential for enzyme immobilization in various biotechnological applications. In this study, chitosan and (hydroxypropyl)methyl cellulose were the polymers used for gel preparation.

Hydrogels have gained great attraction due to their properties. Hydrogels are polymeric three-dimensional networks [12,13,22], that absorb water at a remarkably high capacity, without undergoing dissolution. Their formation that contains great quantity of water, creates the desired microenvironment for the enzymes which are immobilized. The relative activity of the enzyme, the reusability of the biocatalyst as well as the mild conditions that are offered when the enzyme is immobilized on such gels lures towards the use of these biocatalysts in the industry[25].

Microemulsions are stable, isotropic liquid mixtures of oil, water, and surfactant, often in combination with a cosurfactant. They form spontaneously and are thermodynamically stable[26]. In some cases, the incorporation of a microemulsion in these hydrogels offer a promising microemulsion based gel (MBG)[27,28]. The microemulsion alone have been used for the encapsulation of bioactive compounds[29,30], such as enzymes but when it comes to catalysis, the practical utilization of microemulsions can be impeded by the requirement to separate the surfactant from the reaction products. Traditional methods employed for this purpose often result in inefficient separation due to technical challenges, including the formation of emulsions caused by the presence of surfactants[8,31]. Thus, the combination of these two formulations to create a matrix for the enzyme, appear to be rigid and stable for a long time[32]. Additionally, in the majority of circumstances, the gel matrix effectively retains all the components, including surfactant, water, and enzymes, allowing the diffusion of non-polar substrates or products between the non-polar phase and the gel. In the presents work, a water-in-oil (w/o) microemulsion with Sodium bis(2-ethylhexyl)sulfosuccinate (AOT) as surfactant was combined with an (hydroxypropyl)methyl cellulose aqueous suspension, leading to the formation of a matrix that served as an enzyme.

Lipases are highly valuable tools in the field of biocatalysis. They play a crucial role in various industries, including food, pharmaceuticals, detergents, and biofuel production[33]. As lipases are activated in the presence of an interface, they are able to efficiently catalyze reactions involving lipids, which are typically insoluble in water. Additionally, lipases exhibit remarkable substrate specificity and can tolerate a wide range of reaction conditions, making them versatile biocatalysts that can be tailored for various applications[34]. In this study, biocatalysts formed with the natural polymers mentioned above, were used to incorporate lipases from *Mucor miehei* and *Candida antarctica*. Various parameters were analyzed, in order to investigate the characteristics of the biocatalyst using a model esterification reaction.

This research focuses on the investigation of (hydroxypropyl)methyl cellulose microemulsion-based gels and (hydroxypropyl)methyl cellulose-chitosan films as matrices for immobilizing lipase. The primary objective is to enhance our understanding of the structural properties, operational features, and potential utility of these matrices in enzymatic catalysis. The development of systems based on (hydroxypropyl)methyl cellulose and chitosan as the main natural polymers formed promising enzyme immobilization matrix. Two main different gels were developed, namely an MBG system with (hydroxypropyl)methyl cellulose and AOT as surfactant that incorporated lipase from

Candida antarctica, and a combination of (hydroxypropyl)methyl cellulose and chitosan in the form of films with lipase from *Mucor miehei*.

The first system is a well-studied biocatalyst that was investigated structurally after having observed its potential as an excellent biocatalyst. Having observed several interesting features of such a system, inevitably the research could not stop. EPR (Electron Paramagnetic Resonance), SEM (Scanning Electron Microscopy) and SAXs (Small Angle X-ray Scattering) were performed in order to explore the structural properties. EPR can provide an insight of the interface created from the surfactants as well as a plausible position of the enzyme that is immobilized on the matrix. Furthermore, the movement and placement of the water, which plays a crucial role to the matrix, were investigated with the same method. SAXs and SEM on the other hand, were used to clarify the overall formation of the matrix.

On the second project, the development of a film that was easy to handle was achieved. The film was based on the combination of two natural polymers, namely (hydroxypropyl)methyl cellulose and chitosan, without the use of a microemulsion. The biocatalyst was used for the immobilization of lipase from *Mucor miehei*. The biocatalyst 's performance was optimized towards a model esterification reaction and monitored via Gas Chromatography. AFM was used to image the surface of the film and observe the interaction of the polymers combined with the enzyme. Lastly, this biocatalyst was also structurally characterized with several techniques such as SEM, SAXs, FTIR, optical microscopy and profilometry measurements.

The current thesis is organized into the following sections: Theoretical Background, Purpose of the Study, Methods, Conclusion, and Results. The "Theoretical Background" section provides a comprehensive explanation of the necessary knowledge pertaining to biocatalysis. Additionally, it elucidates the necessity of scaffolds, such as natural polymers, for immobilizing enzymes. The section also discusses various methods of immobilization and delves into the nature of the combination formed between the enzyme and the carrier. Supplementary, in this section all the techniques that were used for the measurement of the biocatalytic activity and for the structural and morphological characterization are described thoroughly. The "Purpose of the Study" section presents the objectives of the study by describing the significant findings and highlights derived from the three publications associated with these three projects. In the Methods section, each technique is presented, highlighting their specific contributions to each of the projects. The Conclusion section provides a comprehensive commentary on the results obtained from the projects, emphasizing their contribution to industrial biocatalysis. The final section of the thesis is Results, which encompasses the manuscripts of the three

publications that have been produced. This section provides readers with an overview of the projects, including the objectives of each study and the experimental results, thus presenting a complete picture of the research conducted.

2. Theoretical Background

2.1. Biocatalysis

Biocatalysis is a process that involves the use of natural catalysts, such as whole cells or enzymes, to facilitate chemical reactions[1,9]. These catalysts, which are typically derived from living organisms, can speed up chemical reactions and enable the conversion of various substrates into desired products[33,35]. Biocatalysis is a promising and environmentally friendly alternative to traditional chemical processes, as it offers several advantages:

- High specificity: Enzymes are highly specific in their action, meaning they can catalyze a particular reaction and produce a specific product without generating undesired by-products.
- Mild reaction conditions: Biocatalytic reactions often occur at moderate temperatures and pH levels, reducing energy consumption.
- Environmentally Friendly and sustainable: Biocatalysis typically uses renewable resources, such as biomass, and generates fewer harmful waste products, therefore the procedure is more environmentally sustainable and minimizing the need for hazardous chemicals.
- Reduced costs: In some cases, biocatalysis can lead to cost savings as enzymes can be highly efficient, and the reactions can be carried out with lower energy requirements. Furthermore, the absence of by-products eliminates the necessity for expending additional time and energy on further purification procedures [1,8,17,18,33].

Biocatalysis finds applications in various industries, including pharmaceuticals[1], food[30] and beverages[36], biofuels production[2,5,24], and fine chemicals manufacturing[2,18]. It plays a crucial role in the synthesis of complex molecules that might be challenging or impossible to obtain using traditional chemical methods. To be more specific, biocatalysis is widely used in pharmaceutical manufacturing to synthesize complex molecules required for drugs[1,2]. Enzymes can catalyze specific reactions with high selectivity, allowing the production of pure and chiral compounds[18,33,35], which is crucial in drug development. Furthermore, biocatalysis plays a role in food processing, such as producing sweeteners[37], converting lactose into glucose and galactose in dairy products[38,39], and enhancing flavors in certain foods[40]. Additionally, enzymes are used in the production of biofuels, such as biodiesel and bioethanol[41]. They can break down biomass, which can then be converted into biofuels through[5,42]. fermentation. Also, enzymes are used in laundry detergents to break down stains and improve cleaning efficacy[43,44]. Lastly, biocatalysis is employed to produce fine chemicals[45], flavors[46],

fragrances, and other chemicals that might be challenging to synthesize using traditional chemical methods[47].

Overall, biocatalysis is a valuable tool in the quest for greener and more efficient chemical processes. Researchers and industries continue to explore and develop new enzymes and biocatalytic processes to expand its applications further

2.2. Enzymes

Enzymes are biological molecules, typically proteins, that act as catalysts in living organisms. They play a crucial role in various biological processes by accelerating specific chemical reactions, allowing them to happen at a much faster rate than they would under normal cellular conditions[48]. Enzymes participate in a vast array of biological processes, including metabolism[49], DNA replication and repair[50], cellular signaling and immune response.

Enzymes are critical to life and are found in all living organisms, from simple bacteria to complex multicellular organisms[49]. They are used extensively in biotechnology, medicine, and various industries to catalyze specific reactions, leading to numerous applications in research, manufacturing, and therapeutic interventions. Enzymes remain the most well-known and extensively studied natural catalysts due to their crucial roles in biochemical reactions. Characteristics of enzymes include:

- Specificity: The Nobel Prize-winning organic chemist Emil Fischer initially introduced the "lock-and-key model" for enzymatic catalysis in 1894. Enzymes are highly specific to the reactions they catalyze. Each enzyme is designed to work with a particular substrate, and they bind to these substrates at their active sites, where the reaction takes place[51].
- Reusability: Enzymes, as natural catalysts, are not consumed in the reactions they catalyze. Once a reaction is completed, the enzyme is released and can be used again to catalyze more reactions.[52].
- Sensitivity to environmental factors: Enzymatic activity has specific temperature and pH optima at which the enzymes function most effectively. Deviations from these optimal conditions can reduce their activity or denature them[53,54].

2.3. Lipase

Lipases are a subclass of enzymes, (E.C. 3.1.1.3), that are primarily responsible for the hydrolysis of acylglycerides. They play a significant role in biocatalysis. They are involved in hydrolyzing fats and oils, breaking them down into glycerol and fatty acids. According to a study conducted by Gupta et al.[55], lipases have shown significant potential in the

production of biobased products due to their ability to catalyze diverse reactions, such as esterification, transesterification, and interesterification.

Whilst lipases are water-soluble enzymes, they exhibit their catalytic activity when interacting with lipid substrates, such as fats and oils, where oil and water phases meet. Lipases have a unique characteristic which is interfacial activity. The interfacial activity of lipases is the state in which the enzyme is activated and can perform as a catalyst when it is located at the interface between two immiscible phases, typically oil and water, . Lipase interfacial activity is a critical aspect of its functionality, particularly in the context of lipid metabolism and industrial applications. This phenomenon explains why the environment of the reaction is crucial for the efficient hydrolysis or esterification of the substrates[56]. This ability to work at the interface makes lipases particularly efficient in hydrolyzing or synthesizing lipids. Due to their unique catalytic properties, lipases find applications in various industries. Some notable applications of lipase in biocatalysis are:

- Biodiesel production: Lipases are used to catalyze the transesterification reaction between vegetable oils or animal fats and alcohol to produce biodiesel. This process is more sustainable and environmentally friendly than traditional methods[41,42].
- Food processing: Lipases are employed in the food industry to improve the flavor and texture of various products. For example, they are used in cheese-making to accelerate the ripening process and enhance the development of specific flavors[46].
- Detergent industry: Lipases are added to laundry detergents to break down and remove fatty stains, such as grease and oil, from fabrics[57,58].
- Pharmaceuticals: Lipases are used in the synthesis of pharmaceutical intermediates and active ingredients, especially in the production of lipid-based medications[59].
- Personal care products: Lipases find applications in the cosmetic and personal care industry for the production of soaps, shampoos, and skincare products.
- Flavor and fragrance industry: Lipases are employed to produce various esters and other aromatic compounds used in flavors and fragrances[60,61].
- Environmental applications: Lipases are used in wastewater treatment and bioremediation to degrade fats and oils, helping to clean up environmental pollutants[62].

2.4. Enzyme immobilization

Enzyme immobilization is a process in which enzymes are physically or chemically confined or attached to a solid support or matrix, thereby enabling their reuse and retention in a specific location. Immobilization offers several advantages over using free

(soluble) enzymes, making it a popular technique in various biotechnological and industrial applications[63].

Enzyme immobilization offers several benefits over using free enzymes:

- Reusability: Immobilized enzymes can be reused multiple times, reducing the need for frequent enzyme replacement and lowering operational costs[59,64].
- Stability: Immobilization enhances enzyme stability, protecting them from denaturation and inactivation under harsh conditions, such as changes in temperature, pH, or the presence of organic solvents[65].
- Enhanced Activity: In some cases, immobilization can lead to increased enzyme activity or selectivity compared to their free counterparts[7,66].
- Easy Separation: Immobilized enzymes can be easily separated from the reaction mixture, simplifying downstream processing and reducing contamination of the final product[31].

There are several methods of immobilizing enzymes[8,63,67], each with its unique advantages and applications:

- Physical Adsorption: In this method, enzymes are simply attached to the surface of a solid support through weak non-covalent interactions, such as hydrogen bonding or van der Waals forces. This is a simple and cost-effective method, but the enzymes may not be strongly bound and can potentially leach off from the support[68].
- Covalent Bonding: Enzymes can be covalently attached to the surface of a solid support through chemical reactions. This method provides strong binding, but the modification process must be carefully controlled to avoid enzyme inactivation[14,69,70].
- Encapsulation: Enzymes can be encapsulated within a porous support material, such as hydrogels or microcapsules, which act as a protective barrier. This method offers good stability and allows the controlled release of the enzyme[26].
- Crosslinking: Enzymes can be crosslinked to form a stable enzyme support complex. Crosslinking involves forming chemical bonds between enzyme molecules or with the solid support[71].
- Entrapment: In this method, enzymes are trapped within a gel or matrix without covalent bonding. The enzyme remains physically trapped but can move freely within the support[72–74].

Enzyme immobilization finds applications in various industries and processes. To mention a few, biocatalysis for pharmaceutical drugs, food processing for improved flavor, biosensors, drug delivery systems, and diagnostic assays[63,75]. Overall, enzyme immobilization is a versatile and valuable technique that enhances the stability, reusability,

and efficiency of enzymes, enabling their broader applications in various fields of biotechnology and industry.

2.5. Microemulsions

Microemulsions are thermodynamically stable, optically transparent, and isotropic dispersions of two immiscible liquids (usually oil and water) stabilized by surfactant molecules and sometimes co-surfactants[76]. They are called microemulsions due to their extremely small droplet size[77].

In a typical microemulsion system, the surfactant molecules arrange themselves at the interface between the oil and water phases, forming a stabilizing layer around the tiny droplets of one liquid dispersed in the other. The presence of co-surfactants helps lower the interfacial tension and promotes the formation of these small droplets[78].

Microemulsions can be classified into three main types based on their composition. Firstly, Oil-in-Water (O/W) microemulsions. In this type, small droplets of oil are dispersed in a continuous phase of water, stabilized by surfactant molecules. A second formation is Water-in-Oil (W/O) microemulsions. In W/O microemulsions, small droplets of water are dispersed in a continuous phase of oil, stabilized by surfactant molecules. Lastly, there are bicontinuous microemulsions. Bicontinuous microemulsions have a continuous network of both oil and water phases, separated by surfactant layers. The phases are interconnected, forming a complex structure[79].

Microemulsions have gained significant attention for their diverse and promising applications in various fields. Their unique properties, such as small droplet size, thermodynamic stability, transparency, energy-free spontaneous formation and enhanced solubilization capacity, make them highly suitable for numerous industrial applications[80]. In pharmaceuticals, microemulsions serve as efficient drug delivery systems, enhancing the solubility and bioavailability of poorly water-soluble drugs[81–83]. In the cosmetic industry, they are utilized to improve product stability and deliver active ingredients more effectively[83,84]. Additionally, microemulsions find applications in the food and beverage sector for encapsulating flavors and nutrients, resulting in transparent beverages and improved product stability[85–87]. In the oil industry, microemulsions are employed to enhance oil recovery from reservoirs[88,89]. As a versatile and promising technology, microemulsions continue to be an area of active research, opening up new avenues for innovation and practical applications across a wide range of industries.

Water-in-oil microemulsions have emerged as promising scaffolds for enzyme encapsulation in biocatalysis, revolutionizing the field of enzyme-based processes[76,90–92]. The unique properties of microemulsions, such as their high stability, small droplet size, and large interfacial area, make them ideal candidates for hosting enzymes within

their aqueous nanodomains[26]. By carefully selecting the appropriate surfactants and cosurfactants, researchers can tailor the microemulsion composition to accommodate a wide range of enzymes with varying properties and requirements. The confined environment of w/o microemulsions protects the encapsulated enzymes from denaturation and provides a favorable microenvironment for catalysis.

While microemulsions offer easy separation and reuse of enzymes in theory, in practice, separating the enzymes from the microemulsion matrix can be challenging. It may require additional steps, such as breaking the microemulsion or using specific separation techniques.

2.6. Gels

Gels are semi-solid materials that have a unique structure characterized by a continuous liquid phase trapped within a three-dimensional network of solid particles or polymers. Gels can be categorized by several ways, including by their source, such as natural or synthetic gels; by the type of liquid medium within the polymer network, like hydrogels, organogels or oleogels; and by their cross-linkage, whether it's achieved chemically or physically[93]. Polymers used in gel formation can be natural, such as agarose[94], gelatin[48,53,95], or pectin[17,44,96], chitosan[11,18,62,97,98], cellulose[24,54,99,100], or synthetic, including polyacrylamide or polyvinyl alcohol[94,101]. Furthermore, another category of gels are formed when solid particles, like silica[102,103] or clay[104], disperse in a liquid medium.

Gelation typically occurs through a variety of mechanisms, including chemical cross-linking, physical entanglement, or by cooling a solution containing gel-forming components. These gels find applications across numerous industries due to their unique physical properties. Physical entanglement involves long polymer chains tangling with each other, creating a network that traps the liquid component. Chemical cross-linking, on the other hand, occurs when chemical bonds form between polymer chains, creating a stable network structure. Thermally induced gelation involves cooling a polymer solution, causing the polymers to aggregate and form a gel structure due to decreased molecular motion. Understanding these mechanisms is crucial for designing gels with specific properties for various applications.

Gels are essential in various industries due to their unique properties. Their structure plays a crucial role to achieving the desired properties that can make gels indispensable in various industries, including pharmaceuticals, food, cosmetics, and energy. In the pharmaceutical industry[105–107], gels are used to formulate topical medications, facilitating controlled drug release through the skin[108]. Gels are used in various food products, including jams, jellies, desserts, and yogurt[109] In addition, natural gelling

agents are employed as animal fat replacer in meat products[100,110]. Gels are used in flavoring for food and cosmetics. In the food industry, gels are used as carriers for bioactive ingredients and aroma compounds [111]. They can be used in the preparation of innovative foods and as additives in functional foods due to their bioactivity[112]. In cosmetics, gels are used as delivery systems for active ingredients such as vitamins, antioxidants, and moisturizers[113]. Moreover, in the oil and gas sector, gels are employed for hydraulic fracturing (fracking) to transport proppants and chemicals into underground formations, aiding in the extraction of hydrocarbons[114,115].

In conclusion, understanding the mechanisms of gel formation and the materials involved is essential for tailoring gels to specific applications. As industries continue to innovate, the usefulness of gels ensures their continued importance in countless industrial processes and consumer products.

2.6.1. Hydrogels

Hydrogels are a class of highly water-absorbent, three-dimensional polymeric materials with a unique and handy nature[22,116,117]. Their distinctive property is their ability to retain a significant amount of water or other aqueous solutions while maintaining their structural integrity[118]. This characteristic is due to the presence of hydrophilic groups within their polymer matrix, which attract and bind water molecules[119,120].

The amount of water content can lead to gels that resemble biological tissues, thus making hydrogels ideal for a variety of medical applications, including wound dressings[13,116], drug delivery systems[22,106], and tissue engineering scaffolds[121]. Furthermore, in industry, they find applications in contact lenses[116], food packaging[30,69,122] and food preservation[123]. Their tunable properties, such as porosity, mechanical strength, and responsiveness to external stimuli like temperature or pH, allow for customization to meet specific requirements[29,63].

Hydrogels play a pivotal role in the field of biocatalysis, where they are used as scaffolds to immobilize enzymes, enhancing their stability and reusability while enabling their efficient catalytic activities. The primary function of hydrogel scaffolds in biocatalysis is to provide a supportive and protective environment for enzymes. Enzymes are sensitive to changes in temperature, pH, and mechanical stress, which can significantly affect their activity and longevity. Hydrogels, with their high-water content and tunable properties, offer an ideal platform for enzyme immobilization. They can maintain a stable microenvironment that mimics the natural conditions for enzyme activity, ensuring that the enzymes remain active over extended periods.

Hydrogel scaffolds also facilitate the reusability of immobilized enzymes, making biocatalytic processes more economically viable and environmentally friendly.

Immobilized enzymes can be easily recovered and reused in subsequent reactions, reducing both operational costs and waste generation. This reusability is particularly beneficial in industries like food processing, pharmaceuticals, and biofuel production, where enzymatic reactions are integral to the manufacturing process.

2.6.2. Films

Films made from hydrogels have emerged as promising and innovative scaffolds in the field of biocatalysis, offering unique advantages for immobilizing enzymes and facilitating various biotechnological processes[116,124]. These hydrogel films can be highly biocompatible, water-rich materials that provide a supportive matrix for the immobilization of enzymes, enabling their use in a wide range of applications[98,125,126].

One of the key advantages of hydrogel films in biocatalysis is their flexibility in terms of design and composition[97,98,127]. Researchers can tailor the properties of hydrogel films, including thickness[73,120], porosity, and mechanical strength, to suit the specific requirements of a biocatalytic reaction[18]. This versatility allows for the creation of custom-designed environments that mimic natural conditions, optimizing enzyme activity and stability[19].

The thin and conformal nature of hydrogel films makes them suitable for various substrates and reaction configurations[97,98,127,128]. They can be applied as coatings on solid surfaces or integrated into microreactors[73], enhancing their adaptability and integration into diverse bioprocessing systems.

In practical terms, hydrogel films in biocatalysis have found applications in areas such as biosensors[24,129], pharmaceutical manufacturing[130], and wastewater treatment[118]. For example, in biosensors, hydrogel films can serve as a matrix for the immobilization of enzymes that detect specific biomarkers, enabling rapid and selective analytical techniques[131–133].

Overall, hydrogel films are proving to be valuable tools in biocatalysis[127], offering a versatile and efficient means of immobilizing enzymes and improving the sustainability and efficiency of biotechnological processes thus enabling a wide range of applications in different sectors.

2.6.3. Organogels

Organogels, a unique class of gels formed from polymers and organic solvents, exhibit distinct properties that set them apart from traditional hydrogels[134]. These properties make them valuable in various industrial applications, including biocatalysis[23,111], and offer advantages over other types of gels. The nature of organogels is characterized by their hydrophobicity, derived by the use of organic solvents. This hydrophobic nature

allows them to create a non-aqueous microenvironment, making them ideal for applications involving hydrophobic substrates or reactions that are sensitive to water. Furthermore, organogels allow for the controlled release of reaction products, making them versatile tools for fine chemical synthesis and pharmaceutical production.

While organogels offer several advantages in biocatalysis, they also come with certain disadvantages and limitations that should be considered. Organogels may not be suitable for all types of enzymes. Some enzymes may not function efficiently or may become denatured when immobilized within organogels due to the hydrophobic microenvironment[134]. Compatibility issues can restrict their applicability in certain biocatalytic reactions. The organic solvents used to form organogels can be toxic to enzymes and may negatively impact their stability and catalytic activity. Enzymes may require additional modifications or stabilization strategies to withstand the harsh organic solvent conditions within the gel matrix. Careful consideration of these disadvantages is crucial when selecting organogels for specific biocatalytic applications. Microemulsion Based gels overcome these obstacles offering a more protecting environment for the enzymes.

2.6.4. Microemulsion Based Gels (MBGs)

Microemulsion-based gels (MBGs) are a fascinating class of materials that combine the characteristics of microemulsions and gels, offering a unique blend of versatility[64]. These gels can be tailored with two different techniques. Either they can be formed when a microemulsion transitions into a gel-like state with the use of polymers[91], or when a microemulsion and an already formed gel are combined [28,135].

Microemulsion-based gels find applications in various industries due to their unique properties. In the pharmaceutical sector, they are used for drug delivery systems as well as in topical antifungal therapy, providing controlled release of active compounds[136]. In the cosmetic and personal care industry, these gels are employed for the formulation of transparent and stable emulsions [83,105]. Their texture and ability to incorporate both water-soluble and oil-soluble ingredients make them highly desirable for skincare products such as those applied on the therapy of acne[137,138]. Additionally, microemulsion-based gels are used in the food industry for encapsulating flavor enhancers[111], and bioactive compounds[29,105], enabling their protection and controlled release.

Microemulsion-based gels, characterized by their unique combination of the properties of both, microemulsions and gels, have gained significant attention in the field of biocatalysis. These specialized gels serve as a versatile matrix for enhancing enzymatic activity, offering several advantages in terms of stability, controlled release, and increased

catalytic efficiency[28,32,105]. Enzymes are immobilized within the gel network, which not only protects them from denaturation but also offers an extended catalytic lifetime. The gel's porous structure facilitates the diffusion of reactants and products, leading to improved substrate accessibility and overall catalytic efficiency.

As research in this field continues to advance, microemulsion-based gels are likely to play an increasingly vital role in biocatalytic processes, driving innovation across multiple industries.

2.7. Natural Polymers

Natural polymers are biopolymers derived from living organisms, and they serve as fundamental building blocks in a wide array of industries and applications[2,99,139]. These biologically-sourced materials possess unique properties and biocompatibility, making them highly valuable for both traditional and cutting-edge technologies.

Natural polymers include a broad range of substances, with some of the most notable ones being cellulose, starch, chitin, and proteins like collagen and gelatin[100,140,141]. These polymers are found abundantly in nature, primarily in plants, animals, and microorganisms.

In the food industry, starch and cellulose serve as thickeners, stabilizers, and edible coatings[141]. In pharmaceuticals, natural polymers are used as drug delivery carriers[22,93,107], wound dressings[13,116], and as excipients in tablet formulations[106,107]. They also play a significant role in tissue engineering[22,74,116,121,142], where they are employed as scaffolds for tissue regeneration.

One of the most appealing aspects of natural polymers is their eco-friendliness. They are renewable resources, often derived from agricultural by-products or waste materials[143–145]. Their biodegradability and minimal environmental impact contribute to sustainability efforts, making them an attractive choice for environmentally conscious industries. Their biocompatibility and renewable nature make them particularly well-suited for emerging fields like biotechnology.

In the field of biocatalysis, natural polymers have emerged as necessary components, serving as scaffolds that facilitate enzymatic reactions[23,24,90]. Natural polymers provide essential structural support for enzymes. When used as scaffolds, they can immobilize enzymes and maintain their structural integrity, thus preserving the enzymes' catalytic activity[19,24,146]. This immobilization not only enhances enzyme stability but also allows for easy separation and reuse, reducing operational costs[23,70,128]. Natural polymer scaffolds find applications in various biocatalytic processes. They are used in the

production of biofuels[2,5], pharmaceuticals[140] and chemicals[127]. Their versatility allows them to apply a broad range of industrial and research needs.

While natural polymer scaffolds offer numerous advantages, they also present challenges. Researchers are continually working on modifying and enhancing the properties of natural polymers through chemical and physical treatments to overcome these challenges.

2.7.1. Cellulose and its derivatives

Cellulose, an abundant natural polymer, is an essential structural component found in the cell walls of plants[135,147,148]. Cellulose is composed of repeating glucose units linked together through β-1,4-glycosidic bonds. Its unique linear structure forms microfibrils, which provide strength and rigidity to plant cell walls[149]. Due to its abundance in nature, cellulose is considered a highly sustainable material. The extraction of cellulose can be accomplished from various plant sources, such as wood, cotton, and agricultural residues, making it readily available for industrial use[150].

This biopolymer has captured the attention of scientists and industries worldwide due to its diverse range of applications and its derivatives' exceptional properties. Cellulose derivatives, derived from this renewable resource, have found their way into various sectors, offering sustainable solutions and versatile performance[150]. Cellulose derivatives are synthesized by modifying the hydroxyl groups of cellulose molecules, resulting in compounds with distinct properties and functions. Each derivative is tailored for specific applications, imparting desirable characteristics such as solubility, viscosity, and film-forming capabilities[150,151].

Cellulose derivatives have a wide range of applications. In the food industry they are used as thickeners[141,145], stabilizers[145], and binders in various products. In pharmaceuticals, cellulose derivatives are employed to control drug release in tablet formulations[99,106,107,121]. They are used in the production of films[10,152], fibers, and membranes[153], while methyl cellulose serves as an excellent emulsifier[154,155] and rheology modifier in several products[156].

(Hydroxypropyl)methyl cellulose, commonly known as HPMC, is a cellulose derivative with a multitude of applications across various industries. HPMC retains the fundamental cellulose structure, consisting of glucose units linked by β-1,4-glycosidic bonds. The introduction of hydroxypropyl and methyl groups to cellulose molecules enhances its solubility[150,153]. In the pharmaceutical industry, HPMC plays a pivotal role in drug formulation[157,158]. It is used as a binder, disintegrant, and controlled-release agent in tablet manufacturing. HPMC-based matrices enable precise control over drug release

rates, ensuring medication efficacy. Its biocompatibility and low allergenicity make it an ideal choice for oral dosage forms[159].

As a scaffold material, HPMC-based matrices serve as a solid support for immobilizing enzymes, enabling more efficient and sustainable enzymatic reactions across a spectrum of applications[32,92,98,135,160]. HPMC's properties allow for easy preparation of gels or matrices that can host enzymes while maintaining their structural integrity. HPMC provides a biocompatible and inert matrix that minimizes enzyme denaturation, ensuring long-term catalytic activity.

2.7.2. Chitosan

Chitosan is derived from chitin, which is a biopolymer found abundantly in the exoskeletons of crustaceans and the cell walls of fungi[139,161,162]. Through a deacetylation process, chitin is transformed into chitosan. Chitosan is insoluble in water, organic solvents, and aqueous bases, yet it achieves solubility upon agitation in acids like acetic, nitric, hydrochloric, perchloric, and phosphoric acids. The degree of deacetylation influences chitosan's properties, such as solubility and charge density[163].

One of chitosan's most significant advantages is its biocompatibility and biodegradability. These characteristics make it suitable for various applications. In the pharmaceutical industry, chitosan is used for drug delivery systems[96]. It can encapsulate drugs and release them slowly, enhancing their therapeutic efficacy while minimizing side effects. Chitosan-based wound dressings facilitate tissue regeneration and prevent infection due to their antimicrobial properties[13,164]. Moreover, chitosan's mucoadhesive nature is utilized in nasal drug delivery systems[81]. Chitosan finds applications in tissue engineering[122,139,165]. It serves as a scaffold for cell growth and tissue regeneration. Its porous structure supports the infiltration of cells and the formation of new tissues, making it invaluable in creating artificial skin[166] or repairing damaged ones[164,167].

Chitosan has emerged as a valuable scaffold material in the field of biocatalysis[11,24,97,98,128,168]. This versatile biopolymer offers a solid matrix for immobilizing enzymes, enhancing their stability and catalytic efficiency across a range of applications. Chitosan's ease to form hydrogels allow for the creation of controlled microenvironments around immobilized enzymes. Chitosan-based enzyme scaffolds have found applications across various industries. In the pharmaceutical sector, they are employed for the synthesis of pharmaceutical intermediates, enhancing the efficiency and specificity of chemical reactions[169–171]. In food and beverage production, chitosan-immobilized enzymes are used to modify food ingredients[172,173], improve product quality, and reduce processing time.

3. Purpose of the thesis

The purpose of this thesis is to endorse the field of biocompatible encapsulation and enzyme immobilization using (hydroxypropyl) methyl cellulose (HPMC) and chitosan-based materials. The experiments collectively contribute to the understanding of the structural aspects and applications of these innovative materials in biocatalysis.

As industries increasingly strive for sustainability and cost-effectiveness, the development of biodegradable and biocompatible scaffolds for enzyme immobilization remains a significant focus. The aim is to monitor and optimize a reaction while producing valuable fine chemicals, which hold great scientific and industrial appeal. Natural polymers have gathered substantial attention as promising materials for enzyme immobilization due to their ability to provide stability, operate under mild conditions, and facilitate enzyme reuse.

The structural characterization of HPMC microemulsion-based gels used for enzyme immobilization aims to elucidate the unique properties and structural features of these gels, shedding light on their suitability for immobilizing bioactive compounds. The focus was to explore the formulation, stability, and morphology of these gels.

Moving forward, having previously studied HPMC and chitosan[11,92] separately, the combination was an inevitable step to optimize the properties of the immobilization matrix. HPMC-chitosan films as matrices for lipase immobilization were an attempt to enhance enzyme reusability with a scaffold that is easy to handle and to separate from the reaction solution with no material lose. The study aimed to provide insights into the operational characteristics of these films, including enzyme loading, stability, and catalytic performance. It also delves into the morphological aspects of these films, offering a comprehensive understanding of their structure and functionality in biocatalysis. The research was farther built upon and focused deeper into the structural aspects of HPMC-chitosan films used for lipase immobilization. The aim was to provide a detailed structural analysis, including spectroscopic and microscopic studies, to gain a thorough understanding of the interactions between the film components and the immobilized lipase. This research enhances our knowledge of the structural properties crucial for the catalytic efficiency of the immobilized enzyme.

The research tries to contribute to the broader field of biocompatible encapsulation and enzyme immobilization by offering insights into the structural characteristics and operational functionalities of HPMC and chitosan-based materials. The purpose is to highlight the significance in advancing our understanding of these innovative materials in biocatalysis and biocompatible encapsulations.

This work resulted in three published papers. From now on these three publications will be referred to as Publication 1, *"Structural study of (Hydroxypropyl) methyl cellulose*

microemulsion-based gels used for biocompatible encapsulations", Publication 2, *"(Hydroxypropyl) methyl cellulose-chitosan film as a matrix for lipase immobilization: Operational and morphological study"* and Publication 3, "*(Hydroxypropyl) methyl Cellulose-Chitosan Film as a Matrix for Lipase Immobilization—Part II: Structural Studies ",* where needed.

4. Methods

This section provides details on the methodologies employed in this thesis, which are classified into four sections. Firstly, the focus is on the creation and performance evaluation of the biocatalyst. Subsequently, there is a second section about the structural analysis, followed by morphological analysis, and finally, the last section refers to its application as a drug delivery system.

4.1. Formation of the matrix from natural polymers

In order to investigate the appropriate matrix for the immobilization of lipase, several steps were performed.

Microemulsion-based-gels were developed based on previous work by Biomimetics and Nanobiotechnology group of ICB/NHRF [32,92,174,175]. Hydrated HPMC in various weight ratios were combined with a water-in-oil microemulsion containing AOT in isooctane. To introduce the enzyme into the Microemulsion-Based Gel (MBG), the enzyme was placed in the water phase of the microemulsion by adding a specific amount of 0.05 M Tris-HCl buffer with lipase to a 0.2 M AOT in isooctane solution. This study aimed to assess the enzyme's performance both in the case it is incorporated via a microemulsion or directly in the hydrated HPMC. As found in Publication 1 [135], the use of the microemulsion where the enzyme is included in the water phase is crucial to the performance of the biocatalyst, thus the research focused on the MBGs that were formatted as mentioned above.

In the process of developing hydrogel films (Publication 2 and 3) using HPMC and chitosan, various experiments were conducted. Initially, the hydrated polymers were placed in petri dishes in different ratios. Subsequently, microemulsions were introduced into the solution before drying, and the resulting scaffolds were visually inspected for uniformity. The different film formations were allowed to dry under ambient conditions. Films without microemulsions exhibited a smooth and homogeneous surface, easily detaching from the petri dish. In contrast, films containing microemulsions displayed irregularities and nodules, leading to their exclusion from further investigation. The films that remained were combined with the enzyme solution and were monitored as biocatalyst for the model reaction of propyl laurate esterification. In Fig 1. A visualization of the step-by-step formation of the hydrogel films is shown. As detailed in Publication 2 [98], the most effective biocatalyst was the one composed of HPMC:CS in a 2:1 ratio, with which the rest of the experiments were conducted.

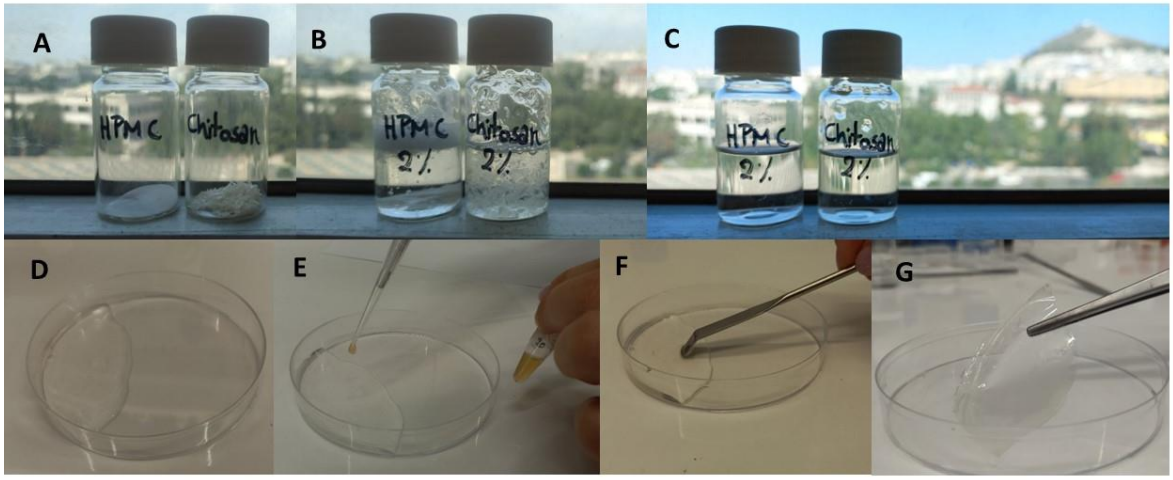

Figure 1 Step by step procedure for the production of the enzyme-loaded film. A: The two polymers, HPMC and Chitosan; B: Dilution of the two polymers in distilled water and acidic water (1%) for HPMC and Chitosan, respectively. They are then left overnight; C: solutions of the two polymers, the next day; D: Mix of the two polymer solutions on a petri dish, HPMC:Chitosan=2:1; E: Addition of the enzyme-containing buffer; F: Gentle stirring with spatula to homogenize the liquid; G: After overnight drying, the film can be peeled off of the petri dish.

4.2. Monitoring of the reaction with Gas Chromatography (GC)

Once the biocatalyst was formed several conditions were tested for the optimization of the reaction. The film was introduced in a solution of propanol and lauric acid (100mM each) inside screwed bottles. The solvent varied depending on the experiment, nevertheless isooctane seems to be the optimum solvent for such reactions[98].

In order to monitor the prosses of the model reactions Gas Chromatography (GC) was employed to track the initial rate of each reaction (Publications 1,2 and 3). Monitoring an enzymatic reaction using GC (Figure 2, [176]) involves tracking changes in the concentration of reactants and/or products over time, to understand the progress of the reaction. The prepared biocatalyst, which included the enzyme immobilized on a matrix formed by HPMC, chitosan or their combination, was placed in the respective reaction solution. To monitor the progress of the reaction, samples were extracted at specific time intervals. This allows the quantification of the substrates and products over time.

Once the sample of the reaction is injected in the apparatus, the individual components of the mixture are separated based on their volatility and affinity for the stationary phase of the column. As the separated compounds exit the GC column, they pass through a flame ionization detector (FID). The data retrieved by the analysis allow the determination of the concentration of the substrates and/or the products over the course of the enzymatic reaction. This analysis can reveal reaction kinetics, enzyme activity, and the progress of the reaction. To ensure the reliability of the results, a triplicate was conducted

to validate the findings. Consistent and reproducible results are crucial for accurate enzymatic reaction monitoring.

For the GC analysis, an Agilent DP5 column was employed (30 m x 0.25 mm i.d. x 0.32 μm film thickness). This column was installed on a Hewlett-Packard (HP) Model GC-6890C chromatograph. Both the injector and detector were maintained at a constant temperature of 280 °C, while the oven temperature was set depending on the experiment in the range of 200°C to 250°C.

When the samples were subtracted from the reaction solution, an external standard was added, i.e., dodecane. To assess and contrast the biocatalyst's effectiveness across various conditions, the initial rate was selected as the most suitable method for comparing these reactions.

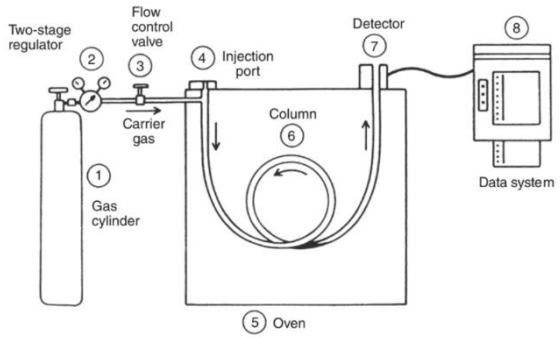

Figure 2 Schematic of a typical gas chromatograph [176]

In a standard GC spectrum, the identification of components within a mixture is provided as the retention time is associated with each compound's appearance. The volume of the peak enables the quantification of concentration. It is measured in picoamperes (pA, y axis in Fig 3), reflecting the intensity of the signal corresponding to the presence of specific compounds in the sample being analyzed.

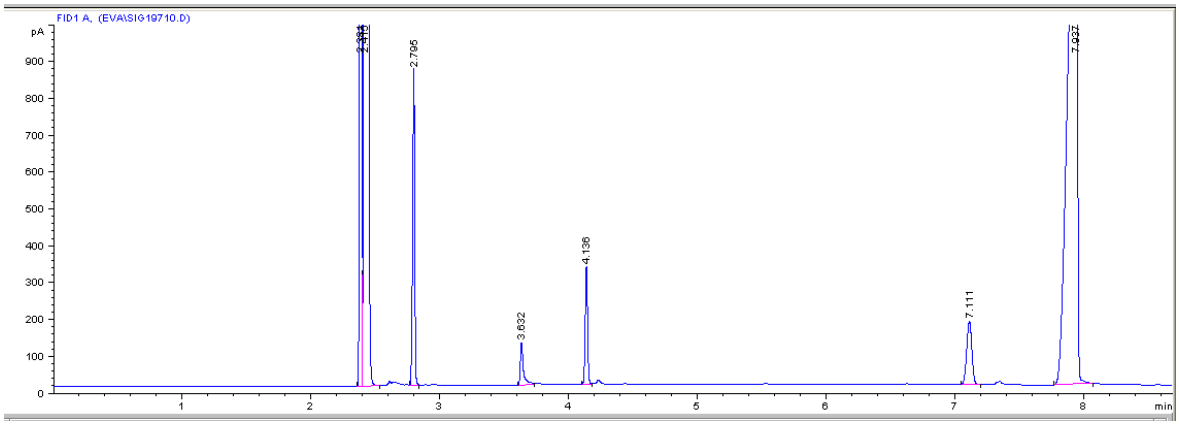

Figure 3. GC spectrum of a model reaction. Each peak represents a compound of the solution. From left to right: Isooctane and propanol (2.3 and 2.4 min, respectively), dodecane (2.8 min), lauric acid (3.6 min), propyl laurate (4.1) and AOT (7.1 and 7.9 min).

Figure 3 shows a standard spectrum analyzed over time (x-axis). Starting from left to right, the dominant solvent peak is displayed in the first few minutes. Subsequently, an external standard, dodecane, is observed, serving as a validation tool of the measurments and allowing comparison with the levels of substrates and products by exhibiting an area proportionate to the other compounds in the mixture. Lauric acid is noteable as it exhibits a distinct "tail" at the end of its peak, aiding in its identification, since using the certain column, it is a characteristic of acids. As the spectrum progresses in the subsequent figure, a peak corresponding to the product emerges at 4.136 minutes. Finally, the presence of AOT from the water-in-oil microemulsion is detectable in the last two peaks of the spectrum. Propanol cannot be easilly observed as it gives its signature peak close to the isooctane peak.

4.3. Structural Characterization

Understanding the structural features of the biocatalyst allows the optimization the design of scaffolds. This includes tailoring properties like porosity, surface area, and charge distribution to enhance enzyme immobilization efficiency and stability. Knowledge of the scaffold's structure aids in predicting how enzymes will interact with the scaffold material. This is crucial for ensuring enzyme-scaffold binding, which is essential for enzyme stability and catalytic efficiency. Structural information assists in designing scaffolds that maintain enzyme stability over multiple reaction cycles and that do not interact with the enzyme. The following techniques were essential for structural characterization of the produced matrices, optimizing the performance of the immobilized enzymes, predicting their behavior in different conditions, and customizing the scaffolds for specific applications.

4.3.1. Electron Paramagnetic Resonance (EPR)

Electron Paramagnetic Resonance (EPR) is a powerful spectroscopic technique used to study paramagnetic species, which are substances with unpaired electrons. This technique enables the identification of samples featuring unpaired electrons, specifically free radicals. The terminology "electron paramagnetic resonance" was introduced to include the influence of both electron orbital and spin angular motion contributions. EPR has found application across diverse disciplines, including chemistry, physics, biology, and material sciences. EPR utilizes spin probes, that is, molecules or ions with unpaired electrons that are introduced into a sample to investigate its properties. Spin probes play a crucial role in EPR spectroscopy, allowing insights into the local environment, dynamics, and interactions of these paramagnetic species. Moreover, in order to investigate the possible conformational changes of the enzymes and to clarify their location when they are immobilized in the gels, spin-labeling of enzyme was performed. The spin labels that are

selected are attached with a covalent bond on the enzyme. For example, a nitroxide spin labeling compound can be attached via a disulfide bond to a specific residue on the enzyme.

In the field of microemulsions, EPR enables the indirect examination of the colloid's microenvironment through the utilization of free radicals. To be more precise, the microwave radiation generated by EPR equipment is assimilated by the free electrons within the free radicals (paramagnetic molecules). In order to quantify the energy splitting in the electrons, induced by a magnetic field, EPR is used as a non-invasive and non-destructive technique. Uses of EPR cover a wide range of applications ranging from the antioxidant activity of a system or a compound to the structural analysis of microemulsions to the investigation of enzyme kinetics as well as the characterization of materials and proteins or biological membranes.

An EPR spectrometer includes a magnet, a microwave bridge including both the microwave source and the detector, and a cavity. A cuvette containing the sample is positioned within the cavity, enhancing the strengthening of faint signals from the sample. The detector, aided by a circulator within the microwave bridge, identifies the signal returning from the cavity as a result of spectroscopic transitions. Subsequently, the microwave power undergoes conversion into an electrical current, generating the distinctive spectrum.

In Publication 1, the exploration of membrane dynamics in microemulsions involved the utilization of nitroxide derivatives, namely doxyl stearic acids (DSAs), with particular emphasis on 5-doxyl stearic acid (5-(1-oxyl-2,2-dimethyl-oxazolidin) stearic acid; 5-DSA), 16-doxyl stearic acid (16-DSA), 12-doxyl methyl stearate (12-DMS) and 4-Hydroxy-2,2,6,6-tetramethylpiperidine-1-oxyl (Hydroxy-TEMPO). The EPR spectra of a nitroxide radical exhibit three distinct peaks arising from the interaction between the spin of the unpaired electron and the nuclear spin.

In order to spin-label our enzyme and observe its interaction with the immobilization matrix, 4-(2-iodoacetamido)-2,2,6,6-tetramethyl-1-piperidinyloxy(4-(2-iodoacetamido)-TEMPO) was chosen to interact and bind with the enzyme. The effectiveness of the enzyme spin-labeling was assessed by observing the reduction in lipase catalytic activity concerning the hydrolysis of 4-Nitrophenyl butyrate (p-NPB).

In the current study, EPR results were analyzed in the terms of three parameters, namely, the rotational correlation time, τ_R; the order parameter, S; and the hyperfine splitting constant, A_N. These parameters are crucial in EPR spectroscopy, offering insights into the rotational dynamics, orientational order, and local microenvironment around a spin probe within a given sample. By analyzing these parameters, researchers understand

the structural and dynamic properties of biological membranes, polymers, or other systems under investigation. More specifically, τ_R represents the average time it takes for a spin probe to undergo a complete rotational motion within its environment. A shorter τ_R indicates faster rotational motion suggesting greater fluidity or flexibility in the surrounding medium. Conversely, a longer τ_R implies slower rotation, indicative of a more constrained or viscous environment. The order parameter, S, characterizes the degree of alignment or orientation of the spin probe within the system. S ranges from 0 (random orientation) to 1 (perfect alignment). Higher values of S indicate a more ordered or aligned orientation of the spin probe within the sample, reflecting a more structured or anisotropic environment. Lastly, A_N is a measure of the separation between the different peaks in the EPR spectrum, resulting from interactions between the electron spin and nearby nuclei. A_N provides information about the local environment of the spin probe. Changes in A_N can indicate alterations in the electron-nuclear interactions, which can be linked to variations in the spin probe's surroundings, such as changes in polarity or the presence of nearby paramagnetic species.

The rotational correlation time τ_R of the spin probe is calculated from the EPR spectrum using the Eq 1:

$$\tau_R = 6 \times 10{-}10\ [(h_0 / h_{+1})\ 1/2 + (h_0 / h_{-1})\ 1/2 - 2]\ \Delta H_0,(s) \qquad \text{Eq 1}$$

Here, ΔH_0 denotes the width of the central field, while h_{+1}, h_0, and h_{-1} represent the intensities of the peaks in the low, central, and high fields of the spectrum, respectively. This formula can be applied only in the fast motion region of the nitroxide time scale, namely for $\tau_R < 3x10^{-9}$ s

For the slow-motion as well as the fast-motion regime EPR spectra simulations were performed using programs in MATLAB platform (MathWorks) employing the EasySpin toolbox in order to acquire the optimal sample's τ_R.

Whereas, the order parameter S is calculated from the EPR spectra using the equation (Eq 2):

$$S = (A_{\parallel} - A_{\perp}) / [A_{ZZ} - 1/2(A_{XX} + A_{YY})]\ k \qquad \text{Eq 2}$$

In the above equation, A_{XX} is 6.3 x 10^{-4}, A_{YY} is 5.8 x 10^{-4}, and A_{ZZ} is 33.6 x 10^{-4} T. $A_{//}$ and $A_{\perp}$ signify the hyperfine splitting constants, which reflects the interaction of the unpaired electron with nuclear spins. $A_{//}$ represents half the distance of the outer hyperfine splitting ($2A_{max}$), while $A_{\perp}$ represents half the distance of the inner hyperfine splitting. The ratio, k = A_0/A_0, serves as the polarity correction factor, where $A_0 = 1/3(A_{XX} + A_{YY} + A_{ZZ})$ is the hyperfine splitting constant for the nitroxide in the crystal state, and $A_0 = 1/3(A_{\parallel} + 2A_{\perp})$ is

the isotropic hyperfine splitting constant for the spin probe in the membrane. A_0 values are depending on the polarity of the spin probe's environment, exhibiting an increase with heightened polarity in the vicinity of the paramagnetic moiety.

WinEPR Processing software was employed to process the experimental spectra.

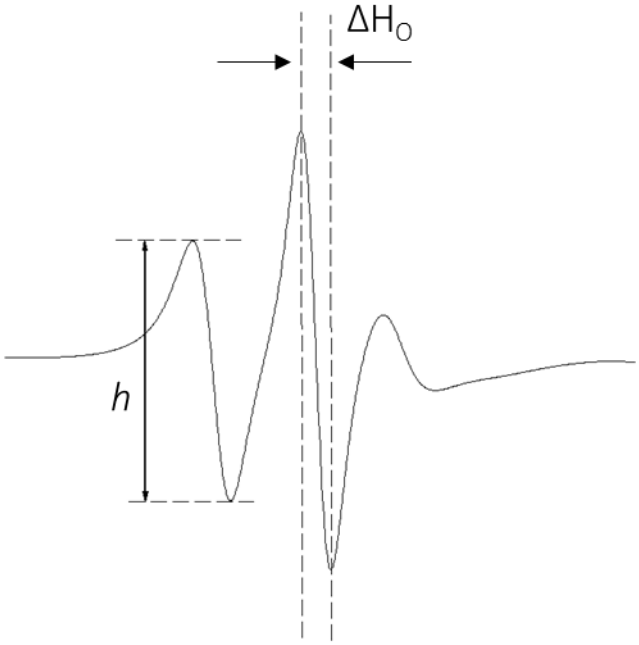

Figure 4. EPR spectrum: h is the height (intensity) of each peak, ΔH_0 is the width of the central field peak".

4.3.2. Small-Angle X-ray Scattering (SAXS) in collaboration with the CNRS Centre de Recherche Paul Pascal

Small-Angle X-ray Scattering (SAXS) was used as an analytical and non-destructive technique, in order to approach the investigation into nanostructures within both liquid and solid matrices. SAXS, with its capability to explore length scales ranging from 10 to 1000 Å, emerged as a robust tool for characterizing gel systems, including films. SAXS begins with an X-ray source, which is directed towards the sample under investigation. The sample can be in various forms, including liquid, solid, or gel. When the X-rays encounter the electrons in the sample, undergo elastic scattering. The scattered X-rays are deflected at different angles depending on the structure of the material, thus creating a diffraction pattern. A detector positioned opposite to the sample collects the scattered X-rays. The intensity of the scattered X-rays at different angles is recorded, creating a scattering profile. The collected data is then analyzed to extract information about the size, shape, and arrangement of nanoscale structures within the sample. The intensity and distribution of scattering angles provide insights into the spatial arrangement of components in the material.

In Publication 3, the experiments were conducted using an XEUSS 2.0 instrument from XENOCS, Grenoble, France, and coupled to a FOX 3D single reflection optical mirror centered on Cu Kα radiation (λ = 1.54 Å). The GeniX 3D source produced an 8 keV beam, precisely collimated and defined by a pair of motorized scatterless slits. Solid samples were placed in capillaries, folded twice to enhance signal strength. The exposure time for the samples was 3 hours. Data collection utilized a two-dimensional PILATUS-300k detector from DECTRIS, Switzerland, positioned perpendicularly to the direct beam at a distance of 1634 mm. Calibration was performed using a Silver behenate standard.

The XENOCS-customized specFE software facilitated the use of the "virtual detector mode", enabling the acquisition of shaped images. This approach provided access to a range of scattering wave vectors, denoted as q, typically spanning from 0.007 $A^{-1}$to 0.24 A^{-1}. The utilization of this mode allowed for a comprehensive exploration of the scattering characteristics during the experiments.

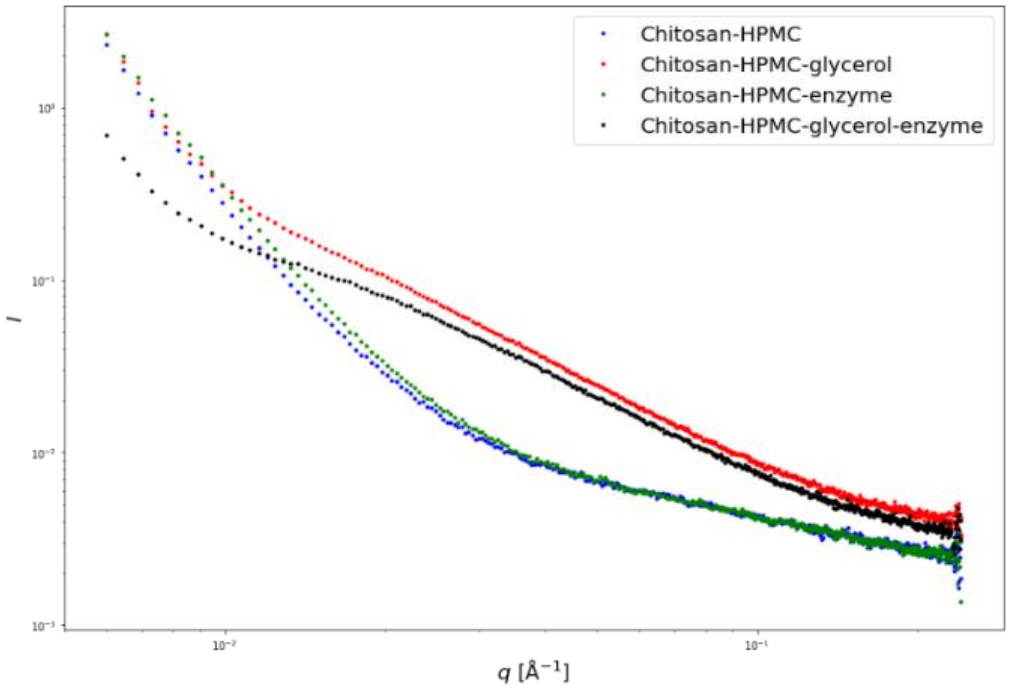

Figure 5. Raw data; Double logarithmic scale; SAXS spectra for different types of films of the present thesis

For this technique, a collaboration with the laboratory of CNRS Centre de Recherche Paul Pascal, University of Bordeaux and Dr. Véronique Schmitt was conducted. The experimental setup, with the guidance of Dr. Federic Nallet, incorporated advancements in X-ray instrumentation and sample handling techniques, ensuring that the SAXs analysis was particularly suited to unraveling the size and structure of these materials [29].

4.3.3. Fourier Transform Infrared spectroscopy (FTIR) with the Faculty of Chemistry, Wrocław University of Science and Technology, Wroclaw, Poland

Fourier Transform Infrared spectroscopy or FTIR is a powerful analytical technique used to study the interaction of infrared light with matter. It provides information about the chemical composition and molecular structure of a sample. FTIR spectroscopy is a nondestructive method that enables the observation of distinct alterations associated with interactions among particular functional groups.

FTIR uses an infrared light source that emits a broad spectrum of wavelength in the infrared area. This spectrum covers the range of frequencies associated with molecular vibrations. The infrared light is directed through or reflected off the sample being analyzed. When the infrared light interacts with the sample, it is selectively absorbed by specific chemical bonds within the molecules. Different chemical bonds vibrate at characteristic frequencies. When these bonds absorb infrared radiation, they undergo vibrational transitions, causing changes in the molecular dipole moment. This absorption is specific to the types of chemical bonds present in the sample. In FTIR, instead of scanning through individual wavelengths, the interferometer is used to simultaneously expose the sample to a broad range of infrared wavelengths. The results contain information about all the frequencies absorbed by the sample. The obtained infrared spectrum is a plot of intensity versus frequency (or wavelength).

In Publication 3, FTIR spectroscopy was employed to examine the polymer functional groups constituting the film, aiming to discern potential interactions between these functional groups and the enzyme within the composite systems. Analysis of the samples occurred in the spectral range of 4000 to 400cm^{-1}, with a resolution of 2cm^{-1}, using a Bruker VERTEX 70 V vacuum spectrometer (Bruker Optik GmbH, Birrika, MA, USA). The spectrometer was equipped with a diamond attenuated total reflectance (ATR) accessory, and spectra analysis was conducted using Opus software (Bruker Optik GmbH, Ettlingen, Germany).

4.4. Morphological Characterization

Morphological characterization is used for the detailed examination of the physical structure and features of a system or material. This includes details about the size, shape, and distribution of polymer chains, as well as any intermolecular interactions. It is essential for optimizing properties, ensuring quality, and tailoring materials for specific applications across various industries. The morphology is directly linked to their functional properties. Understanding the morphology helps elucidate how the material will behave in different conditions, impacting its mechanical, thermal, and barrier properties. In composite systems or when natural polymers are combined with other materials (e.g., enzymes),

morphological characterization provides insights into how these components interact. By characterizing the morphology, researchers can identify factors influencing the performance of the material in order to optimize the synthesis or processing conditions to achieve desired properties in the final product.

4.4.1. Scanning Electron Microscopy (SEM)

Scanning Electron Microscopy (SEM) is a powerful imaging technique that provides detailed and high-resolution three-dimensional images of the surface of a sample. SEM offers high magnification capabilities, allowing researchers to examine samples at the nanoscale. The resolution is typically much higher than that of optical microscopes. SEM data can be used to generate three-dimensional reconstructions of the sample's surface, providing a more comprehensive understanding of its topography.

SEM uses an electron gun as its primary source. The electron gun generates a focused beam of high-energy electrons. When the accelerated electron beam strikes the sample, it interacts with the atoms on the surface. Detectors positioned above the sample collect the emitted secondary electrons. The detected signals are then used to create images that represent the sample's surface morphology. Furthermore, backscattered electrons, which are electrons that are scattered back towards the electron source, provide information about the sample's composition. These electrons have higher energy than secondary electrons and are sensitive to variations in atomic number. The signals collected by the detectors are used to create images. The resulting images can be black and white, false-colored, or even in three dimensions, depending on the information being highlighted.

Scanning Electron Microscopy (SEM) was employed in Publication 1 and 3 to examine intricate aspects of microstructural alterations in the film and gel morphology, both in the absence and presence of the enzyme. Additionally, the impact of the biocatalyst's repeated use (up to 35 times in an organic solvent) on its morphology was investigated.

For the films, an optical microscope model 41-CX (Olympus, Japan) with a 10× magnification, coupled with a 500MI digital camera (Ataray, Turkey), was utilized for imaging. The acquisition and analysis of images were performed using Quick-photo 2.2 software. Additionally, the films were affixed to double-sided carbon tape, coated with carbon, and subjected to examination using a JSM-6601LV scanning electron microscope (JEOL, Akishima, Japan) at an operating voltage of 15 kV.

For the gels, the morphology examination was conducted using a field emission scanning electron microscope (FESEM). The JEOL JSM-7610FPlus Field Emission SEM (Tokyo, Japan) employs a combination of two established technologies—a semi-in-lens detector with an integrated electron energy filter (r-filter) and an in-the-lens Schottky field

emission gun. This configuration allows for ultrahigh spatial resolution over a broad range of probe currents (1 pA to more than 200 nA) across various applications. The JSM-7610FPlus achieves true 1,000,000× magnification with 0.8 nm resolution at 15 kV (1.0 nm at 1 kV) and exceptional beam stability, enabling the detailed observation of the fine surface morphology of nanostructures. Integrating a comprehensive set of detectors for secondary electrons, backscattered electrons, energy dispersive X-ray spectroscopy (EDS), wavelength dispersive X-ray spectroscopy (WDS), scanning transmission electron microscopy (STEM), electron backscatter diffraction (EBSD), and cathodoluminescence (CL), the JSM-7610FPlus provides a versatile analytical platform. The samples were subjected to freeze-drying before analysis, and visualization was carried out without any sputtering process.

4.4.2. Atomic Force Microscopy (AFM) in collaboration with the CNRS Centre de Recherche Paul Pascal

Atomic Force Microscopy (AFM) is a high-resolution imaging technique that operates on the principles of atomic forces between a sharp tip and the surface of the system under investigation.

AFM involves a sharp tip mounted on a flexible cantilever. The tip is usually made of a material with a sharp apex, like silicon or silicon nitride. As the tip approaches the sample, atomic forces such as van der Waals forces, electrostatic forces and chemical bonding forces come into play. These forces cause the cantilever to bend. A cantilever in AFM is a thin beam with a sharp tip at its free end, and it is a crucial component used for scanning and probing surfaces at the atomic and molecular levels. The sample is scanned by moving the tip laterally across the surface in a raster pattern. The vertical movement of the cantilever during scanning creates a topographic map of the sample surface. The collected data is used to generate high-resolution images of the sample surface, revealing details at the atomic and molecular levels. Beyond imaging, AFM can be used in various modes to gather information about material properties, such as stiffness, adhesion and conductivity.

In AFM, height images refer to topographic maps that display the variations in height across a sample's surface. These images provide information about the three-dimensional structure of the sample, revealing surface features such as bumps, valleys and other structural details. On the other hand, phase imaging in AFM is a technique that provides additional information beyond traditional height images. While height images show the variations in the sample's surface topography, phase imaging reveals differences in material properties and surface interactions.

In Publication 2, film morphology was investigated using dynamic force mode (tapping mode) AFM under ambient conditions at 25 °C. The study was conducted with a Dimension-Icon apparatus from Brüker, equipped with Tap 300 Al-G tips obtained from Budget Sensors. Unlike using petri dishes, the mixtures were dried on microscope slides. Various scan sizes were employed for observation, ranging from 300 × 300 nm^2 to 60 × 60 μm^2, depending on the requirements. Simultaneous recording of height and phase images was performed. The assessment of roughness was carried out by determining R_q, the root-mean-square roughness of each sample, calculated over a 100 μm^2 area.

4.4.3. Optical Microscopy in collaboration with the Faculty of Chemistry, Wrocław University of Science and Technology, Wroclaw, Poland

Optical microscopy is an approach predicated on the use of visible light to examine matter, beyond the resolving capacity of the eye. The main principles involve the use of a light source, typically a bulb, to generate light, and a condenser lens to concentrate and uniformly illuminate the sample. The sample, in turn, interacts with the light, either transmitting it through or reflecting it.

Extensive use of optical microscopy can be found in studying the structure, function, and behavior of cells, tissues, analyzing the composition, structure, and properties of materials or examination of chemical reactions, crystal structures, and molecular formations.

In Publication 3, the systems under examination were deposited onto a glass slide. Subsequent microscopic observations were conducted using an optical microscope 41-CX (Olympus, Japan) equipped with 10× magnification and a 500MI digital camera (Ataray, Turkey). The imaging process utilized Quick-photo 2.2 software for both capturing and analyzing pictures. Additionally, the samples were attached to double-sided carbon tape, coated with carbon, and subjected to examination using a JSM-6601LV scanning electron microscope (JEOL, Akishima, Japan) operating at 15 kV.

4.4.4. Profilometry in collaboration with the Department of Chemical and Pharmaceutical Sciences, University of Trieste

Profilometry is a technique used to study the surface profile or topography of an object, providing information about its height variations. This method is commonly employed in fields such as materials science, engineering, and manufacturing to assess surface roughness, wear, and other characteristics. Here, it was used as an additional technique for verification of the AFM results. The mechanical properties and topography of the samples were assessed using an FT-MTA03 (FemtoTools AG, Buchs, Switzerland) equipped with an FT-S2000 microforce sensing probe (range: ±2000 μN, resolution: 0.005 μN), capped with a 50 μm borosilicate glass sphere (BSGMS-2.2 from Cospheric).

For profilometry tests in Publication 3, a single layer (approximately 0.5 cm wide) was meticulously stretched over a glass slide. Indentation measurements were conducted at a fixed height across the width of the sample piece and the surrounding glass slide. Employing a stick-slip actuator (29 mm vertical range, 1 nm positional resolution) in a stepped mode (0.5 µm steps, 0.02 s delay) at a speed of 50 µm s^{-1}, measurements were continued until a force of 1500 µN was reached. Data analysis involved determining the vertical position at which a force of 1000 µN was achieved and calculating the corresponding material height relative to the glass slide.

For mechanical tests, the film samples were initially folded into a 3-layer structure and compressed between two glass slides before measurement. Subsequently, the samples were positioned on a glass slide, and a slight pressure was applied to the sample edges using additional glass slides to maintain flatness during measurement. A piezoscanner (50 µm vertical range, 0.1 nm positional resolution) in a continuous actuation mode was used to indent the probe into the sample. The sample surface was identified by applying a force threshold of 3 µN, retracting the probe 1 µm from the surface for baseline data acquisition. Measurements were conducted at a speed of 1 µm s^{-1}, reaching a maximum force of 30 µN (approximately 0.5 µm maximum indentation depth), and data were collected at a frequency of 200 Hz. Data encompassed the approach, indentation into the material (loading), and retraction back to the initial probe position (unloading).

Custom Python-based application was used for data analysis. The contact point was determined by locating a maximum in the second derivative of force as a function of displacement for each set of force–displacement data. Unloading data beyond the contact point were analyzed using the following method. 50% of the data with the greatest indentation depth were fitted to a power law equation.

$$P = \alpha(h-h_f)^m \qquad \text{Eq. 3}$$

where P is the load at displacement h, m is an exponent set to 1.5 for a spherical indentation probe, and α and h_f are fitting parameters.

Stiffness at peak load was determined, and these values were used to calculate the contact depth and contact area. The reduced modulus and Young's modulus of the film were subsequently calculated using relevant equations, considering the material properties of the borosilicate glass probe and typical Poisson's ratio for biopolymer materials. The Young's modulus of the sample (E_S) is given by:

$$\frac{1}{E_R} = \frac{1-\nu_S^2}{E_S} + \frac{1-\nu_p^2}{E_p} \qquad \text{Eq.4}$$

where E_p and ν_P are the Young's modulus and Poisson's ratio of the probe, and ν_S is the sample Poisson's ratio.

4.5. Drug release study

Franz diffusion cell is mainly used to determine the *ex-vivo* skin permeation and *in-vitro* drug release of many preparations applied over the skin, such as gels, microemulsion, transdermal patches and creams. In the present study, where the results were unpublished, the main method employed for evaluating the transdermal release *in vitro* is Franz Diffusion Cell. A membrane that resembles skin is positioned as a barrier between the donor compartment and the receptor compartment upon a diffusion cell (Fig 4). The transdermal release rate is determined by passive diffusion through the membrane. The diffusion cell includes (a) the donor compartment, where the release system is positioned above a semi-permeable membrane through which the active substance is able to get through, and (b) the receptor compartment, where samples can be drawn using a micropipette for subsequent analysis.

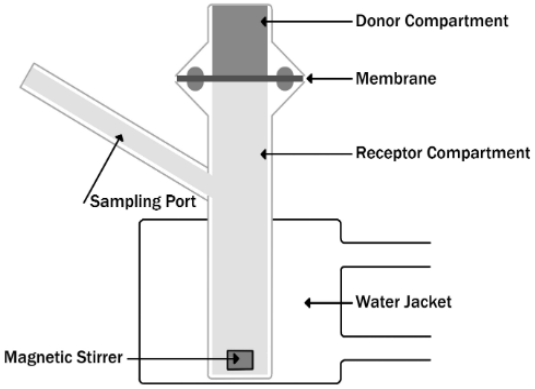

Figure 6. Franz Diffusion Cell [177]

The capacity of the receptor compartment in this case is 5 mL, with an internal diameter of 10 mm. Throughout the experiment, the buffer in the compartment is stirred using a magnetic stirrer. The temperature of the receptor chamber is maintained at a constant 37 °C through a water bath with a circulating pump encompassing the chamber. In contrast, the temperature of the donor chamber remains the same as the ambient temperature.

The methodology used involves the following steps:

- Soak the synthetic membrane for 24 h in an isotonic to blood buffer solution to be allowed to hydrate.
- Fill the receptor compartment with an isotonic to blood buffer solution (pH 7.4).
- Fill the water jacket to maintain a constant temperature around the receptor compartment.

- Place the pre-soaked membrane (synthetic, semisynthetic, or real pig ear skin) on top of the receptor compartment, serving as a barrier between the receptor and donor compartments.
- Place the bioactive-containing system in the donor compartment ensuring its contact with the membrane.
- Withdraw a few microliters from the sampling port at specific time intervals.
- Replace the withdrawn solution with an equal volume of the isotonic buffer to maintain the total volume (5mL). This way, the contact of the receptor solution and the membrane is ensured.
- Measure the withdrawn sample using a photometer to quantify the bioactive compound that crossed the membrane barrier.
- Perform all necessary calculations.

To investigate permeation kinetics and mechanisms through membranes, in the study the following kinetic models were applied:

i. Zero-order model: Widely used for pharmaceutical dosage systems with slow drug release. The equation is expressed as:

$$Q_t = Q_0 + k_0 t \quad \text{Eq.5}$$

where Q_t is the amount of dissolved drug in the receptor solution at time t, Q_0 is the initial amount of drug in the receptor solution (often $Q_0 = 0$), and k_0 is the constant of zero-order release.

ii. First-order model: Commonly used for describing the absorption and release of water-soluble drugs from porous matrices. The equation is:

$$LogQ_t = LogQ_0 - \frac{k_1}{2.303} t \quad \text{Eq.6}$$

where Q_t is the amount of dissolved drug at time t, Q_0 is the initial amount of drug in the solution, and k1 is the constant of first-order release.

iii. Higuchi model: Widely used to describe the release of soluble and sparingly soluble drugs in aqueous media from various semi-solid and/or solid matrices, according to a specific equation:

$$Q_t = k_H t^{1/2} \quad \text{Eq.7}$$

where k_H is the Higuchi dissolution constant, whereas Q_t and t correspond to the parameters described previously.

The films used for this study were three. Namely A film from chitosan, a film from HPMC and a mixture of the two polymers. The film with both polymers that was used for this study was the one composed of HPMC:CS in a 2:1 ratio, as mention in section 4.1. Octyl gallate, being hydrophobic, was added as a 0.5 mM ethanol solution to the

mixture of HPMC and chitosan before the dry film was formed. Once the film was ready it was placed on the donor compartment, and positioned on the upper surface of a Strat M® membrane, a well-known skin-simulating barrier. Since octyl gallate is a hydrophobic molecule, in the receptor section of Franz diffusion cells, ethanol was added to the receptor solution so that the compound could be diluted once it passed the membrane barrier. Samples were collected at specific intervals through the sample port of Franz diffusion cell to analyze the release behavior.

5. Results

In this section, all scientific publications derived by the present study along with unpublished results concerning a drug release study via Franz diffusion cell, will be demonstrated.

5.1. Published results: Scaffolds for the encapsulation of bioactive compounds. Operational, morphological and structural analysis.

Natural polymers can be processed into scaffolds with tailored functionalities that support different bioactive compounds such as enzymes. They can be modified or combined with other materials to enhance their properties. As far as the enzyme is concerned, the immobilization on polymeric supports involves various methodologies, including adsorption, entrapment, encapsulation, covalent linking, and cross-linking. Each method offers unique advantages in terms of enzyme stability, loading efficiency, and biocompatibility. For this research, scaffolds that were formed with the derivatives of the two most abundant natural polymers, chitin and a cellulose, where chitosan and HPMC have been used to carry the enzyme.

In the study marked as Publication 1, as mentioned in section 4.1., an HPMC MBG was formed by hydration of the polymer followed by its combination with a w/o microemulsion based on AOT. This matrix had been well studied [31, 63, 92, 160, 173] as a promising biocatalyst when lipase was incorporated. However, little is known about the structure of these systems. This well studied system attracted attention on clarifying its structure and morphology, thus Publication 1 was thorough research on the system's structure mainly through EPR analysis. In this study, EPR is used to define the polar and non-polar areas of the system and study the existence of interfacial areas. Alongside EPR, scanning electron microscopy (SEM) is used to examine the morphology and bulk of the MBGs, small-angle X-ray scattering (SAXS) to investigate the polar and non-polar areas of the gels, and enzyme-labelling techniques to investigate the location of an enzyme in the matrix. This publication offered insight on the specific arrangement of the ingredients of the system and proposed for the first time a structural model for such systems. The results suggest that although a water-in-oil microemulsion is essential to form the final gel, no microemulsion droplets can be detected after incorporation in the gel. Instead, channels are formed by the organic solvent (oil), which are coated by surfactant molecules and a water layer in which the enzyme can be hosted. The study proposes a structural model for the HPMC matrix based on these findings. The use of HPMC microemulsion-based gels for industrial encapsulations has potential applications in various fields, including catalysis for the formation of significant compounds and high added value products.

For Publications 2 and 3, a second matrix was investigated where HPMC with CS were combined. The two polymers were mixed in different weight ratios and the mixtures were

dried in ambient conditions, with the addition of an enzyme solution. The film that was formed, was an easy-to-handle scaffold that could work as a biocatalyst, in the presence of enzyme. Testing the use of a microemulsion upon matrix formation showed that it leads to an inhomogeneous film with lumps. Thus, the scaffold was formed without any microemulsion and the lipase was incorporated in the polymer mixture that eventually formed a film that was easy to handle. The stable film suitable for enzyme immobilization was investigated towards the biocatalysis of a model reaction, the synthesis of propyl laurate, and was optimized towards several parameters. The operational and morphological properties of the HPMC-chitosan film were studied in Publication 2, and the results showed that the film had high porosity and water uptake capacity, making it an ideal matrix for lipase immobilization. The study also demonstrated that the immobilized lipase retained its activity and stability, even after remarkably multiple cycles of use. The HPMC-chitosan film matrix has potential applications in various fields, including biocatalysis, biosensors, and bioreactors.

The film is found to be successful as a biocatalyst. Thus Publication 3 aimed on understanding the complex structure of the film by employing various analytical techniques such as small-angle X-ray scattering (SAXs), Fourier transform infrared spectroscopy (FTIR), optical microscopy, scanning electron microscopy (SEM), and microindentation measurements. The study found that enzyme loading onto the film had minimal impact on its structure. The combination of HPMC and CS resulted in an increase in pH, and the addition of the enzyme led to a more neutral surface charge. Furthermore, intermolecular hydrogen bonds were observed between the amide groups of the two polymers and the lipase. Weak electrostatic interactions between the polysaccharides and the lipase were also noted. Regarding the mechanical properties of the system, the presence of the enzyme showed no significant differences between the loaded and unloaded films, indicating good interaction between the two polymers. Lastly, after repeated use, the film showed signs of fatigue, with a reduction in humidity, which could explain the decrease in enzyme activity over time.

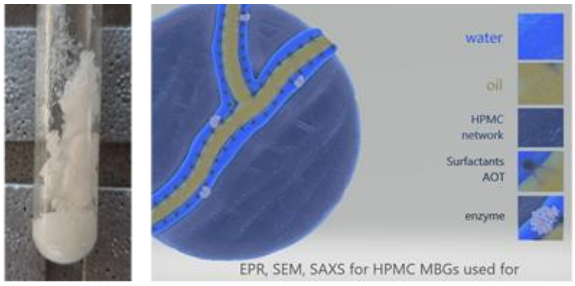

Structural characterization of HPMC MBGS

Publication 1: Vassiliadi, E., Mitsou, E., Avramiotis, S., Chochos, C.L., Pirolt, F., Medebach, M., Glatter, O., Xenakis, A. and Zoumpanioti, M., 2020. Structural study of (Hydroxypropyl) methyl cellulose microemulsion-based gels used for biocompatible encapsulations. *Nanomaterials*, *10*(11), p.2204.

Publication 2: Vassiliadi, E., Aridas, A., Schmitt, V., Xenakis, A. and Zoumpanioti, M., 2022. (Hydroxypropyl) methyl cellulose-chitosan film as a matrix for lipase immobilization: Operational and morphological study. Molecular Catalysis, 522, p.112252.

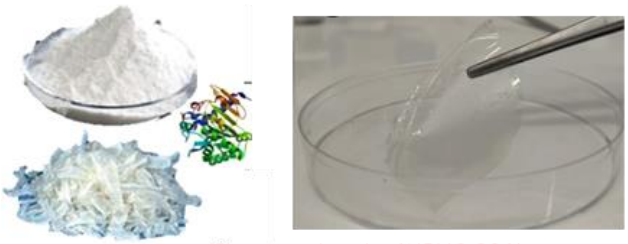

Operational study of HPMC:CS film

Publication 3: Vassiliadi, E., Tsirigotis-Maniecka, M., Symons, H.E., Gobbo, P., Nallet, F., Xenakis, A. and Zoumpanioti, M., 2022. (Hydroxypropyl) methyl Cellulose-Chitosan Film as a Matrix for Lipase Immobilization—Part II: Structural Studies. *Gels*, *8*(9), p.595.

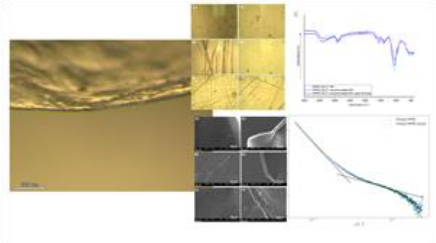

Morphological and structural analysis of the film

Figure 7. Graphical Abstracts of all Publications

5.2. Unpublished results: Release of bioactive compounds

To enhance the versatility of the systems being studied, experiments were conducted to investigate the release of the immobilized bioactive compounds. The Franz diffusion cell, described in section 4.2, was utilized for this purpose.

Octyl gallate, a model chemical compound, was incorporated into a film based on HPMC and chitosan, to study the film's release ability. The data obtained was studied to determine the most suitable release model. Figure 8 demonstrates the concentration of octyl gallate in the receptor solution as calculated by the absorbance using a standard curve, that were released from the different films. As it can be observed the combination of the two polymers accelerated the release of the compound in comparison to the cases where only one of the polymers was used. HPMC seems to be the list effective carrier for the release of the model compound. After this first screening, the film based on the two polymers was thoroughly investigated with the precise calculations mentioned in section 4.5.. Figures 9 and 10 illustrate the Zero Order and Higuchi models of release, respectively. The analysis indicated that the Higuchi model provided a better fit for describing the release behavior of octyl gallate from the system, since the R-squared value of the chart seems to fit better on this model.

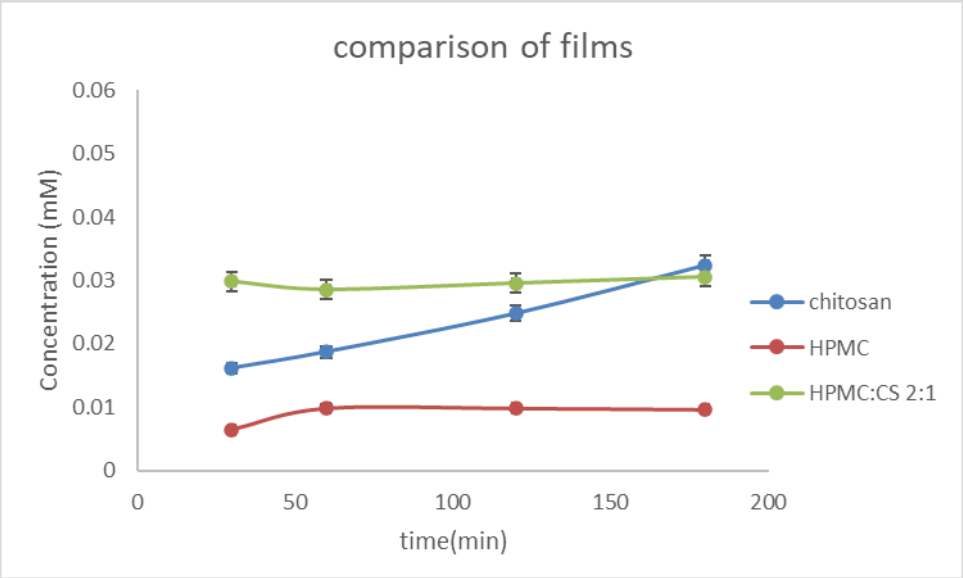

Figure 8. Concentration of octyl gallate that was released from the film/ Comparison between the three types of films (o) Chitosan, (o) HPMC, and (o) HPMC:Chitosan 2:1 , used for the release study

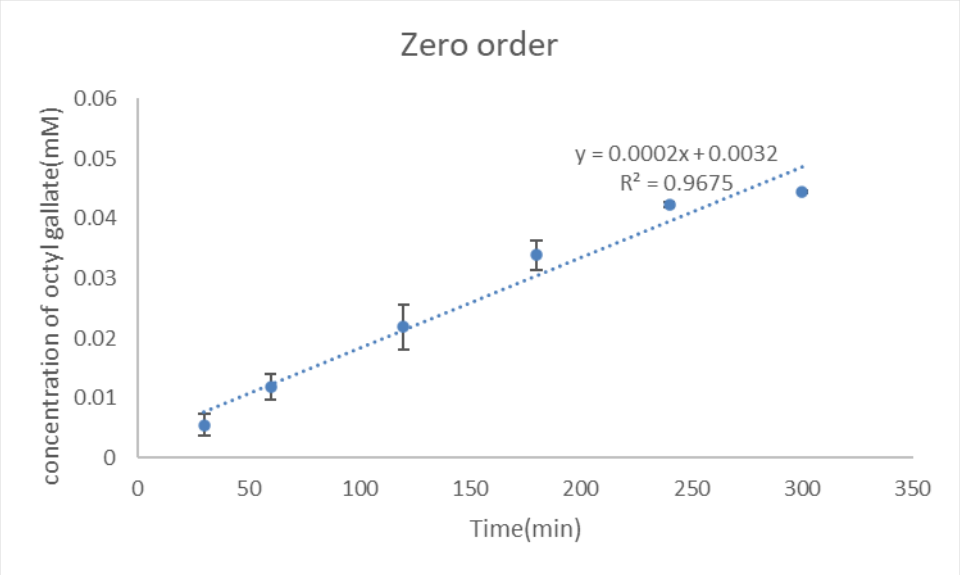

Figure 9. Concentration of octyl gallate (mM) in the receptor solution of Franz diffusion cell over time (min).

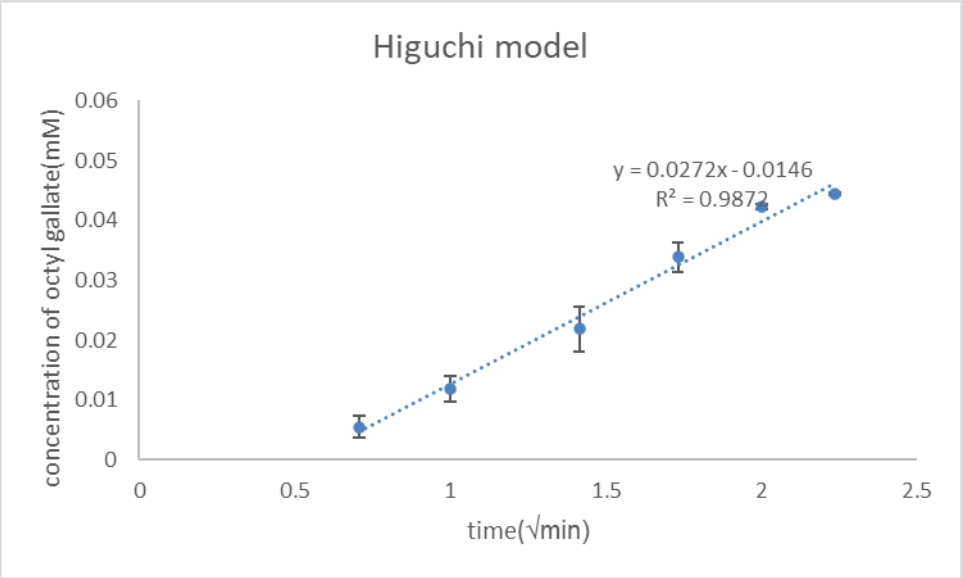

Figure 10. Concentration of octyl gallate (mM) in the receptor solution of Franz diffusion cell in terms of square time in minutes

These results are in agreement with similar studies where chitosan and HPMC were combined. [178–180]. Relevant studies[181] alongside with our findings, observed that by changing the composition of blends, the rate of drug release can be controlled. Depending upon the requirement of pharmaceutical purpose, suitable formulation can be selected. The present study showed the ability of the matrix to incorporate and release a model compound. The prepared blended film made from chitosan and HPMC for potential medicine application might be developed for industrials in the future.

6. Citations

Citations

[1] S.P. France, R.D. Lewis, C.A. Martinez, The Evolving Nature of Biocatalysis in Pharmaceutical Research and Development, JACS Au. 3 (2023) 715–735. https://doi.org/10.1021/JACSAU.2C00712/ASSET/IMAGES/LARGE/AU2C00712_0037.JPEG.

[2] J.M. Choi, S.S. Han, H.S. Kim, Industrial applications of enzyme biocatalysis: Current status and future aspects, Biotechnol. Adv. 33 (2015) 1443–1454. https://doi.org/10.1016/J.BIOTECHADV.2015.02.014.

[3] S. Ferreira-Dias, G. Sandoval, F. Plou, F. Valero, The potential use of lipases in the production of fatty acid derivatives for the food and nutraceutical industries, Electron. J. Biotechnol. (2013). https://doi.org/10.2225/vol16-issue3-fulltext-5.

[4] I. Benucci, K. Liburdi, I. Cacciotti, C. Lombardelli, M. Zappino, F. Nanni, M. Esti, Chitosan/clay nanocomposite films as supports for enzyme immobilization: An innovative green approach for winemaking applications, Food Hydrocoll. (2018). https://doi.org/10.1016/j.foodhyd.2017.08.005.

[5] P. Kalita, B. Basumatary, P. Saikia, B. Das, S. Basumatary, Biodiesel as renewable biofuel produced via enzyme-based catalyzed transesterification, Energy Nexus. 6 (2022) 100087. https://doi.org/10.1016/J.NEXUS.2022.100087.

[6] S. Ray, Applications of Extracellular Microbial Lipase-A Review, Int. J. Res. Biotechnol. Biochem. (2015).

[7] Q. Wang, Z. Yang, Y. Gao, W. Ge, L. Wang, B. Xu, Enzymatic hydrogelation to immobilize an enzyme for high activity and stability, Soft Matter. 4 (2008) 550. https://doi.org/10.1039/b715439a.

[8] D.M. Liu, J. Chen, Y.P. Shi, Advances on methods and easy separated support materials for enzymes immobilization, TrAC Trends Anal. Chem. 102 (2018) 332–342. https://doi.org/10.1016/J.TRAC.2018.03.011.

[9] A. Liese, L. Hilterhaus, Evaluation of immobilized enzymes for industrial applications Motivation and recent developments, Chem. Soc. Rev. Chem. Soc. Rev. (2013).

[10] S. Datta, L.R. Christena, Y.R.S. Rajaram, Enzyme immobilization: an overview on techniques and support materials, 3 Biotech 2012 31. 3 (2012) 1–9. https://doi.org/10.1007/S13205-012-0071-7.

[11] E. Vassiliadi, A. Xenakis, M. Zoumpanioti, Chitosan hydrogels: A new and simple matrix for lipase catalysed biosyntheses, Mol. Catal. (2018).

https://doi.org/10.1016/j.mcat.2017.11.031.

[12] H. Nagahama, H. Maeda, T. Kashiki, R. Jayakumar, T. Furuike, H. Tamura, Preparation and characterization of novel chitosan/gelatin membranes using chitosan hydrogel, Carbohydr. Polym. (2009). https://doi.org/10.1016/j.carbpol.2008.10.015.

[13] X. Shen, J.L. Shamshina, P. Berton, G. Gurau, R.D. Rogers, Hydrogels based on cellulose and chitin: Fabrication, properties, and applications, Green Chem. (2015). https://doi.org/10.1039/c5gc02396c.

[14] C. Sicard, C. Sicard, In Situ Enzyme Immobilization by Covalent Organic Frameworks, Angew. Chemie. 135 (2023) e202213405. https://doi.org/10.1002/ANGE.202213405.

[15] C.S.Z. Battiston, A.M.M. Ficanha, K.L.D. Levandoski, B.A. Da Silva, S. Battiston, R.M. Dallago, M.L. Mignoni, Immobilization of lipase on mesoporous molecular sieve mcm-48 obtained using ionic solid as a structure director and esterification reaction on solvent-free, Quim. Nova. 40 (2017) 293–298. https://doi.org/10.21577/0100-4042.20170011.

[16] C.S.Z. Battiston, A.M.M. Ficanha, C.E.D. Oro, R.M. Dallago, M.L. Mignoni, In Situ Calb Enzyme Immobilization in Mesoporous Material Type MCM-48 Synthesis Using Ionic Solid [C14MI]Cl as Structure-Directing Agent, Appl. Biochem. Biotechnol. 194 (2022) 748–761. https://doi.org/10.1007/S12010-021-03648-Z/FIGURES/6.

[17] A. Flores-Maltos, L. V. Rodríguez-Durán, J. Renovato, J.C. Contreras, R. Rodríguez, C.N. Aguilar, Catalytical properties of free and immobilized aspergillus niger tannase, Enzyme Res. 2011 (2011). https://doi.org/10.4061/2011/768183.

[18] S. Datta, L.R. Christena, Y.R.S. Rajaram, Enzyme immobilization: an overview on techniques and support materials, 3 Biotech. 3 (2013) 1–9. https://doi.org/10.1007/S13205-012-0071-7/FIGURES/1.

[19] S. Gupta, A. Bhattacharya, C.N. Murthy, Tune to immobilize lipases on polymer membranes: Techniques, factors and prospects, Biocatal. Agric. Biotechnol. (2013). https://doi.org/10.1016/j.bcab.2013.04.006.

[20] K.C. Badgujar, B.M. Bhanage, Carbohydrate base co-polymers as an efficient immobilization matrix to enhance lipase activity for potential biocatalytic applications, Carbohydr. Polym. (2015). https://doi.org/10.1016/j.carbpol.2015.08.036.

[21] B. Chen, N. Pernodet, M.H. Rafailovich, A. Bakhtina, R.A. Gross, Protein

Immobilization on Epoxy-Activated Thin Polymer Films: Effect of Surface Wettability and Enzyme Loading, Langmuir. 24 (2008) 13457–13464. https://doi.org/10.1021/LA8019952.

[22] S. Mondal, S. Das, A.K. Nandi, A review on recent advances in polymer and peptide hydrogels, Soft Matter. (2020). https://doi.org/10.1039/c9sm02127b.

[23] H. Stamatis, A. Xenakis, Biocatalysis using microemulsion-based polymer gels containing lipase, J. Mol. Catal. - B Enzym. (1999). https://doi.org/10.1016/S1381-1177(98)00142-8.

[24] R.S. Khan, A.H. Rather, T.U. Wani, S. ullah Rather, T. Amna, M.S. Hassan, F.A. Sheikh, Recent trends using natural polymeric nanofibers as supports for enzyme immobilization and catalysis, Biotechnol. Bioeng. 120 (2023) 22–40. https://doi.org/10.1002/BIT.28246.

[25] J. Meyer, L.E. Meyer, S. Kara, Enzyme immobilization in hydrogels: A perfect liaison for efficient and sustainable biocatalysis, Eng. Life Sci. 22 (2022) 165–177. https://doi.org/10.1002/ELSC.202100087.

[26] E. Mitsou, A. Xenakis, M. Zoumpanioti, Oxidation catalysis by enzymes in microemulsions, Catalysts. (2017). https://doi.org/10.3390/catal7020052.

[27] A. Pastou, H. Stamatis, A. Xenakis, Microemulsion-based organogels containing lipase: application in the synthesis of esters, in: Trends Colloid Interface Sci. XIV, Springer Berlin Heidelberg, Berlin, Heidelberg, 2000: pp. 192–195. https://doi.org/10.1007/3-540-46545-6_39.

[28] M. Zoumpanioti, H. Stamatis, A. Xenakis, Microemulsion-based organogels as matrices for lipase immobilization, Biotechnol. Adv. (2010). https://doi.org/10.1016/j.biotechadv.2010.02.004.

[29] S. Demisli, E. Galani, M. Goulielmaki, F.L. Kyrilis, T. Ilić, F. Hamdi, M. Crevar, P.L. Kastritis, V. Pletsa, F. Nallet, S. Savić, A. Xenakis, V. Papadimitriou, Encapsulation of cannabidiol in oil-in-water nanoemulsions and nanoemulsion-filled hydrogels: A structure and biological assessment study, J. Colloid Interface Sci. 634 (2023) 300–313. https://doi.org/10.1016/J.JCIS.2022.12.036.

[30] S. Demisli, M.D. Chatzidaki, A. Xenakis, V. Papadimitriou, Recent progress on nano-carriers fabrication for food applications with special reference to olive oil-based systems, Curr. Opin. Food Sci. 43 (2022) 146–154. https://doi.org/10.1016/J.COFS.2021.11.012.

[31] C. Wu, S. Bai, M.B. Ansorge-Schumacher, D. Wang, Nanoparticle Cages for Enzyme Catalysis in Organic Media, Adv. Mater. 23 (2011) 5694–5699.

https://doi.org/10.1002/ADMA.201102693.

[32] C. Delimitsou, M. Zoumpanioti, A. Xenakis, H. Stamatis, Activity and stability studies of Mucor miehei lipase immobilized in novel microemulsion-based organogels, Biocatal. Biotransformation. (2002). https://doi.org/10.1080/10242420290025539.

[33] S. Soni, Trends in lipase engineering for enhanced biocatalysis, Biotechnol. Appl. Biochem. 69 (2022) 265–272. https://doi.org/10.1002/BAB.2105.

[34] S. Arana-Peña, N.S. Rios, D. Carballares, L.R.B. Gonçalves, R. Fernandez-Lafuente, Immobilization of lipases via interfacial activation on hydrophobic supports: Production of biocatalysts libraries by altering the immobilization conditions, Catal. Today. 362 (2021) 130–140. https://doi.org/10.1016/J.CATTOD.2020.03.059.

[35] T.C. Bruice, S.J. Benkovic, Chemical basis for enzyme catalysis, Biochemistry. 39 (2000) 6267–6274. https://doi.org/10.1021/BI0003689/ASSET/IMAGES/LARGE/BI0003689H00002.JPEG.

[36] S. Uzuner, D. Cekmecelioglu, Enzymes in the Beverage Industry, Enzym. Food Biotechnol. Prod. Appl. Futur. Prospect. (2019) 29–43. https://doi.org/10.1016/B978-0-12-813280-7.00003-7.

[37] J. Li, Q. Dai, Y. Zhu, W. Xu, W. Zhang, Y. Chen, W. Mu, Low-calorie bulk sweeteners: Recent advances in physical benefits, applications, and bioproduction, Https://Doi.Org/10.1080/10408398.2023.2171362. (2023). https://doi.org/10.1080/10408398.2023.2171362.

[38] M.R. Lawton, S.D. Alcaine, Leveraging endogenous barley enzymes to turn lactose-containing dairy by-products into fermentable adjuncts for Saccharomyces cerevisiae-based ethanol fermentations, J. Dairy Sci. 102 (2019) 2044–2050. https://doi.org/10.3168/JDS.2018-15586.

[39] H. Henriques, C. José, D. Pereira, K. Majore, I. Ciprovica, Bioconversion of Lactose into Glucose–Galactose Syrup by Two-Stage Enzymatic Hydrolysis, Foods 2022, Vol. 11, Page 400. 11 (2022) 400. https://doi.org/10.3390/FOODS11030400.

[40] M. Bilal, H.M.N. Iqbal, State-of-the-art strategies and applied perspectives of enzyme biocatalysis in food sector — current status and future trends, Https://Doi.Org/10.1080/10408398.2019.1627284. 60 (2019) 2052–2066. https://doi.org/10.1080/10408398.2019.1627284.

[41] Z. Amini, Z. Ilham, H.C. Ong, H. Mazaheri, W.H. Chen, State of the art and prospective of lipase-catalyzed transesterification reaction for biodiesel

production, Energy Convers. Manag. 141 (2017) 339–353. https://doi.org/10.1016/J.ENCONMAN.2016.09.049.

[42] E.C.G. Aguieiras, E.D. Cavalcanti-Oliveira, A.M. De Castro, M.A.P. Langone, D.M.G. Freire, Biodiesel production from Acrocomia aculeata acid oil by (enzyme/enzyme) hydroesterification process: Use of vegetable lipase and fermented solid as low-cost biocatalysts, Fuel. 135 (2014) 315–321. https://doi.org/10.1016/J.FUEL.2014.06.069.

[43] Production, purification and characterization of detergent-stable, halotolerant alkaline protease for eco-friendly application in detergents' industry, Int. J. Biosci. 8 (2016) 47–65. https://doi.org/10.12692/IJB/8.2.47-65.

[44] M. Tanwar, M. Debnath, S. Debnath, P. Sharma, A. Mukhopadhay, N. Kakar, S. Ramakrishna, Exploring the utility of nanoprotease as environmentally friendly benign laundry detergent fabric cleaner, J. Clean. Prod. 334 (2022) 130243. https://doi.org/10.1016/J.JCLEPRO.2021.130243.

[45] B. Wiltschi, T. Cernava, A. Dennig, M. Galindo Casas, M. Geier, S. Gruber, M. Haberbauer, P. Heidinger, E. Herrero Acero, R. Kratzer, C. Luley-Goedl, C.A. Müller, J. Pitzer, D. Ribitsch, M. Sauer, K. Schmölzer, W. Schnitzhofer, C.W. Sensen, J. Soh, K. Steiner, C.K. Winkler, M. Winkler, T. Wriessnegger, Enzymes revolutionize the bioproduction of value-added compounds: From enzyme discovery to special applications, Biotechnol. Adv. 40 (2020) 107520. https://doi.org/10.1016/J.BIOTECHADV.2020.107520.

[46] M. Khan, Use of Enzymes in Dairy Industry: A Review of Current Progress, Arch. Razi Inst. 75 (2020) 131–136. https://doi.org/10.22092/ARI.2019.126286.1341.

[47] R. Abu, J.M. Woodley, Application of Enzyme Coupling Reactions to Shift Thermodynamically Limited Biocatalytic Reactions, ChemCatChem. 7 (2015) 3094–3105. https://doi.org/10.1002/CCTC.201500603.

[48] M. Bilal, Y. Zhao, S. Noreen, S. Zakir Hussain Shah, R. Naresh Bharagava, H.M. N Iqbal, S. Zakir Hussain, Biocatalysis and Biotransformation Modifying bio-catalytic properties of enzymes for efficient biocatalysis: a review from immobilization strategies viewpoint, (2019). https://doi.org/10.1080/10242422.2018.1564744.

[49] H. Lee, W.C. DeLoache, J.E. Dueber, Spatial organization of enzymes for metabolic engineering, Metab. Eng. 14 (2012) 242–251. https://doi.org/10.1016/J.YMBEN.2011.09.003.

[50] P.M.J. Burgers, Chromosoma Focus Eukaryotic DNA polymerases in DNA replication and DNA repair, Chromosoma. 107 (1998).

[51] P. Kokkonen, D. Bednar, G. Pinto, Z. Prokop, J. Damborsky, Engineering enzyme access tunnels, Biotechnol. Adv. 37 (2019) 107386. https://doi.org/10.1016/J.BIOTECHADV.2019.04.008.

[52] D.J. Vocadlo, O-GlcNAc processing enzymes: catalytic mechanisms, substrate specificity, and enzyme regulation, Curr. Opin. Chem. Biol. 16 (2012) 488–497. https://doi.org/10.1016/J.CBPA.2012.10.021.

[53] G.A. Evtugyn, H.C. Budnikov, E.B. Nikolskaya, Sensitivity and selectivity of electrochemical enzyme sensors for inhibitor determination, Talanta. 46 (1998) 465–484. https://doi.org/10.1016/S0039-9140(97)00313-5.

[54] Y. Shao, H. Zhou, Q. Wu, Y. Xiong, J. Wang, Y. Ding, Recent advances in enzyme-enhanced immunosensors, Biotechnol. Adv. 53 (2021) 107867. https://doi.org/10.1016/J.BIOTECHADV.2021.107867.

[55] R. Gupta, A. Kumari, P. Syal, Y. Singh, Molecular and functional diversity of yeast and fungal lipases: Their role in biotechnology and cellular physiology, Prog. Lipid Res. 57 (2015) 40–54. https://doi.org/10.1016/J.PLIPRES.2014.12.001.

[56] P.Y. Stergiou, A. Foukis, M. Filippou, M. Koukouritaki, M. Parapouli, L.G. Theodorou, E. Hatziloukas, A. Afendra, A. Pandey, E.M. Papamichael, Advances in lipase-catalyzed esterification reactions, Biotechnol. Adv. 31 (2013) 1846–1859. https://doi.org/10.1016/J.BIOTECHADV.2013.08.006.

[57] C. Hemachander, R. Puvanakrishnan, Lipase from Ralstonia pickettii as an additive in laundry detergent formulations, Process Biochem. 35 (2000) 809–814. https://doi.org/10.1016/S0032-9592(99)00140-5.

[58] R. Devi, | Kesavan, M. Nampoothiri, R. Kumar, S.| Raveendran, S.| M. Arumugam, K.M. Nampoothiri, Lipase of Pseudomonas guariconesis as an additive in laundry detergents and transesterification biocatalysts, J Basic Microbiol. 60 (2020) 112–125. https://doi.org/10.1002/jobm.201900326.

[59] Y.Q. Liu, X. WeiZhuo, X. Wei, A review on lipase-catalyzed synthesis of geranyl esters as flavor additives for food, pharmaceutical and cosmetic applications, Food Chem. Adv. 1 (2022) 100052. https://doi.org/10.1016/J.FOCHA.2022.100052.

[60] H. Abbas, L. Comeau, Aroma synthesis by immobilized lipase from Mucor sp, Enzyme Microb. Technol. 32 (2003) 589–595. https://doi.org/10.1016/S0141-0229(03)00022-X.

[61] A.S.G. Lorenzoni, N.G. Graebin, A.B. Martins, R. Fernandez-Lafuente, M.A. Záchia Ayub, R.C. Rodrigues, Optimization of pineapple flavour synthesis by esterification catalysed by immobilized lipase from Rhizomucor miehei, Flavour Fragr. J. (2012).

https://doi.org/10.1002/ffj.3088.

[62] V.D. Nimkande, A. Bafana, A review on the utility of microbial lipases in wastewater treatment, J. Water Process Eng. 46 (2022) 102591. https://doi.org/10.1016/J.JWPE.2022.102591.

[63] F.T.T. Cavalcante, A.L.G. Cavalcante, I.G. de Sousa, F.S. Neto, J.C.S. Dos Santos, Current Status and Future Perspectives of Supports and Protocols for Enzyme Immobilization, Catal. 2021, Vol. 11, Page 1222. 11 (2021) 1222. https://doi.org/10.3390/CATAL11101222.

[64] I. Itabaiana, K.M. Gonçalves, M. Zoumpanioti, I.C.R. Leal, L.S.M.E. Miranda, A. Xenakis, R.O.M.A. De Souza, Microemulsion-based organogels as an efficient support for lipase-catalyzed reactions under continuous-flow conditions, Org. Process Res. Dev. (2014). https://doi.org/10.1021/op500136c.

[65] M.Y. Chang, R.S. Juang, Activities, stabilities, and reaction kinetics of three free and chitosan-clay composite immobilized enzymes, Enzyme Microb. Technol. 36 (2005) 75–82. https://doi.org/10.1016/J.ENZMICTEC.2004.06.013.

[66] Zhang, Wei Wei, Y.-J. Zhou, H. Ting, X.Q. Yu, Enhancement of activity and stability of lipase by microemulsion-based organogels (MBGs) immobilization and application for synthesis of arylethyl acetate, J. Mol. Catal. B Enzym. 78 (2012) 65–71. https://www.sciencedirect.com/science/article/pii/S1381117712000434?casa_token=ji4UStD_MIcAAAAA:42P--wvA0Piqb8wTWvgjw82Tp2xxB19XsAkvRpatBWIIaXLJAmmSdTTXWufF_4aYIbzkGnhdaw#!

[67] R.A. Sheldon, Enzyme immobilization: The quest for optimum performance, Adv. Synth. Catal. (2007). https://doi.org/10.1002/adsc.200700082.

[68] F. Yagiz, D. Kazan, A.N. Akin, Biodiesel production from waste oils by using lipase immobilized on hydrotalcite and zeolites, Chem. Eng. J. 134 (2007) 262–267. https://doi.org/10.1016/J.CEJ.2007.03.041.

[69] I. Cacciotti, C. Lombardelli, I. Benucci, M. Esti, Clay/chitosan biocomposite systems as novel green carriers for covalent immobilization of food enzymes, J. Mater. Res. Technol. 8 (2019) 3644–3652. https://doi.org/10.1016/J.JMRT.2019.06.002.

[70] R.M. Manzo, R.J. Ceruti, H.L. Bonazza, W.S. Adriano, G.A. Sihufe, E.J. Mammarella, Immobilization of Carboxypeptidase A into Modified Chitosan Matrixes by Covalent Attachment, Appl. Biochem. Biotechnol. 185 (2018) 1029–1043. https://doi.org/10.1007/S12010-018-2708-4.

[71] I. Migneault, C. Dartiguenave, M.J. Bertrand, K.C. Waldron, Glutaraldehyde: Behavior in aqueous solution, reaction with proteins, and application to enzyme crosslinking, Biotechniques. (2004). https://doi.org/10.2144/04375rv01.

[72] M. Matto, Q. Husain, Entrapment of porous and stable concanavalin A-peroxidase complex into hybrid calcium alginate-pectin gel, J. Chem. Technol. Biotechnol. (2006). https://doi.org/10.1002/jctb.1540.

[73] K.A. Batista, F.M. Lopes, F. Yamashita, K.F. Fernandes, Lipase entrapment in PVA/Chitosan biodegradable film for reactor coatings, Mater. Sci. Eng. C. Mater. Biol. Appl. 33 (2013) 1696–1701. https://doi.org/10.1016/J.MSEC.2012.12.082.

[74] M.H. Kim, S. An, K. Won, H.J. Kim, S.H. Lee, Entrapment of enzymes into cellulose-biopolymer composite hydrogel beads using biocompatible ionic liquid, J. Mol. Catal. B Enzym. (2012). https://doi.org/10.1016/j.molcatb.2011.11.011.

[75] C. Garcia-Galan, Á. Berenguer-Murcia, R. Fernandez-Lafuente, R.C. Rodrigues, Potential of different enzyme immobilization strategies to improve enzyme performance, Adv. Synth. Catal. (2011). https://doi.org/10.1002/adsc.201100534.

[76] H. Stamatis, A. Xenakis, F.N. Kolisis, Bioorganic reactions in microemulsions, Biotechnol. Adv. 17 (1999) 293–318. https://doi.org/10.1016/S0734-9750(99)00007-5.

[77] D.P. Acharya, P.G. Hartley, Progress in microemulsion characterization, Curr. Opin. Colloid Interface Sci. 17 (2012) 274–280. https://doi.org/10.1016/J.COCIS.2012.07.002.

[78] M.L. Klossek, J. Marcus, D. Touraud, W. Kunz, The extension of microemulsion regions by combining ethanol with other cosurfactants, Colloids Surfaces A Physicochem. Eng. Asp. 427 (2013) 95–100. https://doi.org/10.1016/J.COLSURFA.2013.03.059.

[79] M. Gradzielski, M. Duvail, P.M. De Molina, M. Simon, Y. Talmon, T. Zemb, Using Microemulsions: Formulation Based on Knowledge of Their Mesostructure, Chem. Rev. 121 (2021) 5671–5740. https://doi.org/10.1021/ACS.CHEMREV.0C00812/ASSET/IMAGES/LARGE/CR0C00812_0032.JPEG.

[80] D. Mitra, Microemulsion and its application: An inside story, Mater. Today Proc. 83 (2023) 75–82. https://doi.org/10.1016/J.MATPR.2023.01.149.

[81] E. Mitsou, V. Pletsa, G.T. Sotiroudis, P. Panine, M. Zoumpanioti, A. Xenakis, Development of a microemulsion for encapsulation and delivery of gallic acid. The role of chitosan, Colloids Surfaces B Biointerfaces. 190 (2020) 110974.

https://doi.org/10.1016/J.COLSURFB.2020.110974.

[82] M. Ohadi, A. Shahravan, N. Dehghannoudeh, T. Eslaminejad, I.M. Banat, G. Dehghannoudeh, Potential Use of Microbial Surfactant in Microemulsion Drug Delivery System: A Systematic Review, (2020). https://doi.org/10.2147/DDDT.S232325.

[83] P. Szumała, A. Macierzanka, Topical delivery of pharmaceutical and cosmetic macromolecules using microemulsion systems, Int. J. Pharm. 615 (2022) 121488. https://doi.org/10.1016/J.IJPHARM.2022.121488.

[84] P. Boonme, Applications of microemulsions in cosmetics, Blackwell Publ. • J. Cosmet. Dermatology. 6 (2007) 223–228. https://doi.org/10.1111/j.1473-2165.2007.00337.x.

[85] M. Saifullah, A. Ahsan, M.R.I. Shishir, Production, stability and application of micro- and nanoemulsion in food production and the food processing industry, Emulsions. (2016) 405–442. https://doi.org/10.1016/B978-0-12-804306-6.00012-X.

[86] A. Amiri-Rigi, S. Abbasi, M.N. Emmambux, Background, Limitations, and Future Perspectives in Food Grade Microemulsions and Nanoemulsions, (2022). https://doi.org/10.1080/87559129.2022.2059808.

[87] M.D. Chatzidaki, E. Mitsou, A. Yaghmur, A. Xenakis, V. Papadimitriou, Formulation and characterization of food-grade microemulsions as carriers of natural phenolic antioxidants, Colloids Surfaces A Physicochem. Eng. Asp. 483 (2015) 130–136. https://doi.org/10.1016/J.COLSURFA.2015.03.060.

[88] A. Bera, T. Kumar, K. Ojha, A. Mandal, Screening of microemulsion properties for application in enhanced oil recovery, Fuel. 121 (2014) 198–207. https://doi.org/10.1016/J.FUEL.2013.12.051.

[89] V.C. Santanna, F.D.S. Curbelo, T.N. Castro Dantas, A.A. Dantas Neto, H.S. Albuquerque, A.I.C. Garnica, Microemulsion flooding for enhanced oil recovery, J. Pet. Sci. Eng. 66 (2009) 117–120. https://doi.org/10.1016/J.PETROL.2009.01.009.

[90] A. Xenakis, H. Stamatis, Lipase immobilization on microemulsion-based polymer gels, Prog. Colloid Polym. Sci. (1999). https://doi.org/10.1007/3-540-48953-3_28.

[91] C. Quellet, H.-F. Eicke, W. Sager, Formation of Microemulsion-Based Gelatin Gels, 350 (1991) 5642–5655. https://doi.org/10.1021/j100167a050.

[92] C. Blattner, M. Zoumpanioti, J. Kröner, G. Schmeer, A. Xenakis, W. Kunz, Biocatalysis using lipase encapsulated in microemulsion-based organogels in supercritical carbon dioxide, J. Supercrit. Fluids. (2006).

https://doi.org/10.1016/j.supflu.2005.06.007.

[93] Y. Osada, J.P. Gong, Y. Tanaka, Polymer Gels, J. Macromol. Sci. Part C Polym. Rev. 44 (2004) 87–112. https://doi.org/10.1081/MC-120027935.

[94] M.P. Thompson, I. Peñafiel, S.C. Cosgrove, N.J. Turner, Biocatalysis Using Immobilized Enzymes in Continuous Flow for the Synthesis of Fine Chemicals, Org. Process Res. Dev. 23 (2019) 9–18. https://doi.org/10.1021/ACS.OPRD.8B00305/ASSET/IMAGES/LARGE/OP-2018-00305W_0017.JPEG.

[95] N.R. Mohamad, N.H.C. Marzuki, N.A. Buang, F. Huyop, R.A. Wahab, An overview of technologies for immobilization of enzymes and surface analysis techniques for immobilized enzymes, Biotechnol. Biotechnol. Equip. 29 (2015) 205–220. https://doi.org/10.1080/13102818.2015.1008192.

[96] A.J. Choi, C.J. Kim, Y.J. Cho, J.K. Hwang, C.T. Kim, Characterization of Capsaicin-Loaded Nanoemulsions Stabilized with Alginate and Chitosan by Self-assembly, Food Bioprocess Technol. 4 (2011) 1119–1126. https://doi.org/10.1007/S11947-011-0568-9/TABLES/1.

[97] V.C. Badgujar, K.C. Badgujar, P.M. Yeole, B.M. Bhanage, Immobilization of Rhizomucor miehei lipase on a polymeric film for synthesis of important fatty acid esters: kinetics and application studies, Bioprocess Biosyst. Eng. (2017). https://doi.org/10.1007/s00449-017-1804-0.

[98] E. Vassiliadi, A. Aridas, V. Schmitt, A. Xenakis, M. Zoumpanioti, (Hydroxypropyl)methyl cellulose-chitosan film as a matrix for lipase immobilization: Operational and morphological study, Mol. Catal. 522 (2022) 112252. https://doi.org/10.1016/J.MCAT.2022.112252.

[99] Y. Wang, J. Wang, Q. Sun, X. Xu, M. Li, F. Xie, Hydroxypropyl methylcellulose hydrocolloid systems: Effect of hydroxypropy group content on the phase structure, rheological properties and film characteristics, Food Chem. 379 (2022) 132075. https://doi.org/10.1016/J.FOODCHEM.2022.132075.

[100] M. Fathi, Á. Martín, D.J. McClements, Nanoencapsulation of food ingredients using carbohydrate based delivery systems, Trends Food Sci. Technol. (2014). https://doi.org/10.1016/j.tifs.2014.06.007.

[101] N. Sharma, R. Sharma, Y.S. Rajput, B. Mann, R. Singh, K. Gandhi, Separation methods for milk proteins on polyacrylamide gel electrophoresis: Critical analysis and options for better resolution, Int. Dairy J. 114 (2021) 104920. https://doi.org/10.1016/J.IDAIRYJ.2020.104920.

[102] D. Alagöz, N.E. Varan, A. Toprak, D. Yildirim, S.S. Tukel, R. Fernandez-Lafuente, Immobilization of xylanase on differently functionalized silica gel supports for orange juice clarification, Process Biochem. 113 (2022) 270–280. https://doi.org/10.1016/J.PROCBIO.2021.12.027.

[103] Q. Chen, G.L. Kenausis, A. Heller, Stability of oxidases immobilized in silica gels, J. Am. Chem. Soc. 120 (1998) 4582–4585. https://doi.org/10.1021/JA971750K/ASSET/IMAGES/LARGE/JA971750KF00002.JPEG.

[104] Y.A. Duman, N. Tekin, Kinetic and thermodynamic properties of purified alkaline protease from Bacillus pumilus Y7 and non-covalent immobilization to poly(vinylimidazole)/clay hydrogel, Eng. Life Sci. 20 (2020) 36–49. https://doi.org/10.1002/ELSC.201900119.

[105] S. Demisli, E. Mitsou, V. Pletsa, A. Xenakis, V. Papadimitriou, Development and Study of Nanoemulsions and Nanoemulsion-Based Hydrogels for the Encapsulation of Lipophilic Compounds, Nanomater. 2020, Vol. 10, Page 2464. 10 (2020) 2464. https://doi.org/10.3390/NANO10122464.

[106] J.E. Hogan, Hydroxypropylmethylcellulose sustained release technology, Drug Dev. Ind. Pharm. 15 (1989) 975–999. https://doi.org/10.3109/03639048909043660.

[107] P. Colombo, R. Bettini, P. Santi, N.A. Peppas, Swellable matrices for controlled drug delivery: gel-layer behaviour, mechanisms and optimal performance, Pharm. Sci. Technolo. Today. 3 (2000) 198–204. https://doi.org/10.1016/S1461-5347(00)00269-8.

[108] K. Rehman, M.H. Zulfakar, Recent advances in gel technologies for topical and transdermal drug delivery, Drug Dev. Ind. Pharm. 40 (2014) 433–440. https://doi.org/10.3109/03639045.2013.828219.

[109] P.C. Nath, S. Debnath, K. Sridhar, B.S. Inbaraj, P.K. Nayak, M. Sharma, A Comprehensive Review of Food Hydrogels: Principles, Formation Mechanisms, Microstructure, and Its Applications, Gels 2023, Vol. 9, Page 1. 9 (2022) 1. https://doi.org/10.3390/GELS9010001.

[110] C. de S. Paglarini, G. de F. Furtado, J.P. Biachi, V.A.S. Vidal, S. Martini, M.B.S. Forte, R.L. Cunha, M.A.R. Pollonio, Functional emulsion gels with potential application in meat products, J. Food Eng. (2018). https://doi.org/10.1016/j.jfoodeng.2017.10.026.

[111] T. Raghavendra, D. Sayania, D. Madamwar, Synthesis of the "green apple ester" ethyl valerate in organic solvents by Candida rugosa lipase immobilized in MBGs in organic solvents: Effects of immobilization and reaction parameters, J. Mol. Catal. B Enzym. (2010). https://doi.org/10.1016/j.molcatb.2009.11.015.

[112] M.J. Dille, K.I. Draget, M.N. Hattrem, The effect of filler particles on the texture of food gels, Modifying Food Texture Nov. Ingredients Process. Tech. (2015) 183–200. https://doi.org/10.1016/B978-1-78242-333-1.00009-7.

[113] S. Javed, R. Atta-Ur, Aloe Vera Gel in Food, Health Products, and Cosmetics Industry, Stud. Nat. Prod. Chem. 41 (2014) 261–285. https://doi.org/10.1016/B978-0-444-63294-4.00009-7.

[114] A. Ellafi, H. Jabbari, O.S. Tomomewo, M.D. Mann, M.B. Geri, C. Tang, Future of Hydraulic Fracturing Application in Terms of Water Management and Environmental Issues: A Critical Review, Soc. Pet. Eng. - SPE Canada Unconv. Resour. Conf. 2020, URCC 2020. (2020). https://doi.org/10.2118/199993-MS.

[115] R. Barati, J.T. Liang, A review of fracturing fluid systems used for hydraulic fracturing of oil and gas wells, J. Appl. Polym. Sci. 131 (2014) 40735. https://doi.org/10.1002/APP.40735.

[116] L. Cui, Y. Yao, E.K.F. Yim, The effects of surface topography modification on hydrogel properties, APL Bioeng. 5 (2021) 31509. https://doi.org/10.1063/5.0046076/1025090.

[117] T. Wang, L. Chen, T. Shen, D. Wu, Preparation and properties of a novel thermo-sensitive hydrogel based on chitosan/hydroxypropyl methylcellulose/glycerol, Int. J. Biol. Macromol. (2016). https://doi.org/10.1016/j.ijbiomac.2016.09.038.

[118] M.K. Yazdi, V. Vatanpour, A. Taghizadeh, M. Taghizadeh, M.R. Ganjali, M.T. Munir, S. Habibzadeh, M.R. Saeb, M. Ghaedi, Hydrogel membranes: A review, Mater. Sci. Eng. C. 114 (2020) 111023. https://doi.org/10.1016/J.MSEC.2020.111023.

[119] R.W. Korsmeyer, R. Gurny, E. Doelker, P. Buri, N.A. Peppas, Mechanisms of solute release from porous hydrophilic polymers, Int. J. Pharm. 15 (1983) 25–35. https://doi.org/10.1016/0378-5173(83)90064-9.

[120] M. Tsirigotis-Maniecka, L. Szyk-Warszyńska, A. Michna, P. Warszyński, K.A. Wilk, Colloidal characteristics and functionality of rationally designed esculin-loaded hydrogel microcapsules, J. Colloid Interface Sci. 530 (2018) 444–458. https://doi.org/10.1016/J.JCIS.2018.07.006.

[121] H.U. Ali, D.N. Iqbal, M. Iqbal, S. Ezzine, A. Arshad, R. Zeeshan, A.A. Chaudhry, S.Z. Alshawwa, A. Nazir, A.F. Khan, HPMC crosslinked chitosan/hydroxyapatite scaffolds containing Lemongrass oil for potential bone tissue engineering applications, Arab. J. Chem. 15 (2022) 103850. https://doi.org/10.1016/J.ARABJC.2022.103850.

[122] S.C. Barros, A.A. da Silva, D.B. Costa, I. Cesarino, C.M. Costa, S. Lanceros-Méndez,

A. Pawlicka, M.M. Silva, Thermo-sensitive chitosan–cellulose derivative hydrogels: swelling behaviour and morphologic studies, Cellulose. 21 (2014) 4531–4544. https://doi.org/10.1007/S10570-014-0442-9/TABLES/2.

[123] P. Laurienzo, M. Malinconico, R. Pizzano, C. Manzo, N. Piciocchi, A. Sorrentino, M.G. Volpe, Natural polysaccharide-based gels for dairy food preservation, J. Dairy Sci. (2006). https://doi.org/10.3168/jds.S0022-0302(06)72558-9.

[124] E.M. Ahmed, Hydrogel: Preparation, characterization, and applications: A review, J. Adv. Res. 6 (2015) 105–121. https://doi.org/10.1016/J.JARE.2013.07.006.

[125] A. Pinotti, M.A. García, M.N. Martino, N.E. Zaritzky, Study on microstructure and physical properties of composite films based on chitosan and methylcellulose, Food Hydrocoll. 21 (2007) 66–72. https://doi.org/10.1016/J.FOODHYD.2006.02.001.

[126] C. Ding, M. Zhang, G. Li, Preparation and characterization of collagen/hydroxypropyl methylcellulose (HPMC) blend film, Carbohydr. Polym. 119 (2015) 194–201. https://doi.org/10.1016/J.CARBPOL.2014.11.057.

[127] K.P. Dhake, P.J. Tambade, Z.S. Qureshi, R.S. Singhal, B.M. Bhanage, HPMC-PVA Film immobilized rhizopus oryzae lipase as a biocatalyst for transesterification reaction, ACS Catal. (2011). https://doi.org/10.1021/cs100162t.

[128] K.C. Badgujar, K.P. Dhake, B.M. Bhanage, Immobilization of Candida cylindracea lipase on poly lactic acid, polyvinyl alcohol and chitosan based ternary blend film: Characterization, activity, stability and its application for N-acylation reactions, Process Biochem. 48 (2013) 1335–1347. https://doi.org/10.1016/J.PROCBIO.2013.06.009.

[129] A. Mateescu, Y. Wang, J. Dostalek, U. Jonas, Thin hydrogel films for optical biosensor applications, Membranes (Basel). (2012). https://doi.org/10.3390/membranes2010040.

[130] S. Andreasen, B. Fejerskov, A.N. Zelikin, Biocatalytic polymer thin films: optimization of the multilayered architecture towards in situ synthesis of anti-proliferative drugs, Nanoscale. 6 (2014) 4131–4140. https://doi.org/10.1039/C3NR05999E.

[131] Z.S. Nishat, T. Hossain, M.N. Islam, H.P. Phan, M.A. Wahab, M.A. Moni, C. Salomon, M.A. Amin, A.A.I. Sina, M.S.A. Hossain, Y.V. Kaneti, Y. Yamauchi, M.K. Masud, Hydrogel Nanoarchitectonics: An Evolving Paradigm for Ultrasensitive Biosensing, Small. 18 (2022) 2107571. https://doi.org/10.1002/SMLL.202107571.

[132] Z. Zhou, Z. Wang, Y. Tang, Y. Zheng, Q. Wang, Optical detection of anthrax biomarkers in an aqueous medium: the combination of carbon quantum dots and

europium ions within alginate hydrogels, J. Mater. Sci. 54 (2019) 2526–2534. https://doi.org/10.1007/S10853-018-2955-3/FIGURES/10.

[133] F. Fathi, M.R. Rashidi, P.S. Pakchin, S. Ahmadi-Kandjani, A. Nikniazi, Photonic crystal based biosensors: Emerging inverse opals for biomarker detection, Talanta. 221 (2021) 121615. https://doi.org/10.1016/J.TALANTA.2020.121615.

[134] W.L. Hinze, I. Uemasu, F. Dai, J.M. Braun, Analytical and related applications of organogels, Curr. Opin. Colloid Interface Sci. (1996). https://doi.org/10.1016/s1359-0294(96)80119-1.

[135] E. Vassiliadi, E. Mitsou, S. Avramiotis, C.L. Chochos, F. Pirolt, M. Medebach, O. Glatter, A. Xenakis, M. Zoumpanioti, Structural study of (Hydroxypropyl)methyl cellulose microemulsion-based gels used for biocompatible encapsulations, Nanomaterials. (2020). https://doi.org/10.3390/nano10112204.

[136] H. Liu, Y. Wang, F. Han, H. Yao, S. Li, Gelatin-stabilised microemulsion-based organogels facilitates percutaneous penetration of cyclosporin A in vitro and dermal pharmacokinetics in vivo, J. Pharm. Sci. (2007). https://doi.org/10.1002/jps.20898.

[137] N. Üstündağ Okur, E.Ş. Çağlar, M.D. Arpa, H.Y. Karasulu, Preparation and evaluation of novel microemulsion-based hydrogels for dermal delivery of benzocaine, Pharm. Dev. Technol. 22 (2017) 500–510. https://doi.org/10.3109/10837450.2015.1131716.

[138] M.R. Patel, R.B. Patel, J.R. Parikh, B.G. Patel, Novel microemulsion-based gel formulation of tazarotene for therapy of acne, Pharm. Dev. Technol. 21 (2016) 921–932. https://doi.org/10.3109/10837450.2015.1081610.

[139] H.J. Malmiri, M.A.G. Jahanian, A. Berenjian, Potential Applications of Chitosan Nanoparticles as Novel Support in Enzyme Immobilization, Am. J. Biochem. Biotechnol. 8 (2012) 203–219. https://doi.org/10.3844/AJBBSP.2012.203.219.

[140] E. Bouyer, G. Mekhloufi, V. Rosilio, J.L. Grossiord, F. Agnely, Proteins, polysaccharides, and their complexes used as stabilizers for emulsions: Alternatives to synthetic surfactants in the pharmaceutical field?, Int. J. Pharm. 432 (2012) 359–378. https://doi.org/10.1016/j.ijpharm.2012.06.052.

[141] C. Arancibia, S. Bayarri, E. Costell, Comparing Carboxymethyl Cellulose and Starch as Thickeners in Oil/Water Emulsions. Implications on Rheological and Structural Properties, Food Biophys. 8 (2013) 122–136. https://doi.org/10.1007/S11483-013-9287-2/FIGURES/9.

[142] Q. Chai, Y. Jiao, X. Yu, Hydrogels for Biomedical Applications: Their Characteristics

and the Mechanisms behind Them, Gels. (2017). https://doi.org/10.3390/gels3010006.

[143] A. Nanni, M. Parisi, M. Colonna, Wine By-Products as Raw Materials for the Production of Biopolymers and of Natural Reinforcing Fillers: A Critical Review, Polym. 2021, Vol. 13, Page 381. 13 (2021) 381. https://doi.org/10.3390/POLYM13030381.

[144] B.E. DiGregorio, Biobased Performance Bioplastic: Mirel, Chem. Biol. 16 (2009) 1–2. https://doi.org/10.1016/J.CHEMBIOL.2009.01.001.

[145] R. Mu, X. Hong, Y. Ni, Y. Li, J. Pang, Q. Wang, J. Xiao, Y. Zheng, Recent trends and applications of cellulose nanocrystals in food industry, Trends Food Sci. Technol. 93 (2019) 136–144. https://doi.org/10.1016/J.TIFS.2019.09.013.

[146] M. Harguindeguy, C. Antonelli, M.P. Belleville, J. Sanchez-Marcano, C. Pochat-Bohatier, Gelatin supports with immobilized laccase as sustainable biocatalysts for water treatment, J. Appl. Polym. Sci. (2021). https://doi.org/10.1002/app.49669.

[147] D. Zhao, Y. Zhu, W. Cheng, W. Chen, Y. Wu, H. Yu, Cellulose-Based Flexible Functional Materials for Emerging Intelligent Electronics, Adv. Mater. 33 (2021) 2000619. https://doi.org/10.1002/ADMA.202000619.

[148] M.H. Kim, S. An, K. Won, H.J. Kim, S.H. Lee, Entrapment of enzymes into cellulose–biopolymer composite hydrogel beads using biocompatible ionic liquid, J. Mol. Catal. B Enzym. 75 (2012) 68–72. https://doi.org/10.1016/J.MOLCATB.2011.11.011.

[149] J.R. Barnett, V.A. Bonham, Cellulose microfibril angle in the cell wall of wood fibres, Biol. Rev. 79 (2004) 461–472. https://doi.org/10.1017/S1464793103006377.

[150] H. Seddiqi, E. Oliaei, H. Honarkar, J. Jin, L.C. Geonzon, R.G. Bacabac, J. Klein-Nulend, Cellulose and its derivatives: towards biomedical applications, Cellul. 2021 284. 28 (2021) 1893–1931. https://doi.org/10.1007/S10570-020-03674-W.

[151] Q. Shen, Surface Properties of Cellulose and Cellulose Derivatives: A Review, (n.d.). https://www.researchgate.net/publication/284340323 (accessed November 1, 2023).

[152] F. Bigi, H. Haghighi, H.W. Siesler, F. Licciardello, A. Pulvirenti, Characterization of chitosan-hydroxypropyl methylcellulose blend films enriched with nettle or sage leaf extract for active food packaging applications, Food Hydrocoll. 120 (2021) 106979. https://doi.org/10.1016/J.FOODHYD.2021.106979.

[153] K. Jedvert, T. Heinze, Cellulose modification and shaping - A review, J. Polym. Eng. 37 (2017) 845–860. https://doi.org/10.1515/POLYENG-2016-

0272/ASSET/GRAPHIC/J_POLYENG-2016-0272_FIG_007.JPG.

[154] Z. Meng, K. Qi, Y. Guo, Y. Wang, Y. Liu, Effects of thickening agents on the formation and properties of edible oleogels based on hydroxypropyl methyl cellulose, Food Chem. 246 (2018) 137–149. https://doi.org/10.1016/J.FOODCHEM.2017.10.154.

[155] J. Floury, A. Desrumaux, M.A.V. Axelos, J. Legrand, Effect of high pressure homogenisation on methylcellulose as food emulsifier, J. Food Eng. 58 (2003) 227–238. https://doi.org/10.1016/S0260-8774(02)00372-2.

[156] E. Perez, J.R. Fernandez, J.B. Stock, M. Hartson, C. Coyle, S. Amin, Methylcellulose-Chitosan Smart Gels for Hairstyling, Cosmet. 2022, Vol. 9, Page 69. 9 (2022) 69. https://doi.org/10.3390/COSMETICS9040069.

[157] K.C. Sung, P.R. Nixon, J.W. Skoug, T.R. Ju, P. Gao, E.M. Topp, M. V. Patel, Effect of formulation variables on drug and polymer release from HPMC-based matrix tablets, Int. J. Pharm. 142 (1996) 53–60. https://doi.org/10.1016/0378-5173(96)04644-3.

[158] J. Siepmann, N.A. Peppas, Modeling of drug release from delivery systems based on hydroxypropyl methylcellulose (HPMC), Adv. Drug Deliv. Rev. 64 (2012) 163–174. https://doi.org/10.1016/J.ADDR.2012.09.028.

[159] C. Benetti, P. Colombo, T.W. Wong, In vitro and in vivo particle coating for oral targeting and drug delivery, Handb. Mod. Coat. Technol. Fabr. Methods Funct. Prop. (2021) 231–258. https://doi.org/10.1016/B978-0-444-63240-1.00009-7.

[160] M. Zoumpanioti, M. Karali, A. Xenakis, H. Stamatis, Lipase biocatalytic processes in surfactant free microemulsion-like ternary systems and related organogels, Enzyme Microb. Technol. (2006). https://doi.org/10.1016/j.enzmictec.2005.03.030.

[161] J. Song, H. Feng, M. Wu, L. Chen, W. Xia, W. Zhang, Development of a bioactive chitosan HPMC-based membrane with tea polyphenols encapsulated in β-cyclodextrin as an effective enhancement, Mater. Today Commun. 27 (2021) 102324. https://doi.org/10.1016/J.MTCOMM.2021.102324.

[162] M. Imran, A. Klouj, A.M. Revol-Junelles, S. Desobry, Controlled release of nisin from HPMC, sodium caseinate, poly-lactic acid and chitosan for active packaging applications, J. Food Eng. 143 (2014) 178–185. https://doi.org/10.1016/J.JFOODENG.2014.06.040.

[163] E.S. de Alvarenga, C. Pereira de Oliveira, C. Roberto Bellato, An approach to understanding the deacetylation degree of chitosan, Carbohydr. Polym. 80 (2010) 1155–1160. https://doi.org/10.1016/J.CARBPOL.2010.01.037.

[164] V. Patrulea, V. Ostafe, G. Borchard, O. Jordan, Chitosan as a starting material for wound healing applications, Eur. J. Pharm. Biopharm. 97 (2015) 417–426. https://doi.org/10.1016/J.EJPB.2015.08.004.

[165] J.D. dos Santos Carvalho, R.S. Rabelo, M.D. Hubinger, Thermo-rheological properties of chitosan hydrogels with hydroxypropyl methylcellulose and methylcellulose, Int. J. Biol. Macromol. 209 (2022) 367–375. https://doi.org/10.1016/J.IJBIOMAC.2022.04.035.

[166] J. Mao, L. Zhao, K. De Yao, Q. Shang, G. Yang, Y. Cao, Study of novel chitosan-gelatin artificial skin in vitro, J. Biomed. Mater. Res. Part A. 64A (2003) 301–308. https://doi.org/10.1002/JBM.A.10223.

[167] T. Dai, M. Tanaka, Y.Y. Huang, M.R. Hamblin, Chitosan preparations for wounds and burns: antimicrobial and wound-healing effects, Expert Rev. Anti. Infect. Ther. 9 (2011) 857–879. https://doi.org/10.1586/ERI.11.59.

[168] E.B. Pereira, G.M. Zanin, H.F. Castro, IMMOBILIZATION AND CATALYTIC PROPERTIES OF LIPASE ON CHITOSAN FOR HYDROLYSIS AND ESTERIFICATION REACTIONS, Brazilian J. Chem. Eng. 20 (n.d.) 343–355.

[169] M.L. Verma, S. Kumar, A. Das, J.S. Randhawa, M. Chamundeeswari, M.L. Verma, S. Kumar, T. Api, U. Pradesh, I.A. Das, J.S. Randhawa, M. Chamundeeswari, Enzyme Immobilization on Chitin and Chitosan-Based Supports for Biotechnological Applications, (2019) 147–173. https://doi.org/10.1007/978-3-030-16538-3_4.

[170] M.L. Verma, S. Kumar, A. Das, J.S. Randhawa, M. Chamundeeswari, Chitin and chitosan-based support materials for enzyme immobilization and biotechnological applications, Environ. Chem. Lett. 18 (2020) 315–323. https://doi.org/10.1007/S10311-019-00942-5.

[171] Y. Bai, Z. Jing, R. Ma, X. Wan, J. Liu, W. Huang, A critical review of enzymes immobilized on chitosan composites: characterization and applications, Bioprocess Biosyst. Eng. (2023). https://doi.org/10.1007/S00449-023-02914-0.

[172] I. Benucci, K. Liburdi, I. Cacciotti, C. Lombardelli, M. Zappino, F. Nanni, M. Esti, Chitosan/clay nanocomposite films as supports for enzyme immobilization: An innovative green approach for winemaking applications, Food Hydrocoll. 74 (2018) 124–131. https://doi.org/10.1016/J.FOODHYD.2017.08.005.

[173] M.L. Verma, S. Kumar, A. Das, J.S. Randhawa, M. Chamundeeswari, Chitin and chitosan-based support materials for enzyme immobilization and biotechnological applications, Environ. Chem. Lett. 18 (2020) 315–323. https://doi.org/10.1007/S10311-019-00942-5/METRICS.

[174] M. Zoumpanioti, P. Parmaklis, P.D. De María, H. Stamatis, J. V. Sinisterra, A. Xenakis, Esterification reactions catalyzed by lipases immobilized in organogels: Effect of temperature and substrate diffusion, Biotechnol. Lett. (2008). https://doi.org/10.1007/s10529-008-9734-1.

[175] M. Zoumpanioti, E. Merianou, T. Karandreas, H. Stamatis, A. Xenakis, Esterification of phenolic acids catalyzed by lipases immobilized in organogels, Biotechnol. Lett. (2010). https://doi.org/10.1007/s10529-010-0305-x.

[176] M. Harold, M. James, H. Nicholas, J. Wiley, Basic Gas Chromatography Qualitative and Quantitative, (2021). https://books.google.com/books/about/Basic_Gas_Chromatography.html?hl=el&id=VimjDwAAQBAJ (accessed January 24, 2024).

[177] L. Bartosova, J. Bajgar, Transdermal Drug Delivery In Vitro Using Diffusion Cells, Curr. Med. Chem. 19 (2012) 4671–4677. https://doi.org/10.2174/092986712803306358.

[178] R.S. Nair, B. Manickam, T.M. Sheng, Design and evaluation of Chitosan-HPMC polymeric films for transdermal delivery of captopril, Indian Drugs. 57 (2020) 69. https://doi.org/10.53879/ID.57.06.12317.

[179] D. Datta, D.S. Panchal, V.V.K. Venuganti, Transdermal delivery of vancomycin hydrochloride: Influence of chemical and physical permeation enhancers, Int. J. Pharm. 602 (2021) 120663. https://doi.org/10.1016/J.IJPHARM.2021.120663.

[180] S. Sangboonruang, N. Semakul, M.A. Obeid, M. Ruano, K. Kitidee, U. Anukool, K. Pringproa, P. Chantawannakul, V.A. Ferro, Y. Tragoolpua, K. Tragoolpua, Potentiality of Melittin-Loaded Niosomal Vesicles Against Vancomycin-Intermediate Staphylococcus aureus and Staphylococcal Skin Infection, (2021). https://doi.org/10.2147/IJN.S325901.

[181] Siddaramaiah, P. Kumar, K.H. Divya, B.T. Mhemavathi, D.S. Manjula, Chitosan/HPMC polymer blends for developing transdermal drug delivery systems, J. Macromol. Sci. - Pure Appl. Chem. 43 (2006) 601–607. https://doi.org/10.1080/10601320600575231.

7. Published scientific papers

nanomaterials

MDPI

Article

Structural Study of (Hydroxypropyl)Methyl Cellulose Microemulsion-Based Gels Used for Biocompatible Encapsulations

Evdokia Vassiliadi [1,2], Evgenia Mitsou [1], Spyridon Avramiotis [1], Christos L. Chochos [1], Franz Pirolt [3], Martin Medebach [3], Otto Glatter [4], Aristotelis Xenakis [1] and Maria Zoumpanioti [1,*]

1 Institute of Chemical Biology, National Hellenic Research Foundation, 48, Vassileos Constantinou Ave., 11635 Athens, Greece; evassiliadi@eie.gr (E.V.); emitsou@eie.gr (E.M.); spavramiotis@yahoo.com (S.A.); chochos@eie.gr (C.L.C.); arisx@eie.gr (A.X.)

2 Laboratory of Biotechnology, Department of Biological Applications and Technologies, University of Ioannina, 45110 Ioannina, Greece

3 Anton Paar GmbH, Anton Paar Straße 20, 8054 Graz, Austria; franz.pirolt@anton-paar.com (F.P.); martin.medebach@anton-paar.com (M.M.)

4 Institute of Inorganic Chemistry, Graz University of Technology, Stremayrgasse 9, 8010 Graz, Austria; otto.glatter@uni-graz.at

* Correspondence: mariaz@eie.gr; Tel.: +30-210-727-3796

Received: 29 September 2020; Accepted: 30 October 2020; Published: 5 November 2020

Abstract: (Hydroxypropyl)methyl cellulose (HPMC) can be used to form gels integrating a w/o microemulsion. The formulation in which a microemulsion is mixed with a hydrated HPMC matrix has been successfully used as a carrier of biocompatible ingredients. However, little is known about the structure of these systems. To elucidate this, scanning electron microscopy was used to examine the morphology and the bulk of the microemulsion-based gels (MBGs) and small-angle X-ray scattering to clarify the structure and detect any residual reverse micelles after microemulsion incorporation in the gel. Electron paramagnetic resonance spectroscopy was applied using spin probes to investigate the polar and non-polar areas of the gel. Furthermore, the enzyme-labelling technique was followed to investigate the location of an enzyme in the matrix. A structural model for HPMC matrix is proposed according to which, although a w/o microemulsion is essential to form the final gel, no microemulsion droplets can be detected after incorporation in the gel. Channels are formed by the organic solvent (oil), which are coated by surfactant molecules and a water layer in which the enzyme can be hosted.

Keywords: scanning electron microscopy (SEM); small angle X-ray scattering (SAXS); electron paramagnetic resonance (EPR); (hydroxypropyl)methyl cellulose (HPMC); lipase

1. Introduction

Gels are defined as three-dimensional macromolecule networks swollen by large amounts of solvent and are divided in different categories according to their ingredients and formation procedure. Their properties allow their use in various fields, including catalysis, drug delivery, and food applications [1–5]. Various gels based on biopolymers have been prepared using alginates, agarose, starch, gelatin, cellulose, chitosan, and their derivatives, as they have exceptional properties combining efficiency and biocompatibility [6,7]. Especially, mixtures of biodegradable and biocompatible polymers belonging to well-known families of natural polysaccharides (such as cellulose, starch, chitin) have already been approved for use in food industry [8].

Cellulose is the most abundant-in-nature, renewable biopolymer. It has excellent thermal and mechanical properties and biocompatibility [9]; therefore, it has been used in a wide range of applications such as tissue engineering, water purification, encapsulation, and delivery of biocompatible ingredients and as the Supporting Material for immobilizing enzymes. In most cases, cellulose derivatives are used [10,11], because of their physico-chemical properties [12–14]. Especially, methylcellulose (MC) and hydroxypropyl-methylcellulose (HPMC) are considered the principal cellulose derivatives [15]. HPMCs are non-ionic cellulose derivatives with methyl (hydrophobic) and hydroxypropyl (hydrophilic) groups added to the anhydro-glucose backbone. HPMCs are water-swelling polymers that provide their promissory usage as vehicles for encapsulation of active ingredients, serving at the same time as humidity absorption agents [16].

The combination of microemulsions and gels [17,18] led to the so-called microemulsion-based organogels (MBGs), which were first reported in 1986 by the groups of Eicke [19] and Luisi [20]. Later, new systems were proposed by our group [21,22], where the combination of a microemulsion and a gel based on HPMC, created very promising MBGs [2]. Several variations of the MBGs have since been prepared, combining HPMC with different ingredients. The microemulsion used can be based on natural surfactants such as lecithin [2,22], the organic solvent can be a vegetable oil or other biocompatible oil [2], and the encapsulated ingredients can be drugs [2], enzymes [23], or other bioactive compounds. Nevertheless, most of the studies were carried out on MBGs formed with an bis-(2-ethylhexyl)sulfosuccinate sodium salt (AOT) in isooctane microemulsion. For the present structural study, we focused on the latter system since, AOT/HPMC is a well-studied system used in several applications [24], and an enzyme was used as a model-encapsulated molecule. Replacement of these ingredients with biocompatible or even edible ones can offer a possibility to further develop interesting applications in various domains.

Therefore, in the present work HPMC-based MBGs were studied in order to clarify their structural properties. Scanning electron microscopy (SEM) was used to examine the morphology of the MBGs and small angle X-ray scattering (SAXS) to detect any residual reverse micelles after microemulsion incorporation in the HPMC matrix and clarify its structure. Moreover, electron paramagnetic resonance (EPR) spectroscopy was applied using hydrophilic, amphiphilic as well as hydrophobic spin probes to investigate the polar and non-polar areas. The enzyme-labelling technique was also followed to investigate the location of the enzyme in the immobilization matrix. The necessity of the presence of an enzyme-carrying microemulsion was tested following an esterification reaction.

Finally, the results were combined to propose a structural model for HPMC MBGs.

2. Materials and Methods

Materials: Lipase from *Candida rugosa* Type VII (specific activity of 724 U mg^{-1}; 1 U corresponds to the amount of enzyme, which hydrolyzes 1 microequivalent of fatty acid from a triglyceride per hour at pH 7.2 and 37 °C), bis-(2-ethylhexyl)sulfosuccinate sodium salt (AOT), (hydroxypropyl)methyl cellulose (HPMC) (3600–5500 cP), lauric acid as well as the iodoacetamido-TEMPO, and 4-Nitrophenyl butyrate (p-NPB) were obtained from Sigma, Darmstadt, Germany. The spin probe 4-Hydroxy-2,2,6,6-tetramethylpiperidine-1-oxyl (Hydroxy-TEMPO), the spin-labelled doxylated derivatives 5-doxyl stearic acid (5-(1-oxyl-2,2-dimethyl-oxazolidin) stearic acid; 5-DSA), 16-doxyl stearic acid (16-DSA), 12-doxyl methyl stearate (12-DMS), 10-doxyl nonadecane (10-DN), 5-doxyl decane (5-DD), and the spin label 4-(2-iodoacetamido)-2,2,6,6-tetramethyl-1-piperidinyloxy (4-(2-iodoacetamido)-TEMPO) were obtained from Sigma, Darmstadt, Germany. All other reagents were of the highest commercially available purity.

2.1. HPMC MBGs Formulation

HPMC gels based on AOT-microemulsions were prepared, as described elsewhere [22]. The weight composition of the studied HPMC-based MBGs ranged in terms of HPMC content, w_o and H_2O. In a typical experiment, 1 mL of AOT microemulsion (w_o = 15) was prepared by adding the

appropriate amount of 0.05 M Tris-HCl buffer or lipase solution to a 0.2 M AOT in isooctane solution. The microemulsion was then added to a mixture of 1 g HPMC and water (1 to 4 g), which was then vigorously stirred with a spatula until homogeneous.

2.2. Scanning Electron Microscopy (SEM) Measurements

The morphology of the gels was observed via scanning electron microscopy on a field emission scanning electron microscope (FESEM). The JEOL JSM-7610FPlus Field Emission SEM (Tokyo, Japan) combines two proven technologies—a semi-in-lens detector with integrated electron energy filter (r-filter) and an in-the-lens Schottky field emission gun—to deliver ultrahigh spatial resolution with a wide range of probe currents for all applications (1 pA to more than 200 nA). The JSM-7610FPlus offers true 1,000,000× magnification with 0.8 nm resolution at 15 kV (1.0 nm at 1 kV) and unmatched beam stability, making it possible to observe the fine surface morphology of nanostructures. The JSM-7610FPlus successfully integrates a full set of detectors for secondary electrons, backscattered electrons, energy dispersive X-ray spectroscopy (EDS), WDS, STEM, EBSD, and CL. The samples were freeze-dried before analysis and visualized without any sputtering process.

2.3. Electron Paramagnetic Resonance (EPR) Measurements

Electron paramagnetic resonance (EPR) measurements were carried out at ambient temperature, using a Bruker EMX EPR spectrometer (Rheinstetten, Germany) operating at the X-band, and the CW spectra were accumulated using Bruker WinEPR Acquisition Software (Rheinstetten, Germany) for EMX by Bruker Biospin GmbH (Rheinstetten, Germany). Gel samples were placed in an ER 162 TC-Q Tissue cell, Bruker, while aqueous and microemulsion samples were contained in a flat E-248 cell. Typical instrument settings were as follows: center field, 0.3480 T; scan range, 10.0 mT; gain, 5.64×10^4; time constant, 5.12 s; conversion time, 5 ms; modulation amplitude, 0.4 mT; microwave power, 2.147 mW; frequency, 9.8 GHz.

2.3.1. Spin-Probing

In order to obtain a concentration of 10^{-3} M of 5-DSA, 16-DSA, 12-DMS, 10-DN, and 5-DD in the w/o AOT microemulsions, w_o = 15, 1 mL of the microemulsion was added to a tube into which the appropriate amount of amphiphilic or lipophilic probe had previously been deposited. This was obtained by placing 10 µL of a stock probe solution in ethanol (7.8×10^{-3} M) in the tube and by further evaporating the ethanol. The same concentration was used for the hydrophilic Hydroxy-TEMPO, which was diluted in water. After gel preparation, the final probe concentration in the systems was 3.5×10^{-5} g to 1.4×10^{-4} g of spin probe per 1 g of gel. In the microemulsions that were used as a reference system, a concentration of 5×10^{-4} M of the probe was used, for comparison reasons.

2.3.2. Spin-Labeling Lipase

The lipase from *C. rugosa* was spin-labelled by the iodoacetamido-TEMPO in a 0.05 M Tris-HCl buffer, pH 7.5 at 25 °C. For this, 45 mg of *C. rugosa* lipase was dissolved in 1.5 mL of 0.05 M Tris-HCl buffer; pH 7.5. Twenty microliters of iodoacetamido-TEMPO 5.3 mM in acetonitrile were added. The reaction mixture was gently agitated for 12 h. The unreacted spin label was removed by extensive dialysis against 0.05 M Tris-HCl buffer, pH 7.5. The spin-labelled enzyme solution was then removed from the dialysis bag and stored in a freezer. A control sample was prepared following the same procedure without the spin-label reagent.

The efficiency of the enzyme spin-labeling was measured by monitoring the loss of lipase catalytic activity towards the hydrolysis of p-Nitrophenylbutyrate (p-NPB). For this purpose, enzyme solution was prepared by adding 30 µL of free or labelled *C. rugosa* lipase in 50 mM Tris/HCl buffer, pH = 8. For the hydrolysis reaction a solution of 1.5 mg p-NPB in 5 mL 2-propanol was added at a ratio 1:9 to the solution of 0.1 g Triton X-100 and 0.025 g Arabic gum containing the enzyme (27 µL). The rate of p-NPB hydrolysis catalyzed by the lipase was followed spectrophotometrically by means of the

produced p-nitrophenol (pNP) absorbance at 410 nm. Values reported correspond to the production of pNP versus time. Experiments were performed at room temperature.

2.3.3. Interpretation of the EPR Data

The WinEPR Processing program was used for the processing of EPR experimental spectra. The results reported in this work were analyzed in terms of rotational correlation time, τ_R, order parameter, S, and hyperfine splitting constant, A_N. The above-mentioned parameters can monitor the dynamics of a spin probe in membranes or in viscous media and the polarity of the microenvironment as sensed by the spin probe molecules [25–29]. The simulations of the EPR spectra were performed using programs in the MATLAB platform (MathWorks), employing the EasySpin toolbox in order to acquire the optimal sample's τ_R. For the slow-motion regime EPR spectra simulations as well as the fast-motion regime EPR spectra simulations, the "chili" function and the "garlic" function were selected, respectively [30,31]. For the EPR spectra of 10-DND and the spin-labelled enzyme, a two-component analysis computation was used through EasySpin simulations. Simulation of experimental EPR spectra were decomposed into components using SimLabel, a program working on the MATLAB platform, which employs the EasySpin chili function [32]. More details can be found in the Supporting Information section.

2.4. Small-Angle X-ray Scattering (SAXS) Measurements

The SAXS experiments were performed on a SAXSpoint 2.0 camera, Anton Paar, Graz, Austria. The equipment is operated at 50 W (50 kV/1 mA) with a Primux 100 microsource, using Cu Kα radiation (λ = 0.1542 nm). The X-ray beam was collimated by scatterless slits. The samples were measured in transmission, and the scattered signal was collected by a 2D Eiger R 1M hybrid photon counting (HPC) detector with 75 μm^2 pixel size. The investigated q range was 0.055–5.2 nm^{-1}. q is defined by $q = 4\pi (\sin \theta)/\lambda$, with 2θ being the scattering angle with respect to the incident beam and λ the wavelength of the X-rays. The exposure time for each sample was 10 min. Microemulsions were measured in a 1 mm diameter quartz capillary, and MBG samples were measured in a multiple paste holder (Kapton windows). All measurements were performed at 25 °C. The measured scattering curves were corrected for transmission losses and put on absolute scale.

3. Results

HPMC MBGs have been successfully used as biocatalysts [24] or as drug carriers [2]. In both cases, it has been observed that the nature and amount of each ingredient influences the catalytic activity and the release profile of the encapsulated compound, respectively. A characteristic example has been reported [24], where the different water concentrations affect the efficiency of the system by means of catalytic activity. Those alterations of the gel's composition are able to cause changes to the structure, thus creating the urge to understand the morphology of the HPMC MBGs. The structural study can offer an insight on how each component affects the final matrix and therefore the behavior and properties of the system. In addition, an extensive structural characterization will contribute to the rational development of various systems according to the application.

3.1. Catalytic Activity

Previous works have demonstrated that the HPMC-based MBGs hosting lipases are excellent biocatalysts [33–35]. In order to investigate the contribution of the microemulsion in the final catalyst, three different systems were prepared using 1 g HPMC, 2 g H_2O with or without 1 mL of AOT microemulsion (0.2 M, w_o = 7.5). For the first system, the enzyme was added in the microemulsion, which was then mixed with the HPMC/water mixture. In the second one, the enzyme was added in the water used to dissolve HPMC prior to the addition of the microemulsion, whereas in the third one, there was no microemulsion in the gel. The total amount of the enzyme in each system was 0.3 mg. The experimental protocol was designed aiming to observe the differences of the

encapsulated and "free" lipase inside the matrix. The results are shown in Figure 1. It can be noted that in the absence of a microemulsion, the enzyme is practically inactive. Then, the activity is much more important when the enzyme is included in the microemulsion when added to the MBG than when it is added separately. Obviously, the enzyme is in need of the microemulsion ingredients. This can be attributed to the surfactants that create protected surfaces between the organic and water domains. Furthermore, the necessity of the microemulsion as a carrier of the enzyme in the final system is essential, as the enzyme does not come in contact with the organic phase, which would lead to the protein denaturation.

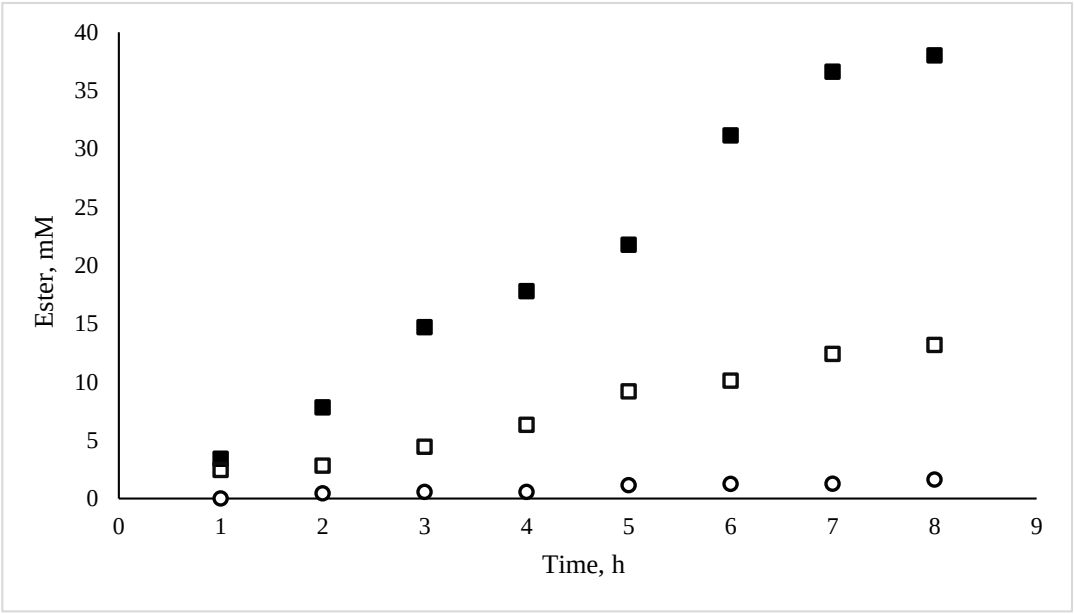

Figure 1. Effect of microemulsion-based gels (MBG) preparation on the rate of propyl laurate synthesis, catalyzed by *C. rugosa* lipase. [1-propanol], [lauric acid]: 100 mM, each; isooctane as solvent (10 mL); *C. rugosa* content per MBG 0.3 mg. (■): (hydroxypropyl)methyl cellulose (HPMC)-based MGB; (□): HPMC matrix with the enzyme and the microemulsion added separately; (○): HPMC matrix with the enzyme (no microemulsion).

3.2. Morphological Analysis

Three HPMC-based MBGs were studied with different weight compositions (Figure 2), namely, System A containing 71% *w/w* water, System B containing 55% *w/w* water, and System C containing 43% *w/w* water. The exact compositions of the systems are shown in Table 1. Since HPMC with microemulsion forms a gel matrix within a narrow window of polymer mass fraction [22], the systems studied here have been chosen to represent the whole range of polymer/water ratios that can lead to final gel matrix formation. It should be mentioned here that the chosen systems have been used in previous studies that determined the state of water that they contain [36].

Table 1. Weight composition of the studied HPMC-based MBGs.

MBG	HPMC	H_2O	μE
		% *w/w*	
System A	18	71	11
System B	28	55	17
System C	44	43	13

μE = AOT/isooctane microemulsion.

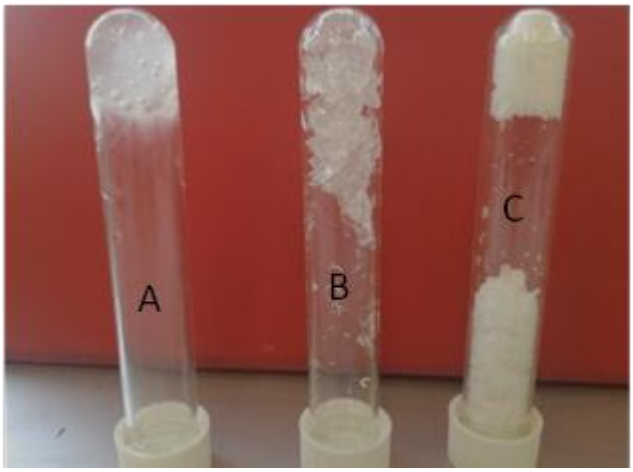

Figure 2. HPMC-based MBGs of different water content. System A: HPMC = 18% *w/w*, H_2O = 71% *w/w*, μE = 11% *w/w*; System B: HPMC = 28% *w/w*, H_2O = 55% *w/w*, μE = 17% *w/w*; System C: HPMC = 44% *w/w*, H_2O = 43% *w/w*, μE = 13% *w/w*. μE: AOT microemulsion w_o = 15. Tubes are reversed to visualize their sticky shape.

The morphology of the different systems was observed via SEM images revealing the formation of a three-dimensional network. In order to monitor the role of each component of the microemulsion on the gel structure, images were taken for HPMC/water mixture without any organic solvent. Then pure isooctane was added to a HPMC/water mixture corresponding to System A, and finally, AOT microemulsion was used as the organic component to form System A. A comparison of the images taken for the freeze-dried systems reveals that when no organic solvent is used the matrix appears to be compact, without a network of pores (Figure 3a). When isooctane is added, the appearance of pores in the coherent, otherwise, material can be observed (Figure 3b). This could be attributed to the fact that the organic solvent congregates in the surrounding polar environment assembling enclaves that after freeze-drying leave the observed pores. The addition of micelles in the organic solvent by using microemulsion instead of pure isooctane, leads to a more porous matrix, although the water content does not change (Figure 3c). The effect of water content was also studied. For the three systems studied, namely Systems A, B, and C, the images are shown in Figure 3c–e, respectively. As can be seen, the addition of water facilitates the appearance of pores. Increasing water, the pores population increases (Figure 3e to 3c, respectively) until a sponge-like structure can be seen for the system with 71% *w/w* water (System A, Figure 3c). We can also notice a broadening of the pores for the system with higher water content. Similar results for the structural investigation of gelatin MBGs were also observed by Dandavate and Madamwar. Gelatin MBGs showed pore widening after use, which was attributed to the accumulation of water molecules that cause swelling of the assumed coexisting w/o microemulsion droplets [37].

Moreover, the influence of the surfactant concentration was studied for System B based on microemulsion with 0.1 M or 0.2 M AOT concentration (Figure 3d,f). As can be seen, when the surfactant concentration is higher the gel appears to have a more uniform network consisting of more, smaller, and evenly distributed pores. The same effect of smooth and uniform network formation was observed over the addition of polyethylene glycol (PEG) on gelatin MBGs [38].

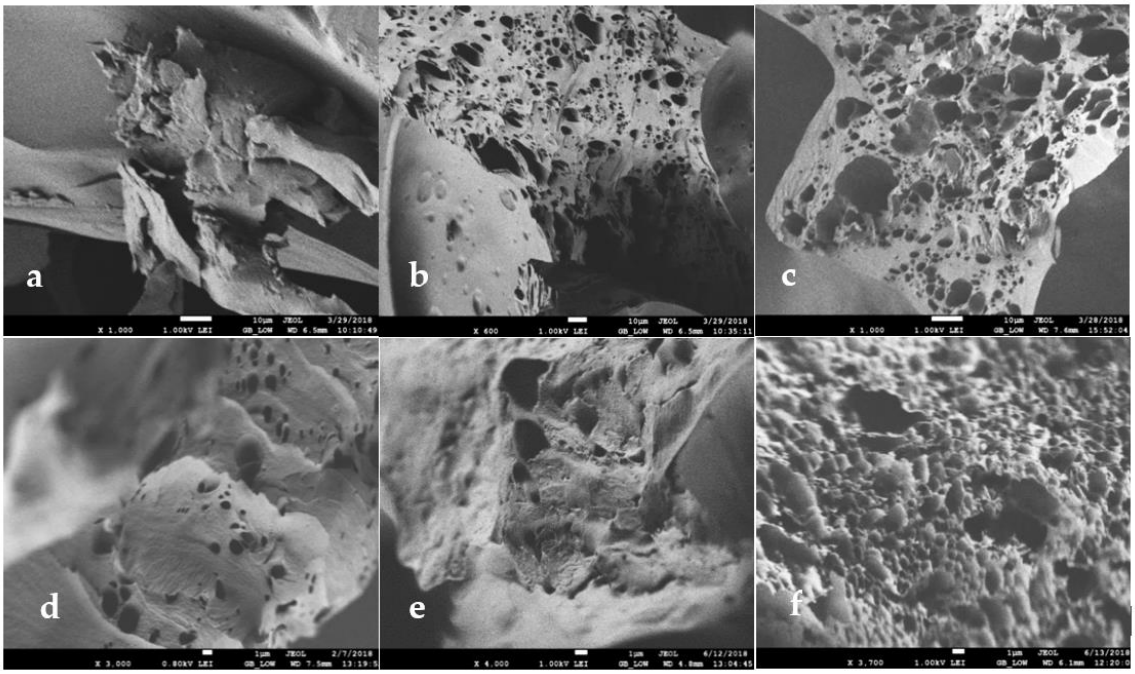

Figure 3. SEM images of freeze-dried HPMC-based MBGs. (**a**) System A prepared without organic components; (**b**) System A prepared with isooctane; (**c**) System A prepared with 0.1 M AOT μE; (**d**) System B prepared with 0.1 M AOT μE; (**e**) System C prepared with 0.1 M AOT μE; (**f**) System B prepared with 0.2 M AOT μE. μE = microemulsion.

3.3. Interfacial Properties

In order to study the properties of the interfaces as well as the polar or non-polar areas of the constructed gels, Electron paramagnetic resonance (EPR) spectroscopy was engaged using different probes, polar, non-polar, and amphiphilic ones.

3.3.1. Hydrophilic Spin-Probe

The hydrophilic probe Hydroxy-TEMPO was used to study the properties of the polar areas of the MBGs. For this purpose, the probe was dissolved (a) in the water pools of the microemulsion, which was then added to the HPMC/water mixture or (b) in the water used to hydrate HPMC prior to the addition of the microemulsion. The following reference systems were chosen: (i) microemulsions formed with water and 0.1 M or 0.2 M AOT, with w_o = 15 or w_o = 7.5, respectively, (ii) HPMC/water mixtures (ratios corresponding to Systems A, B, and C), and (iii) HPMC with water and isooctane (without AOT). The results are presented in Table 2. As Table 2 shows, the A_N parameter value obtained in microemulsion ((AOT) = 0.1 M, w_o = 15) reflects a less polar microenvironment comparing the one obtained in water. A lower hyperfine splitting constant value also occurs when a different microemulsion is used ((AOT) = 0.2 M, w_o = 7.5). This can be attributed to the different nature of the water molecules that form the microemulsion's water pools, comparing to the ones in bulk water [39,40]. On the other hand, τ_R values calculated for the spin-probe Hydroxy-TEMPO molecules in both microemulsions used showed lower mobility, since they are higher than the value obtained in aqueous solution. This reflects the existence of bound water in the microemulsion's water core.

Table 2. τ_R and A_N values of hydrophilic spin-probe Hydroxy-TEMPO in water, AOT microemulsions, and HPMC-based MBGs systems.

Hydrophilic Probe Hydroxy-TEMPO		
System	**τ_R, ns**	**A_N, 10^{-4} T**
Water	0.03 ± 0.00	17.49 ± 0.04
System A*	0.07 ± 0.01	17.29 ± 0.11
System B*	0.15 ± 0.01	17.25 ± 0.03
System C*	0.40 ± 0.01	17.07 ± 0.04
System C**	0.40 ± 0.06	17.07 ± 0.03
(AOT) = 0.1 M μE w_o = 15	0.13 ± 0.01	16.25 ± 0.02
(AOT) = 0.2 M, μE w_o = 7.5	0.21 ± 0.01	15.84 ± 0.01
Probe incorporated in the HPMC-based MBGs via *the AOT microemulsion*		
System A	0.06 ± 0.01	17.31 ± 0.01
System B	0.14 ± 0.01	17.21 ± 0.02
System C	0.40 ± 0.01	17.14 ± 0.01
System C†	0.40 ± 0.06	17.11 ± 0.05
Probe incorporated in the HPMC-based MBG via *the HPMC/water mixture*		
System A	0.08 ± 0.01	17.35 ± 0.04
System B	0.15 ± 0.02	17.22 ± 0.03
System C	0.38 ± 0.03	17.11 ± 0.02

Systems A*, B*, and C*: mixtures of HPMC and water at ratios that correspond to the Systems A, B, and C, respectively; System C**: mixture of HPMC, water, and isooctane at ratios that correspond to System C; System C†: System C prepared with 0.2 M AOT microemulsion.

A remarkable increase in immobilization of the hydrophilic spin probe occurs when incorporated into the gel via solubilization in the microemulsion. Immobilization, as expressed by τ_R values, increased when the water content of the gel decreased from 71% to 55% and to 43% *w*/*w*, respectively (Systems A, B and C), while at the same time, the polarity as expressed by hyperfine splitting constant decreased. Quite similar τ_R and A_N values occurred for System C independently on the microemulsion used (Table 2, Systems C and C†).

Table 2 also shows the corresponding τ_R and A_N values for the same spin-probe incorporated in the gels prior the addition of the microemulsion. Comparing the obtained values, it becomes obvious that the microenvironment polarity as "sensed" by the hydrophilic spin probe as well as its mobility are quite similar in both cases, when the spin probe molecules are either incorporated in the water pool of the AOT microemulsion used for the construction of the gel or incorporated directly in the "outer" water. The polarity slightly decreased when the water content of the gel decreased, and the calculated values are much higher than the ones calculated in the microemulsion. The values obtained for gels with the same water content can be considered equal within experimental error, regardless how the spin-probe was incorporated in them. In addition, both τ_R and A_N values of this hydrophilic spin probe indicate a linear dependence on the amount of water as can be seen in Supporting Information Figures S1 and S2. Furthermore, the values of the τ_R and A_N for the same spin-probe in the HPMC/water or HPMC/water/isooctane mixtures (Systems A*, B*, C*, and C**) follow a similar pattern showing similar behavior.

This finding gives strong evidence that no form of microemulsion droplets exist after the addition of the microemulsion in the HPMC/water mixture, and consequently, the micellar water is mixed with the "outer" water and absorbed by the HPMC network.

3.3.2. Amphiphilic Spin-Probes

Table 3 presents the τ_R, S, and A_N values obtained when the amphiphilic spin-probe molecules 5-DSA and 16-DSA were incorporated in the three HPMC-based MBGs examined. These spin-probes were incorporated in the gels via the AOT microemulsion, where they were previously solubilized. The calculated values shown in Table 3 for both probes correspond to the expected locations of n-DSA

molecules located in the interface of w/o microemulsions, where n refers to the carbon atom of the fatty acid to which the doxy1 group is anchored. Indeed, for 5-DSA molecule where the paramagnetic group is closer to the carboxyl group, i.e., deeper in the water/oil interface, a stronger mobility restriction is evident giving higher τ_R and S values, while being closer to the water core leads to higher A_N values [3,41].

Table 3. τ_R, S, and A_N values of amphiphilic spin-probes 5-doxyl stearic acid (5-DSA) and 16-doxyl stearic acid (16-DSA) in AOT microemulsion (μE) and HPMC MBGs.

Amphiphilic Probes						
System	**5 DSA**			**16 DSA**		
	τ_R, **ns**	S	A_N, 10^{-4} **T**	τ_R, **ns**	S	A_N, 10^{-4} **T**
μE w_o = 15	3.45 ± 0.10	0.29 ± 0.02	15.06 ± 0.03	0.07 ± 0.01	0.06 ± 0.01	14.39 ± 0.08
μE w_o = 7.5	2.30 ± 0.08	0.14 ± 0.01	14.01 ± 0.05	0.09 ± 0.02	0.09 ± 0.01	14.26 ± 0.06
System A	6.02 ± 0.47	0.49 ± 0.03	15.08 ± 0.12	0.95 ± 0.01	0.05 ± 0.01	14.97 ± 0.02
System B	6.57 ± 0.05	0.55 ± 0.01	15.37 ± 0.05	1.39 ± 0.05	0.07 ± 0.01	14.85 ± 0.01
System C	6.96 ± 0.14	0.61 ± 0.03	15.69 ± 0.17	3.31 ± 0.04	0.17 ± 0.01	14.21 ± 0.14

Figure 4 shows the experimental and the simulation spectra of 5-DSA in AOT microemulsion and in Systems A, B, and C. More pronounced immobilization (τ_R) occurred when amphiphilic spin probes were involved. As can be seen in Figure 4, the alterations of spectrum characteristics are obvious. The observed differences between spectra obtained in microemulsion and in MBGs can be attributed to the immobilization of the spin probe in the AOT layer in the gel matrix. As the gel water content decreased, Figure 4b–d, the outer hyperfine splitting, $2A_{max}$, increased, while the $2A_{min}$ decreased. τ_R values appear to have a drastic increase when the microemulsion is incorporated in the HPMC/water matrix (Table 3) corresponding to the slow-motion regime. The order parameter value, S, is also increased, due to the highly ordered arrangement of the amphiphilic probe molecules among the surfactant molecules. This gradually increasing high-ordered state occurs both at that depth of the interface corresponding to the 5th carbon atom (5-DSA) and to the 16th carbon atom (16-DSA), as it can be seen in Table 3. It is also clear that the τ_R and S calculated values for 16-DSA in the final gels are much lower than the corresponding values for 5-DSA; therefore, 16-DSA molecules are less restricted. This could be explained by the closer location of the paramagnetic ring of 16-DSA to the oily phase than the carbon chains of AOT and 5-DSA. The calculated values for both probes follow the same pattern; however, for 16-DSA, they correspond to the fast motion regime. Spectra of 16-DSA can be seen in Supporting Information Figure S3.

The calculated polarity of the microenvironment of the paramagnetic ring of 5-DSA and 16-DSA as expressed by A_N values (Table 3) follows a different pattern, as the water decreases in the MBGs. More specifically, the hyperfine splitting constant issued from the 5-DSA spectra increases, while the one corresponding to 16-DSA decreases. Plots of the above mobility (τ_R) and hyperfine splitting constant (A_N) data of the amphiphilic probes versus the water content appear to follow linearity for the 5-DSA, while the ones for 16-DSA deviate remarkable from linearity. The behavior of 16-DSA is similar to the one of the lipophilic probes, the alkane 5-DD (Supporting Information Figures S1, S2, and S4).

Given the strong binding of the polar head –COOH of both DSA's with the water molecules, in the case of 5-DSA, the paramagnetic ring is closer to water molecules, and the results indicate that it "senses" an increased polarity, showing a smaller distance between the hydrophobic tails of AOT. As water reduces progressively from Systems A to C, the water/isooctane interface seems more rigid, giving remarkably less freedom in the probe's mobility and the two amphiphilic probes tend to detect quite different polarity regarding the position of the paramagnetic ring on their aliphatic chain. This can be explained if we assume a tight, almost parallel arrangement of the surfactant molecules, which is in agreement with the assumption of channel formation of AOT layers.

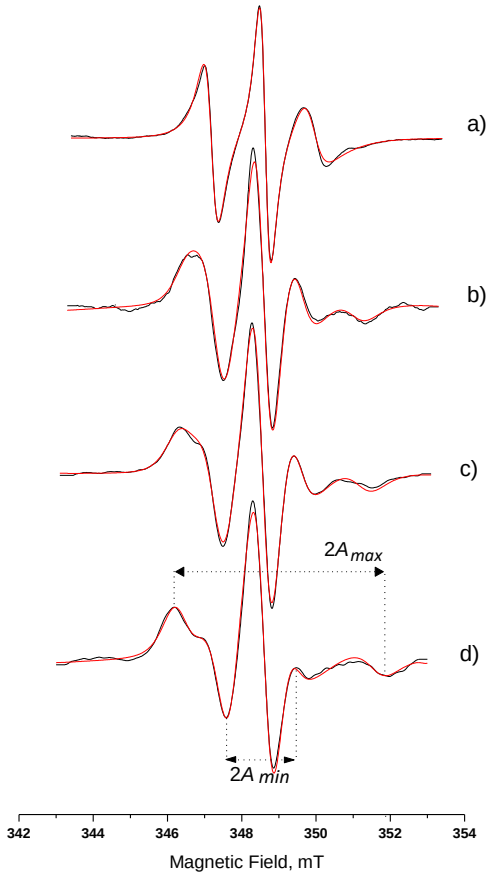

Figure 4. Spectra of 5-DSA in (**a**) AOT microemulsion w_o = 15; (**b**) System A; (**c**) System B; (**d**) System C. Black line, experimental; red line, simulation. (A_{max} and A_{min} as described in the Supporting Information section).

3.3.3. Lipophilic Spin-Probes

In order to examine the role of the organic phase, i.e., isooctane introduced through the AOT-isooctane microemulsion into the HPMC-based MBGs, three lipophilic spin probes were followed, namely, 10-doxyl nonadecane (10-DND), 5-doxyl decane (5-DD), and 12-doxyl methyl stearate (12-DMS). Considering the two spin-probes, 10-DND and 12-DMS, a quite similar behavior was detected. Figure 5 shows the experimental as well as the relative simulation spectra of 10-DND in AOT microemulsion and in Systems A, B, and C. From these spectra, it can be observed that as the water decreases the spectral characteristics show two main spectral shape alterations. Firstly, the spectrum of 10-DND recorded in the AOT microemulsion is a typical spectrum of nitroxide, showing three equal peaks (first derivate of the original spectrum), which is characteristic of fast molecular motion in a non-polar medium, in the EPR spectroscopy time scale. When 10-DND was embedded in the final gel structure, the three peaks became progressively (i) unequal and (ii) in different position as regards the base line, i.e., a scale shape. The arrows in Figure 5 show spectral characteristics that indicate immobilization as the water decreases (broadening in the low field—splitting in the high field), and this is more pronounced when the water content is low (System C). For the 10-DND spectra analysis, we applied computer-aided (MATLAB/EasySpin/SimLabel) single component simulation. When this probe was embedded in the AOT microemulsion and System A, the calculated rotational correlation time, τ_R, values were 0.06 ns and 0.88 ns, respectively (Figure 5a,b). However, when the probe was embedded in Systems B and C a two-component analysis gave more consistent results during the fitting process. The rotational correlation time, τ_R, calculated values for System B were 1.45 ns and 5.86 ns for the mobile (22%) and the immobile component (78%) (Figure 5c). The τ_R calculated values for System C were 3.59 ns and 6.43 ns

for the mobile (21%) and the immobile component (79%), respectively (Figure 5d). Simulation trials using two-component analysis for System A gave a 92% mobile component with τ_R, value 0.08 ns and an 8% immobile component with τ_R, value 8.43 ns. These results give evidence of a dramatic alteration of the structure of the final gel systems between System A on one hand and B, C on the other hand. The calculated hyperfine splitting constant values, A_N, as "sensed" by the 10-DND probe were 14.14 ± 0.04 × 10^{-4}, 13.9 ± 0.03 × 10^{-4}, 14.01 ± 0.02 × 10^{-4}, and 14.12 ± 0.03 × 10^{-4} for the AOT microemulsion and the three systems A, B, and C, respectively.

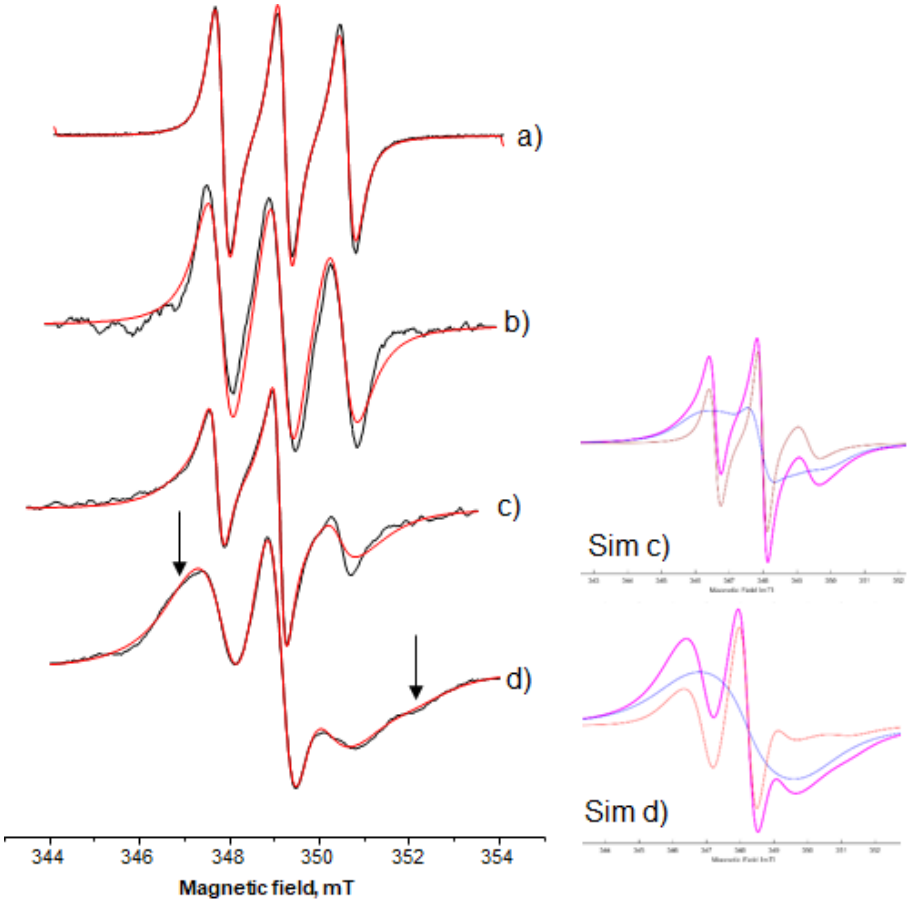

Figure 5. Ten-doxyl nonadecane (10-DND) in (**a**) AOT microemulsion w_o = 15; (**b**) System A; (**c**) System B; (**d**) System C. Black line, experimental; red line, simulation. In the inserts show the simulations (violet line) of the spectra (**c**) and (**d**) (Sim (c) and Sim (d), respectively) and the analysis of its components (mobile: orange line, immobile: blue line).

The second characteristic is indicative that, as the water decreases, the spin system undergoes an increasing spin–spin interaction [42]. This is a result of high local spin probe concentration or partially molecular aggregation of the spin probes. This is confirmed by the simulation analysis of the spectra shown in Figure 5c,d. The immobile component is also reflecting the accumulated 10-DND molecules (Figure 5, the blue line of the decomposed spectra).

The spectra of the second hydrophobic spin probe, namely, 5-doxyl decane (5-DD) recorded in the same systems, follow a different pattern. This smaller molecule also shows gradual immobilization in the fast motion region but did not show high local concentration. More specifically, the rotational correlation time, τ_R, values calculated were 0.03 ns, 0.62 ns, 1.26 ns, 2.52 ns; the order parameter, S, values were 0.04, 0.06, 0.08, 0.17; and the measure of hyperfine splitting constant, A_N, values were 14.36 × 10^{-4} T, 14.67 × 10^{-4} T, 14.5 × 10^{-4} T, 14.05 × 10^{-4} T in the AOT microemulsion and in Systems A, B, and C, respectively.

This deferent behavior of the two lipophilic probes is interesting and can be explained by the assumption that a remarkable part of the organic solvent, i.e., the isooctane molecules, is absorbed through the HPMC-based MBG lattice in the hydrophobic regions of propyl- and methyl-groups of the HPMC molecules. This absorption is most effective when water content is low (Systems B and C). A similar result was reported for gelatin–AOT organogels [43]. The larger molecules of 10-DND and 12-DMS probably cannot diffuse through the HPMC/water matrix and therefore are accumulated inside the channels of the remaining organic solvent, while the smaller molecule of 5-DD preferably follows the behavior of isooctane. The relative indicative spectra for the 5-DD and the 12-DMS are presented in the Supporting Information section, Figures S3 and S4.

3.3.4. Spin-Labelled Lipase

While these gels have been used as immobilization matrices for several lipases, among which is the lipase VII from *Candida rugosa*, their structure and the location of the enzyme is yet to be described. In order to investigate the possible conformational changes in the lipase and to clarify its location when immobilized in the gels, the spin-labelling technique was applied and followed by EPR spectroscopy using the iodoacetamido-TEMPO as a spin label. The iodoacetamide group has an iodine leaving group and attaches rather selectively to thiol groups, -SH, which are present in cysteine residues, forming a stable irreversible thioether bond. Spin labelling of other amino acids cannot be excluded if the reagent is in excess and in acidic pH. The chosen lipase has five cysteine residues at the positions 60, 97, 217, 268, and 277. Four of them are linked as pairs by a disulfide bridge, Cys60-Cys97 and Cys268-Cys277, while Cys217 is a single cysteine residue with the free -SH group, not bound with an S-S bridge [44–46]. Enzyme labelling was verified following the hydrolysis of p-NPB. The labelled enzyme lost 80% of its activity, while the non-labelled enzyme that followed the same treatment lost only 20% of activity.

Figure 6 shows the spectra of (a) free spin-label recorded in aqueous solution and spin-labelled lipase recorded in (b) aqueous solution, (c) AOT microemulsion w_o = 15, (d) System A, (e) System B. The respective calculated relative τ_R, S, and A_N values are presented in Table 4. The spectrum characteristics of the free spin label in water (Figure 6a), showing three narrow peaks of equal height, is indicative of highly fast movement. The spectrum of the labelled enzyme in aqueous solution, Figure 6b, shows an "immobilized" part and a "mobile" one (indicated with arrows). It is assumed that the spin label can be traced in two different states, one strongly bound to the cysteine residue and another one with a weaker bond on the surface of the protein, sensing thus, a different microenvironment [47]. This observation leads us to use a two-component computation analysis. It was calculated that in aqueous solution the immobile component was 44%, while the mobile one was 56%. The calculated S value (0.41) is an overall estimated value for the ordering behavior of the bound on the protein molecule spin label. The calculated A_N value shows an environment less polar than water, however, the polarity is still quite high.

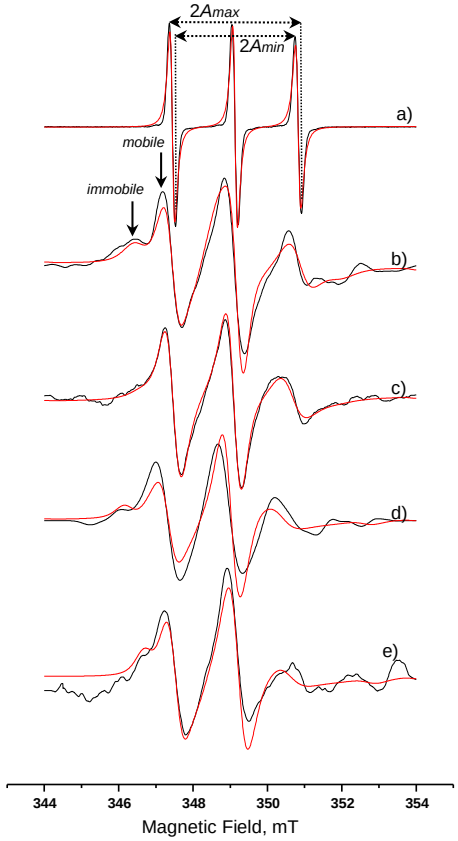

Figure 6. EPR spectra of (**a**) free spin-label iodoacetamido-TEMPO in aqueous solution; and spin-labelled *C. rugosa* lipase in: (**b**) aqueous solution; (**c**) AOT microemulsion w_o = 15; (**d**) System A; (**e**) System B. Black line, experimental; red line, simulation.

Table 4. τ_R, S, and A_N values of free iodoacetamido-TEMPO in water and spin-labelled *C. rugosa* lipase in aqueous solution, AOT microemulsion, and Systems A and B.

Spin-Labelled Lipase from *Candida rugosa*—Iodoacetamide Tempo					
	τ_R, ns			**S**	**A_N, 10^{-4}T**
Free spin label in water	0.06 ± 0.01			0.01 ± 0.01	17.48 ± 0.09
Spin-labelled *Candida rugosa* in aqueous solution					
Two components	Immobile	–	mobile		
	10.83 ns (44%)	–	1.66 ns (56%)	0.41 ± 0.03	17.23 ± 0.14
Spin-labelled *Candida rugosa* in AOT microemulsion, w_o = 15					
Two components	Immobile	–	mobile		
	8.92 ns (20%)	–	1.78 ns (80%)	0.14 ± 0.06	16.00 ± 0.03
Spin-labelled *Candida rugosa* in HPMC-based MBGs					
Two components	Immobile	–	mobile		
System A	19.85 ns (45%)	–	3.16 ns (55%)	0.35 ± 0.04	16.48 ± 0.13
System B	21.87 ns (43%)	–	3.31 ns (57%)	0.39 ± 0.05	16.73 ± 0.08

The spectrum in Figure 6c (spin-labeled lipase in microemulsion) is indicative of a more relaxed form of the enzyme. The peaks at 346 and 353 mT that correspond to the strongly bound spin label almost disappeared. More specifically, the immobile and mobile component ratio is altered to 20% and 80%, respectively, followed by altered rotational correlation time values (Table 4). The increase in the ratio of the relaxed form of the enzyme can be explained considering that the environment in the microemulsion is less polar due to the presence of AOT molecules, and this is in agreement with the

calculated A_N value. It should be noted here that the calculated percentages do not correspond to the actual weight percentages of the two states of the spin label, but they can be considered as the average movement of the spin-label/lipase complex in the AOT microemulsion's water-pool. The *S* value calculated from the spectral characteristics is also lower than the one in aqueous solution, and this confirms the above observations.

When the spin-labelled lipase is incorporated in System A, the spectral characteristics are again indicative of two different states of spin label. From Table 4, we can see that the A_N value lays between the values obtained in aqueous solution and in microemulsion. The values of the rotational correlation time for the immobile and mobile component indicate that a quite strict environment affects the movement of the lipase. The immobilization is also confirmed from the order parameter value S. The spectrum for the spin-labelled lipase in System B (Figure 6e) is similar to the one recorded in System A (Figure 6d). The relative calculated values, as they are reported in Table 4, indicate a higher immobilization as both τ_R values increase with a percentage of 43% and 57% for the two states of the spin label, respectively. The hyperfine splitting constant value, A_N, also lays between the values obtained in aqueous solution and in the microemulsion. It is obvious that the simulation spectra in Figure 6d,e are less well fitted to the relative experimental spectra. Considering the multi-compartmental structure and the variable stiffness of MBGs under investigation, we can say that there are many immobilized states of the lipase molecule and this fact implies more than two states of the anchored spin label. This also consequently results in the increase in the Gaussian participation in the simulation spectra.

Taking into account this study, we can assume that there is evidence that the lipase molecules in both gels tested are preferably located close to the AOT interface. In parallel, less water content in the gel leads to more restricted lipase molecules.

3.4. Small-Angle X-ray Scattering (SAXS) Measurements

SAXS was used to verify whether there are residual reverse micelles after incorporation in the MBGs as well as to clarify our perspective of the MBGs morphology. Data shown in Figure 7 were transmission-corrected and put on absolute scale [48]. The Kapton background was subtracted from the curves of the gel samples. To approach the amount of microemulsion in the MBG, the intensities of the microemulsions have been scaled to 20% scattering intensity (green curves). The microemulsions show clear scattering features of nanometer-sized droplets. These can be analyzed in detail by the indirect Fourier transformation [49]. The microemulsion containing 0.05 M AOT forms spherical micelles of approximately 11 nm in diameter, while the one containing 0.2 M AOT has a mean diameter of approximately 5 nm. This is the reason for the decay at lower q-values for the 0.05 M AOT sample. The comparison of the microemulsions with the corresponding gel samples shows no remaining contribution of the microemulsion signal, confirming, thus, EPR findings.

Of the available models that were tested against SAXS data, the so-called Gel Fit Model (in SasView) was used to gain further knowledge of the gel properties, since this was the model that best fitted our data. Therefore, the data were fit to the Correlation Length Model shown in Equation (1):

$$I(Q) = A/Q^n + C/[1 + (Q\xi)^m] + B \quad (1)$$

The first term describes the Porod scattering from clusters, and the second term is a Lorentzian function describing scattering from polymer chains. The two multiplicative factors A and C, the constant background B, and the two exponents n and m are used as fitting parameters. The final parameter ξ is a correlation length for the polymer chains [50,51], while the Porod and Lorentzian exponents are used for the fractal structure and polymer/solvent interaction, respectively.

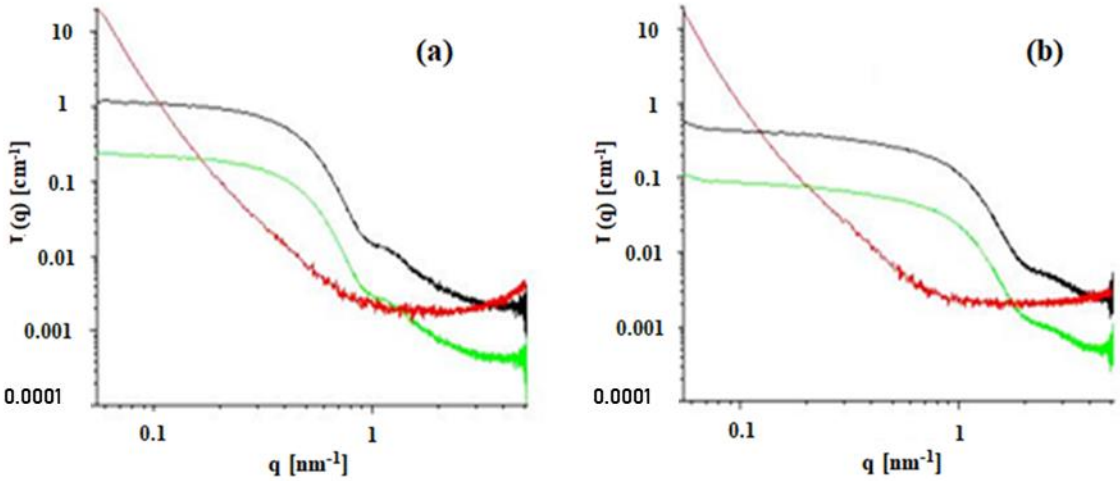

Figure 7. Scattering curves on absolute scale for HPMC-based MBGs (System C, red curves) and microemulsions with 0.05 M (**a**) and 0.2 M (**b**) AOT (black curves). A factor of 0.2 was applied to the microemulsions (green curves) to show the expected contribution of the micellar signal in the gel.

The structural parameters obtained from the Correlation Length Model (Table 5) for the MBGs formed with 0.05 M and 0.2 M AOT microemulsion show that the correlation length (ξ) increases with the increased surfactant concentration. Higher AOT concentration in the microemulsion—and as a result, in the final gel—leads to an increased entanglement length of HPMC, creating an environment of higher stiffness in comparison to the systems prepared with isooctane instead of a microemulsion. The equation's first term (A/Qn) describes the Porod scattering from clusters where the network collapses and forms compact particle-like structures. The Porod exponent (n) values (Table 5) calculated for the HPMC/water mixture in the presence or absence of isooctane are similar. The n value increases when AOT is added via the microemulsion with further increase for higher AOT concentration, indicating increased compactness of the formulated clusters. In contrast, the Lorentz exponent (m) does not change (Table 5), showing that while the compactness of the cluster grows, that of the network remains unchanged. This indicates a stronger effect of AOT on the local nanostructure. The increased compactness of HPMC clusters in MBGs prepared with 0.2 M AOT microemulsion may create an environment, where the organic solvent can be more easily distributed in comparison to the MBGs prepared with 0.05 M AOT, due to the space that the compact clusters leave among them. As a result, the evaporation of the solute prior SEM observations creates the pores, which as mentioned before, are more uniform (Figure 3f).

Table 5. Correlation length, Porod, and Lorentz exponential.

Parameters	System C*	System C**	System C‡	System C†
Correlation length (Å)	44.6	44.1	66.9	71.6
Porod exponent (n)	4.5	4.5	4.8	5.1
Lorentzian exponent (m)	3.0	3.2	2.8	3.1

System C*: mixture of HPMC and water at ratios that correspond to System C; System C**: mixture of HPMC, water, and isooctane at ratios that correspond to System C; C‡: System C prepared with 0.05 M AOT microemulsion; C†: System C prepared with 0.2 M AOT microemulsion.

4. Discussion

The use of HPMC network combined with a microemulsion as a successful enzyme immobilization matrix has led to the investigation of the system's structural characteristics. The fact that those gels have shown a catalytic activity only in the presence of microemulsion, with much better results when the enzyme is introduced to the gel entrapped in the microemulsion rather than separately,

has given the motive to study the structure of such systems in order to gain basic knowledge regarding the use of the biocatalyst. The preparation of such gels differs from the gelatin-based gels studied in the past [19,20,52,53], where the polymer is dissolved in the water of the microemulsion rather than the preparation of a gel that would absorb the microemulsion [35]. Luisi's group [20] prepared MBGs by adding solid gelatin to an already prepared AOT microemulsion. On the other hand, the groups of Eicke [19] and Robinson [52] prepared MBGs by adding an aqueous gelatin solution to an AOT/oil solution. On the contrary, HMPC-based MBGs studied here are prepared by adding AOT microemulsion to an HPMC/water mixture [21,22]. Nevertheless, due to the similarity of application and the use of polymers and microemulsions for the formulation, questions arose about whether the models proposed in the past could also apply to HMPC-based gels.

According to our EPR and SAXS findings, after incorporation in the gel, the microemulsion cannot be detected in the form of reverse micelles. There is no distinction between the aqueous phase of the microemulsion and the water used to hydrate HPMC, therefore, independently of how the water is introduced in the gel matrix, it is rearranged. The use of lipophilic spin probes to obtain EPR spectra leads to the conclusion that the organic solvent seems to congregate. This is obvious not only by the higher immobilization detected, but mainly by the increased local concentration that the longer carbon chain probe molecules exhibit. Moreover, according to the SEM images recorded for HPMC gels in the presence and absence of organic solvent, it becomes obvious that the organic solvent is essential for the formation of pores or channels.

The results obtained by using amphiphilic probes and EPR spectroscopy lead to the conclusion that in the MBGs, the molecules of the surfactant are still ordered. However, their arrangement is different than the one they present in the initial microemulsion, since there are indications that the AOT tails are packed more tightly showing a parallel arrangement. The surfactant molecules create a layer via which the enzyme can be protected in the aqueous phase of the system, while a non-polar channel on the other side of the layer ensures the diffusion of the substrates. Therefore, the location of the enzyme near the surfactant molecules allows the protein to always be close to the reaction's substrate. On the other hand, when the enzyme is introduced in the MBG via the HPMC/water mixture before adding the microemulsion, although the surfactant-coated channels are still formed, the enzyme might be located anywhere in the matrix and not necessarily close to the channels. Therefore, although it is still active, the observed activity is significantly lower. These findings clarify the necessity of the enzyme-containing microemulsion for the construction of the biocatalyst, even though after its incorporation the initial structure of the microemulsion droplets disappear.

Combining our previous work [36]—in which following Differential Scanning Calorimetry (DSC), different types of water were identified in the HPMC MBGs—with the present findings, we can conclude that the identified type of water with the strongest interactions can be water molecules bound strongly on the heads of the surfactant molecules. Nevertheless, it has been proven before [54] that two molecules of water are more tightly bound to the heads of AOT than the rest of the water of hydration. The identified interfacial water [36] can be the rest of the AOT hydration molecules that accumulate on the side of the heads of AOT molecules that cover the channels formed by the organic solvent. As the water content in the system increases, free, bulk water appears where the water molecules can be dissolved among the polymer chains presenting very weak interactions with the matrix. This is in agreement with the findings of SEM study, where the system with a higher amount of water leaves broader pores after solute evaporation. Moreover, EPR study of lipophilic probes allows the assumption that the higher the water content of the MBG (with bulk-like water appearance) the lower the organic solvent that dissolves in the HPMC mesh.

Finally, in the present study, SEM images and SAXS profile prove that the surfactant concentration is crucial for the distribution of the organic solvent in the gel matrix.

Taking all these into account, we propose a structural model presented in Figure 8 (corresponding to System B), according to which the organic solvent forms channels (Figure 8, yellow area) surrounded by surfactant molecules. These surfactant-coated channels are surrounded by water molecules among

which the enzyme could be located (Figure 8, blue area). This water layer is narrower for MBGs with low water content and wider for MBGs with higher water content. The water can be found bound on the heads of the surfactant molecules or bound on the substitutes of the cellulose molecules. In systems with higher water content, a lower amount of organic solvent and higher water amount dissolves in the HPMC mesh, where water accumulates as bulk-like water. The opposite takes place in low water systems.

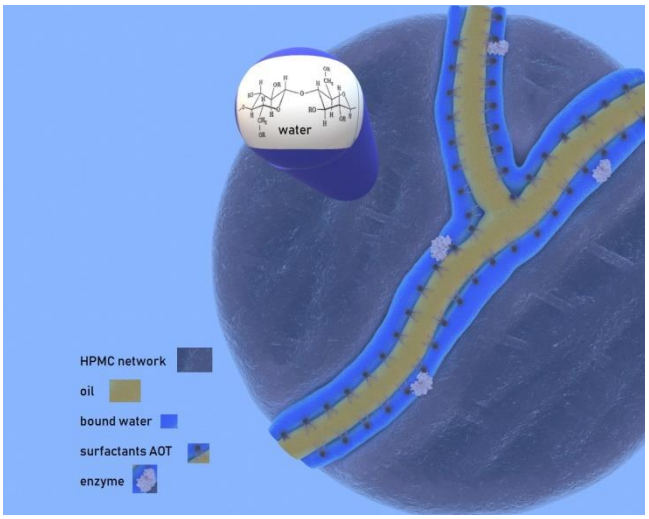

Figure 8. Proposed structural model for HPMC-based MBGs.

Overall, the results of the present work led to understanding the structure of such systems that have been so effectively used as biocatalysts. The applied techniques offer an overall view of the matrix created from the polymer, the surfactants of the microemulsion, the polar and non-polar solvents of the system as well as the enzyme.

5. Conclusions

Although the HPMC MBG has been successfully used as matrices for enzyme immobilization or biocompatible ingredients encapsulation, little is known about the structure of these systems and the role of their components. Deeper knowledge would aid the catalyst optimization as well as ease the encapsulation of bioactive compounds. Therefore, in the present study, we applied SEM to study the morphology, SAXS to detect the presence of droplets, and EPR to investigate the polar and non-polar areas of the matrix. Furthermore, we spin-labelled a model enzyme to investigate the possible conformational changes i the lipase and to clarify its location when immobilized in the MBGs. It should be noted here that this is the first work to combine these techniques to demonstrate an insight of the structure of these immobilization matrices. According to our findings, an organic solvent-based microemulsion is essential to form the MBGs; however, after the preparation procedure, the microemulsion droplets can no longer be detected. Our study leads to a proposed structural model for HPMC-based MBGs, according to which in the HPMC network the organic solvent forms channels that are surrounded by surfactant molecules. These surfactant-coated channels are covered by water molecules among which the enzyme can be located. No microemulsion droplets can be detected after its incorporation in the MBG. The channels could facilitate the diffusion of the substrates during a reaction. Taking into account our findings on how water, the organic solvent, and the surfactant influence the structure of the catalyst, in the future it will be easier to optimize the system according to the application that it will facilitate.

Supplementary Materials: The following are available online at http://www.mdpi.com/2079-4991/10/11/2204/s1, Details of EPR analysis. Figure S1: Plots of rotational correlation time, τ_R, vs. water content of Systems A, B, and C for the different spin probes used. Figure S2. Plots of hyperfine splitting constant, A_N, vs. water content of MBG Systems A, B, and C for the different spin probes used. Figure S3. Spectra of 12-doxyl methyl stearate (12-DMS) in AOT microemulsion and in Systems A, B, C. Figure S4. Spectra of 5-doxyl decane (5-DD) in AOT microemulsion and Systems A, B, and C.

Author Contributions: Conceptualization, S.A. and M.Z.; methodology, C.L.C., F.P., M.M., E.V., and E.M. software, S.A.; validation, S.A., A.X., and M.Z.; data curation, S.A., C.L.C., F.P., and M.Z.; writing—original draft preparation, E.V., E.M., F.P., and S.A.; writing—review and editing, M.Z., A.X., and O.G.; supervision, M.Z. All authors have read and agreed to the published version of the manuscript.

Funding: This research was financially supported by the project "STHENOS-b" (MIS 5002398), which is funded by the Operational Programme "Competitiveness, Entrepreneurship and Innovation" (NSRF 2014–2020) and co-financed by Greece and the EU (European Regional Development Fund).

Acknowledgments: The National Hellenic Research Foundation (NHRF) acknowledges the General Secretariat for Research and Technology (GSRT) for the financial support through the Research Programs for Excellence under the Programmatic agreement between Research Centers—GSRT (2015–2017), funded by Siemens SA. EV acknowledges support by the project "STHENOS-b: Targeted therapeutic approaches against degenerative diseases with special focus on cancer and ageing-optimisation of the targeted bioactive molecules" (MIS 5002398) which is implemented under the "Action for the Strategic Development on the Research and Technological Sector", funded by the Operational Program "Competitiveness, Entrepreneurship and Innovation" (NSRF 2014–2020) and co-financed by Greece and the European Regional Development Fund of the European Union.

Conflicts of Interest: The authors declare no conflict of interest.

References

1. Chai, Q.; Jiao, Y.; Yu, X. Hydrogels for Biomedical Applications: Their Characteristics and the Mechanisms behind Them. *Gels* **2017**, *3*, 6. [CrossRef]
2. Zoumpanioti, M.; Karavas, E.; Skopelitis, C.; Stamatis, H.; Xenakis, A. Lecithin organogels as model carriers of pharmaceuticals. *Progr. Colloid Polym. Sci.* **2004**, *123*, 199–202.
3. Avramiotis, S.; Papadimitriou, V.; Hatzara, E.; Bekiari, V.; Lianos, P.; Xenakis, A. Lecithin organogels used as bioactive compounds carriers. A microdomain properties investigation. *Langmuir* **2007**, *23*, 4438–4447. [CrossRef]
4. De Souza Paglarini, C.; de Figueiredo Furtado, G.; Biachi, J.P.; Vidal, V.A.S.; Martini, S.; Forte, M.B.S.; Cunha, R.L.; Pollonio, M.A.R. Functional emulsion gels with potential application in meat products. *J. Food Eng.* **2018**, *222*, 29–37. [CrossRef]
5. Huang, Y.; Mei, L.; Chen, X.; Wang, Q. Recent developments in food packaging based on nanomaterials. *Nanomaterials* **2018**, *8*, 830. [CrossRef]
6. Kim, M.H.; An, S.; Won, K.; Kim, H.J.; Lee, S.H. Entrapment of enzymes into cellulose-biopolymer composite hydrogel beads using biocompatible ionic liquid. *J. Mol. Catal. B Enzym.* **2012**, *75*, 68–72. [CrossRef]
7. Vassiliadi, E.; Xenakis, A.; Zoumpanioti, M. Chitosan hydrogels: A new and simple matrix for lipase catalysed biosyntheses. *Mol. Catal.* **2018**, *445*, 206–212. [CrossRef]
8. Laurienzo, P.; Malinconico, M.; Pizzano, R.; Manzo, C.; Piciocchi, N.; Sorrentino, A.; Volpe, M.G. Natural polysaccharide-based gels for dairy food preservation. *J. Dairy Sci.* **2006**, *89*, 2856–2864. [CrossRef]
9. Bilal, M.; Iqbal, H.M.N. Naturally-derived biopolymers: Potential platforms for enzyme immobilization. *Int. J. Biol. Macromol.* **2019**, *130*, 462–482. [CrossRef]
10. Turner, M.B.; Spear, S.K.; Holbrey, J.D.; Rogers, R.D. Production of bioactive cellulose films reconstituted from ionic liquids. *Biomacromolecules* **2004**, *5*, 1379–1384. [CrossRef]
11. Dalla-Vecchia, R.; Sebrão, D.; Nascimento, M.D.G.; Soldi, V. Carboxymethylcellulose and poly(vinyl alcohol) used as a film support for lipases immobilization. *Process Biochem.* **2005**, *40*, 2677–2682. [CrossRef]
12. Arboleya, J.C.; Wilde, P.J. Competitive adsorption of proteins with methylcellulose and hydroxypropyl methylcellulose. *Food Hydrocoll.* **2005**, *19*, 485–491. [CrossRef]
13. Pérez, O.E.; Sánchez, C.C.; Pilosof, A.M.R.; Rodríguez Patino, J.M. Kinetics of adsorption of whey proteins and hydroxypropyl-methyl-cellulose mixtures at the air-water interface. *J. Colloid Interface Sci.* **2009**, *336*, 485–496. [CrossRef]
14. Rodriguez Patino, J.M.; Pilosof, A.M.R. Protein-polysaccharide interactions at fluid interfaces. *Food Hydrocoll.* **2011**, *25*, 1925–1937. [CrossRef]

15. Pérez, O.E.; Carrera Sánchez, C.; Pilosof, A.M.R.; Rodríguez Patino, J.M. Impact of hydroxypropylmethylcellulose on whey protein concentrate spread film at the air-water interface: Structural and surface dilatational characteristics. *Colloids Surfaces A Physicochem. Eng. Asp.* **2015**, *465*, 1–10. [CrossRef]
16. Fathi, M.; Martín, Á.; McClements, D.J. Nanoencapsulation of food ingredients using carbohydrate based delivery systems. *Trends Food Sci. Technol.* **2014**, *39*, 18–39. [CrossRef]
17. Raghavendra, T.; Sayania, D.; Madamwar, D. Synthesis of the "green apple ester" ethyl valerate in organic solvents by Candida rugosa lipase immobilized in MBGs in organic solvents: Effects of immobilization and reaction parameters. *J. Mol. Catal. B Enzym.* **2010**, *63*, 31–38. [CrossRef]
18. Nagayama, K.; Karaiwa, K.; Doi, T.; Imai, M. Esterification activity and stability of Candida rugosa lipase in AOT microemulsion-based organogels. *Biochem. Eng. J.* **1998**, *2*, 121–126. [CrossRef]
19. Quellet, C.; Eicke, H.-F. Mutual gelation of gelatin and water-in-oil microemulsions. *Chimia* **1986**, *40*, 233–238.
20. Haering, G.; Luisi, P.L. Hydrocarbon Gels from Water-in-Oil Microemulsions. *J. Phys. Chem.* **1986**, *16*, 5892–5895. [CrossRef]
21. Pastou, A.; Stamatis, H.; Xenakis, A. Microemulsion-based organogels containing lipase: Application in the synthesis of esters. *Progr. Colloid Polym. Sci.* **2000**, *115*, 192–195.
22. Delimitsou, C.; Zoumpanioti, M.; Xenakis, A.; Stamatis, H. Activity and stability studies of Mucor miehei lipase immobilized in novel microemulsion-based organogels. *Biocatal. Biotransform.* **2002**, *20*, 319–327. [CrossRef]
23. Zoumpanioti, M.; Merianou, E.; Karandreas, T.; Stamatis, H.; Xenakis, A. Esterification of phenolic acids catalyzed by lipases immobilized in organogels. *Biotechnol. Lett.* **2010**, *32*, 1457–1462. [CrossRef]
24. Zoumpanioti, M.; Stamatis, H.; Xenakis, A. Microemulsion-based organogels as matrices for lipase immobilization. *Biotechnol. Adv.* **2010**, *28*, 395–406. [CrossRef]
25. Griffith, O.H.; Jost, P.C. Lipid Spin Labels in Biological Membranes. In *Spin Labeling*; Academic Press: Cambridge, MA, USA, 1976; Volume 1, pp. 453–523.
26. Papadimitriou, V.; Sotiroudis, T.G.; Xenakis, A. Olive Oil Microemulsions: Enzymatic Activities and Structural Characteristics. *Langmuir* **2007**, *23*, 2071–2077. [CrossRef]
27. Fanun, M.; Papadimitriou, V.; Xenakis, A. Characterization of Cephalexin Loaded Nonionic Microemulsions. *J. Colloid Interface Sci.* **2011**, *361*, 115–121. [CrossRef] [PubMed]
28. Knauer, B.R.; Napier, J.J. The Nitrogen Hyperfine Splitting Constant of the Nitroxide Functional Group as a Solvent Polarity Parameter. The Relative Importance for a Solvent Polarity Parameter of Its Being a Cybotactic Probe vs. Its Being a Model Process. *J. Am. Chem. Soc.* **1976**, *98*, 4395–4400. [CrossRef]
29. Marsh, D. Spin-Label EPR for Determining Polarity and Proticity in Biomolecular Assemblies: Transmembrane Profiles. *Appl. Magn. Reson.* **2010**, *37*, 435–454. [CrossRef] [PubMed]
30. Stoll, S.; Schweiger, A. EasySpin, a comprehensive software package for spectral simulation and analysis in EPR. *J. Magn. Reson.* **2006**, *178*, 42–55. [CrossRef] [PubMed]
31. Hemminga, M.A.; Berliner, L. *ESR Spectroscopy in Membrane Biophysics*; Biological Magnetic Resonance; Springer US: Boston, MA, USA, 2007; Volume 27.
32. Etienne, E.; Le Breton, N.; Martinho, M.; Mileo, E.; Belle, V. SimLabel: A graphical user interface to simulate continuous wave EPR spectra from site-directed spin labeling experiments. *Magn. Reson. Chem.* **2017**, *55*, 714–719. [CrossRef]
33. Zoumpanioti, M.; Karali, M.; Xenakis, A.; Stamatis, H. Lipase biocatalytic processes in surfactant free microemulsion-like ternary systems and related organogels. *Enzym. Microb. Technol.* **2006**, *39*, 531–539. [CrossRef]
34. Stamatis, H.; Xenakis, A. Biocatalysis using microemulsion-based polymer gels containing lipase. *J. Mol. Catal. B Enzym.* **1999**, *6*, 399–406. [CrossRef]
35. Itabaiana, I.; Gonçalves, K.M.; Zoumpanioti, M.; Leal, I.C.R.; Miranda, L.S.M.E.; Xenakis, A.; De Souza, R.O.M.A. Microemulsion-based organogels as an efficient support for lipase-catalyzed reactions under continuous-flow conditions. *Org. Process Res. Dev.* **2014**, *18*, 1372–1376. [CrossRef]
36. Blattner, C.; Zoumpanioti, M.; Kröner, J.; Schmeer, G.; Xenakis, A.; Kunz, W. Biocatalysis using lipase encapsulated in microemulsion-based organogels in supercritical carbon dioxide. *J. Supercrit. Fluids* **2006**, *36*, 182–193. [CrossRef]
37. Dandavate, V.; Madamwar, D. Reusability of surfactant-coated Candida rugosa lipase immobilized in gelatin microemulsion-based organogels for ethyl isovalerate synthesis. *J. Microbiol. Biotechnol.* **2008**, *18*, 735–741.

38. Zhang, W.W.; Wang, N.; Zhang, L.; Wu, W.X.; Hu, C.L.; Yu, X.Q. Effects of additives on lipase immobilization in microemulsion-based organogels. *Appl. Biochem. Biotechnol.* **2014**, *172*, 3128–3140. [CrossRef] [PubMed]
39. Moulik, S.P.; Paul, B.K. Structure, dynamics and transport properties of micro emulsions. *Adv. Colloid Interface Sci.* **1998**, *78*, 99–195. [CrossRef]
40. González-Blanco, C.; Rodríguez, L.J.; Velázquez, M.M. Effect of the solvent on the water properties of water/oil microemulsions. *J. Colloid Interface Sci.* **1999**, *211*, 380–866. [CrossRef]
41. Haering, G.; Luisi, P.L.; Hauser, H. Characterization by electron spin resonance of reversed micelles consisting of the ternary system AOT-isooctane-water. *J. Phys. Chem.* **1988**, *92*, 3574–3581. [CrossRef]
42. Schreier, S.; Polnaszek, C.F.; Smith, I.C.P. Spin labels in membranes problems in practice. *BBA Rev. Biomembr.* **1978**, *515*, 395–436. [CrossRef]
43. Caldararu, H.; Timmins, G.S.; Gilbert, B.C. The Structure of Gelatin-Water/Oil Microemulsion Sols and Gels. An EPR Spin-Probe and Spin-Labelling Study. *Phys. Chem. Chem. Phys.* **1999**, *1*, 5689–5695. [CrossRef]
44. Alberghina, L.; Lotti, M. [14] Cloning, sequencing, and expression of Candida rugosa lipases. In *Methods in Enzymology*; Academic Press: Cambridge, MA, USA, 1997; Volume 284, pp. 246–260.
45. Grochulski, P.; Li, Y.; Schrag, J.D.; Bouthillier, F.; Smith, P.; Harrison, D.; Rubin, B.; Cygler, M. Insights into interfacial activation from an open structure of Candida rugosa lipase. *J. Biol. Chem.* **1993**, *268*, 12843–12847.
46. Grochulski, P.; Li, Y.; Schrag, J.D.; Cygler, M. Two conformational states of Candida rugosa lipase. *Protein Sci.* **1994**, *3*, 82–91. [CrossRef]
47. Mukherjee, S.; Yang, L.; Vincent, C.; Lei, X.; Ottaviani, M.F.; Ananthapadmanabhan, K.P. A comparison between interactions of triglyceride oil and mineral oil with proteins and their ability to reduce cleanser surfactant-induced irritation. *Int. J. Cosmet. Sci.* **2015**, *37*, 371–378. [CrossRef]
48. Bösecke, P.; Diat, O. Small-angle X-ray scattering at the ESRF high-brilliance beamline. *J. Appl. Crystallogr.* **1997**, *30*, 867–871. [CrossRef]
49. Glatter, O. A new method for the evaluation of small-angle scattering data. *J. Appl. Crystallogr.* **1977**, *10*, 415–421. [CrossRef]
50. Hammouda, B.; Ho, D.L.; Kline, S. Insight into clustering in poly(ethylene oxide) solutions. *Macromolecules* **2004**, *37*, 6932–6937. [CrossRef]
51. Bhattacharjee, S.M.; Giacometti, A.; Maritan, A. Flory theory for polymers. *J. Phys. Condens. Matter* **2013**, *25*, 503101. [CrossRef]
52. Atkinson, P.J.; Heenan, R.K.; Grimson, M.J.; Howe, A.M.; Robinson, B.H. Structure of microemulsion-based organo-gels. *Progr. Colloid Polym. Sci.* **1990**, *23*, 1807–1809.
53. Petit, C.; Zemb, T.; Pileni, M.P. Structural Study of Microemulsion-Based Gels at the Saturation Point. *Langmuir* **1991**, *7*, 223–231. [CrossRef]
54. Hauser, H.; Haering, G.; Pande, A.; Luisi, P.L. Interaction of water with sodium bis(2-ethyl-1-hexyl) sulfosuccinate in reversed micelles. *J. Phys. Chem.* **1989**, *93*, 7869–7876. [CrossRef]

Molecular Catalysis 522 (2022) 112252

Contents lists available at ScienceDirect

Molecular Catalysis

journal homepage: www.journals.elsevier.com/molecular-catalysis

(Hydroxypropyl)methyl cellulose-chitosan film as a matrix for lipase immobilization: Operational and morphological study

Evdokia Vassiliadi [a,b], Anastasios Aridas [a,b], Véronique Schmitt [c], Aristotelis Xenakis [a], Maria Zoumpanioti [a,*]

[a] National Hellenic Research Foundation (NHRF), Institute of Chemical Biology, 48 Vassileos Constantinou Ave., Athens 11635, Greece
[b] Department of Biological Applications and Technology, University of Ioannina, Ioannina 45110, Greece
[c] Centre de Recherche Paul Pascal (CRPP) UMR 5031 CNRS, University of Bordeaux, Bordeaux, France

ARTICLE INFO

Keywords:
Biocatalysis
Lipase
Ester synthesis
Atomic force microscopy

ABSTRACT

The present work reports on the use of a hybrid blend of biopolymers as a matrix for lipase immobilization. (Hydroxypropyl)methyl cellulose (HPMC) and Chitosan (CS) were combined in order to formulate a film on which *Mucor miehei* lipase was immobilized. The biocatalyst was studied upon the model reaction of propyl laurate synthesis. The system was examined in terms of its capability to provide an appropriate environment where lipase will maintain its activity. The ratio of the polymers used was examined and HPMC:CS=2:1 proved to form the most promising matrix. Increasing the amount of the immobilized enzyme appears to improve the reaction yield indicating, however, mass transfer limitations. Apparent activation energy was calculated and energy input showed that ultra-sonication accelerated the initial rate of the reaction. Different reaction solvents were tested with isooctane being the most effective. The enzyme-containing film showed a remarkable reusability, since it can be used for up to 35 times without loss of activity. Finally, Atomic Force Microscopy (AFM) was performed to observe the morphology of the most promising films. The HPMC/CS film exhibits a nanostructure without a unique characteristic length and a roughness of 42.8 nm while the presence of enzyme smoothens the film as the roughness decreases to 5.5 nm.

1. Introduction

Hydrogels are defined as three-dimensional macromolecule networks swollen by large amounts of water. They are divided in different categories according to their ingredients and formation procedure, such as beads, and thin films [1]. Their properties allow their use in various fields, including catalysis, drug delivery and food applications [2]. Their catalytic applications are related to their ability to provide a suitable environment for the immobilization of enzymes, thus offering a unique medium for maximizing their activity and stability [3]. Various hydrogels based on biopolymers have been prepared by using alginate, agarose, starch, gelatin, cellulose, chitosan, and their derivatives, since they have exceptional properties combining efficiency and biocompatibility [4–6].

Lipases (triacylglycerol ester hydrolases, EC 3.1.1.3) are capable of catalyzing several reactions including esterification, transesterification, hydrolysis, epoxydations [7] and aminolysis [8–12]. The immobilization of enzymes on various polymeric carriers has gained interest due to numerus advantages [13]. Among several immobilization methods [14–16] entrapment in polymeric hydrogels has been proposed as alternative solution to acquire a biocatalyst with good mechanical properties [14,17]. In most cases, enzyme immobilization is accomplished with the aid of a cross-linker, such as glutaraldehyde [18–20].

Thus far, several natural polymers have been used for the design of an efficient support for enzymes. The use of a blend of biopolymers provides enhanced immobilization capability, biodegradability and flexibility [14,21]. What is more, mixtures of biodegradable and biocompatible polymers belonging to well-known families of natural polysaccharides (cellulose, starch, chitin) [22] are already approved for use in food industry.

Cellulose and chitin are the two most abundant natural polymers [5, 23]. Cellulose ethers such as methylcellulose (MC) and (hydroxypropyl) methyl cellulose (HPMC) are water-soluble derivatives of cellulose [24]. Chitosan is a natural polymer derived by deacetylation of chitin.

Abbreviations: AFM, atomic force microscopy; CS, chitosan; GLY, glycerol; HPMC, (Hydroxypropyl)methyl cellulose.

* Corresponding author.
E-mail address: mariaz@eie.gr (M. Zoumpanioti).

https://doi.org/10.1016/j.mcat.2022.112252
Received 26 October 2021; Received in revised form 22 March 2022; Accepted 23 March 2022
Available online 28 March 2022

Cellulose derivatives can interact with chitosan via hydrogen bonds, electronic or hydrophobic associations, chain entanglements, and van der Waals forces, resulting in the formation of hydrogels [24]. One of the biggest advantages of chitosan over chitin and other potential support/protective materials (e.g. silica) is that slightly acidic solutions of chitosan can be readily cast into beads, films or fibres [25]. HPMC, in contrast to chitosan has large hydrophobic segments and consequently exhibits strong surface activity. Therefore, simultaneous use of HPMC and chitosan could expand their potential uses.

Furthermore, plasticizers can be introduced to reduce frictional forces between polymer chains, such as those derived from hydrogen bonds or ionic forces. The incorporation of glycerol (GLY) into the film formulation also has the effect of retaining the film's mechanical properties [26]. In addition, the elongation of blended films increases with plasticizer content, even if a high content also produces a loss in tensile strength [27].

In the present study chitosan and a cellulose derivative (HPMC) were combined in order to formulate a promising enzyme carrier used as a biocatalyst, as tested upon propyl laurate synthesis. The biocatalyst was studied in terms of its capability to provide an appropriate environment where lipase from *Mucor miehei* can maintain its activity and stability in organic media. Several parameters were tested to optimize the biocatalyst, such as the ratio of the two polymers and the enzyme loading. The reusability was also tested with excellent results. Furthermore, the biocatalyst was observed via Atomic Force Microscopy (AFM) to assess the film topology in presence or absence of enzyme and/or plasticizer. The aim of the present study is to develop and optimize a biocatalyst which will subsequently be proposed for the synthesis of high added value products of industrial interest.

2. Experimental

2.1. Materials

Lipase from *Mucor miehei* (*M. miehei*) was supplied by Fluka, Basel, Switzerland and had a specific activity of 1.19 U/mg of protein (1 U corresponds to the amount of enzyme which liberates 1 μmol butyric acid per min at pH 8.0 and 40°C using tributyrin as substrate). Chitosan (CS) from shrimp and other crustacean shells (viscosity 200–600 mPa.s, 0.5% in 0.5% Acetic acid, 20°C; Deacetylation value: 80%, molecular mass 1526.464 g/mol) was purchased from TCI, Belgium. (Hydroxypropyl)methyl cellulose (HPMC) (3600–5500 cP) as well as lauric acid were obtained from Sigma, Darmstadt, Germany. Acetic acid and glycerol were obtained from LachNer, Neratovice, Czech Republic. All other materials were at least reagent grade. Millipore Milli-Q water was used for the preparation of gels and buffer solutions.

2.2. Methods

2.2.1. Film preparation

Films based on CS/HPMC were prepared by solubilizing CS in acidic water (1% acetic acid) and HPMC in distilled water, resulting in a 2% w/w solution, each. The solutions were left overnight until homogeneous. Then a mixture was prepared at the proper ratio and placed on a petri dish to dry overnight. After drying, approximately 0.3 g of film is produced. It is worth noting that after mixture of the two solutions, no phase separation could be observed whatever the composition, showing the good biopolymers' compatibility.

To prepare films containing glycerol, 0.15 g anhydrous glycerol was added to 3 g of the solution of polymers prior to drying, resulting in producing a film with 0.5 g of glycerol/g.

2.2.2. Lipase-containing film preparation

To formulate the biocatalyst, the appropriate amount of Tris/HCl buffer, pH 7.5 containing lipase was added in the polymers solution, prior to drying. In a typical experiment, 1 g of CS solution 2% w/w was mixed with 2 g HPMC solution 2% w/w, followed by the addition of 30 μL buffer solution containing 0.3 mg of lipase (commercially available) and stirred at room temperature. The mixture was left overnight on a petri dish to dry, thus formulating a dehydrated film where the enzyme is immobilized. This way a biocatalyst is produced with final lipase concentration of 1 mg/g of film. Before use, the film was washed three times with 5 mL of isooctane to remove enzyme molecules that may not be effectively immobilized on the gel network. After enzyme immobilization on the film, it was examined whether the solution with which the biocatalyst was washed, contained any amount of the lipase. Since proteins tend to have a characteristic absorbing peak at about 280 nm, the wash was spectrophotometrically evaluated [3] and no traces of the enzyme were found. These results show that there is no enzyme leakage after the procedure of drying.

2.2.3. Lipase-catalyzed reactions

The esterification reactions took place under ambient conditions, unless otherwise stated. Approximately, 0.3 g of a film containing 0.3 mg of lipase was placed in a screw cap bottle with 10 mL of the appropriate organic solvent containing lauric acid and 1-propanol (100 mM, each). The bottles were preserved at room temperature without stirring, unless stated otherwise. At fixed time intervals samples of 10 μL each were withdrawn and analyzed by GC. Each experiment was performed in duplicate and conversions were calculated by using calibration curves of butyl laurate ester in the presence of dodecane as an external standard. After plotting the amount of produced ester against time, the slope was calculated giving the initial rate in terms of mM/min.

In order to compare and evaluate the performance of the biocatalyst under different conditions, the initial rate was chosen as the most appropriate means to compare given heterogeneous reactions [28]. Therefore, each reaction was monitored until approximately 10% yield.

For the gas chromatography (GC) analysis a DP5 column, Agilent, (30 m x 0.25 mm i.d. x 0.32 μm film thickness) was mounted on a Hewlett-Packard (HP) Model GC-6890C. Injector as well as detector temperature was 270 °C and oven temperature was held constant at 200 °C.

2.2.4. Energy input

To study the effect of energy input on the biocatalytic activity of *M. miehei* lipase immobilized on the films, different methods were tested. In the first case, the reaction took place in controlled temperature by placing the reaction vials in a water bath (Memmert water bath W 200), at 45 °C. In the second case, the reaction took place under mechanical agitation, by placing the reaction vials on an orbital shaker at 200 rpm. In the third case, the reaction vials were placed in a sonicator (Ultrasonic bath UCI-150). As a control, a reaction that took place at room temperature, without stirring or any energy input was used.

2.2.5. Effect of incubation temperature

To study the effect of temperature on the biocatalytic activity of *M. miehei* lipase immobilized on the films, its catalytic activity against propyl laurate synthesis was tested after incubation at different temperatures. For this purpose, a water bath was used under controlled temperature at 30, 40, 50, and 60 °C.

2.2.6. Products diffusion

To study the ability of the products to diffuse in the biocatalyst, films were prepared in the absence of enzyme and placed in vials with isooctane as an external solvent, containing 100 mM butyl laurate. At fixed time intervals, samples were withdrawn and ester concentration in the external solvent was calculated by GC analysis.

2.2.7. Morphological analysis via Atomic Force Microscopy (AFM)

Film morphology was examined by dynamic force mode (tapping mode) AFM in air at 25 °C using a Dimension-Icon, Brüker apparatus equipped with Tap 300 Al-G tips from Budget Sensors. Films were

prepared as described in 2.2.1 in the absence and 2.2.2 in the presence of enzyme. In each case, the mixtures were left to dry on microscope slides instead of petri dishes. Each sample was observed in different scan sizes adapted to the observation (going from 300 × 300 nm2 to 60 × 60 μm2). Height and phase images were recorded, simultaneously. The roughness is estimated through Rq the root-mean-square roughness of the sample over a 100 μm^2 area.

3. Results and discussion

The aim of the present study was to develop a potential enzyme biocatalyst based on the blend of two polymers, CS and HPMC, offering a system with improved properties. In order to optimize the biocatalyst, a model esterification reaction was used and several parameters were examined. More specifically, the effect on the esterification rate of the amount of enzyme immobilized on the films, the use of different reaction solvents, the use of glycerol as a plasticizer and the energy input were tested.

3.1. Biocatalyst optimization

To investigate the effect of the polymers' ratio of the film on the biocatalytic activity of *M. miehei* lipase, film hydrogels were prepared with different CS to HPMC ratios. The lipase-containing films were used to catalyze propyl laurate synthesis in isooctane, as described in Materials and Methods section. Fig. 1 presents the effect of HPMC/CS ratio on the esterification rate.

As can be seen from Fig. 1, increasing the CS content in the film initially increases the reaction's initial rate, with the highest efficiency achieved for polymer ratio HPMC:CS 2:1. Further increase of the CS content leads to lower esterification rates. This could be attributed to changes in the surface properties of the carrier, such as hydrophobicity and hydrogen bond forming ability. It has been reported in literature [29] that HPMC forms hydrogen bonding interactions with chitosan. Furthermore, it has been shown that there is an increase in the values of the polar surface free energy and the hydrophilic character of the film, when HPMC ratio is increased in the blend [30]. Thus, change of the polymer ratio could lead to changes of the surface properties, affecting the interaction between the enzyme and the carrier. Surface hydrophilicity is a very important parameter since it affects the interaction between the enzyme and the carrier [31], affecting the activity of the immobilized enzyme and thus the performance of the biocatalyst. Our results are also in agreement with the findings of Badgujar and co-workers [21]. Badgujar et al. reported for films based on chitosan and hydroxyl-methyl cellulose (HMC) containing lipase that the gradual addition of chitosan to the film leads to increased lipase activity; however, after a certain chitosan concentration lipase activity decreases.

3.2. Addition of glycerol

It is reported in literature that glycerol, when added to a film, induces changes to its morphology playing the role of a plasticizer [32]. To investigate whether the addition of glycerol can improve the mixed chitosan-HPMC films, glycerol was added to the blend of the two polymers alongside with enzyme addition and the mixture was left to dry overnight on a petri dish to form a film.

As can be seen from Fig. 2, the addition of glycerol to the film results in a slight raise of 7% of the reaction's initial rate. As reported in literature, glycerol increases the intensity of the hydrogen bonds in chitosan films, affecting the water affinity of the films [33]. In another study [34], the addition of glycerol increased the mobility of amylase and amylopectin chains, increasing the film's flexibility. Therefore, in our case the increased lipase activity may be attributed to a more flexible matrix. Moreover, it was observed that when glycerol was used for film preparation, a more fragile film was produced that was easily shred when removed from the dish. The smaller film parts offer increased interface, leading to higher conversion rates. However, the high error bar shown in Fig. 2 for the glycerol-containing biocatalyst reveals that these films give results with low reproducibility. This could be attributed to the fact that glycerol is also a substrate for the immobilized lipase. Therefore, glycerol consumption by the enzyme leads to matrix decomposition, thus affecting the model reaction that is being investigated. It should be mentioned here that all experiments involving films in the absence of glycerol had a high reproducibility (small error bars; Figs. 1 and 2) and as a result, films prepared without glycerol were chosen for further study.

3.3. Effect of lipase concentration on the reaction rate

To study the effect of the amount of lipase immobilized in HPMC/CS films on the esterification reaction, several films were prepared with different *M. miehei* lipase concentration. Fig. 3 shows the effect of varying the lipase concentration, calculated in terms of mg of lipase per g of gel, on the esterification rate of 1-propanol (100 mM) with lauric acid (100 mM) in isooctane. As can be seen from Fig. 3, the esterification rate increases with the increase of lipase content. This is in agreement with many studies that show that increasing the amount of enzyme has a positive effect on the reaction rate [35–37]. However, as shown in Fig. 3,

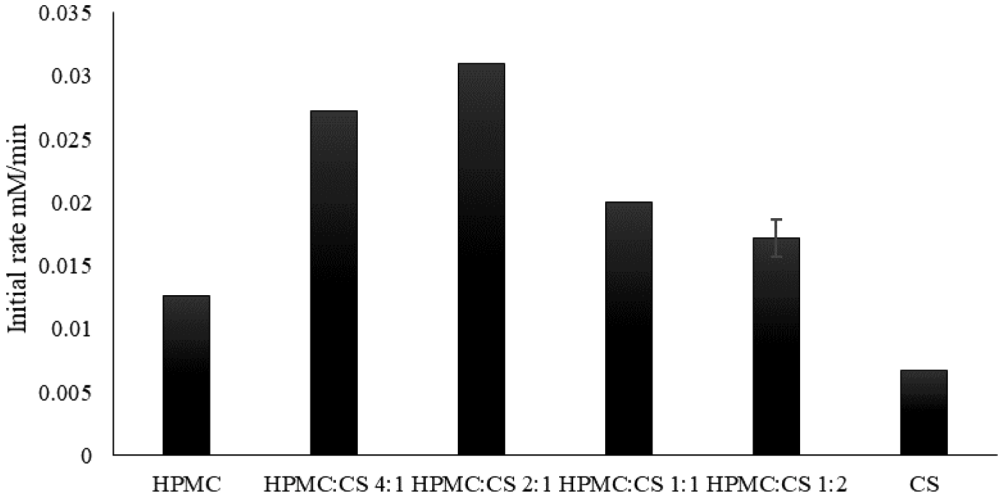

Fig. 1. Effect of polymer ratio (HPMC:CS) on the activity of *M. miehei* lipase as expressed by the initial rate of esterification reaction of lauric acid with 1-propanol. Reaction conditions as described in the Materials and Methods section.

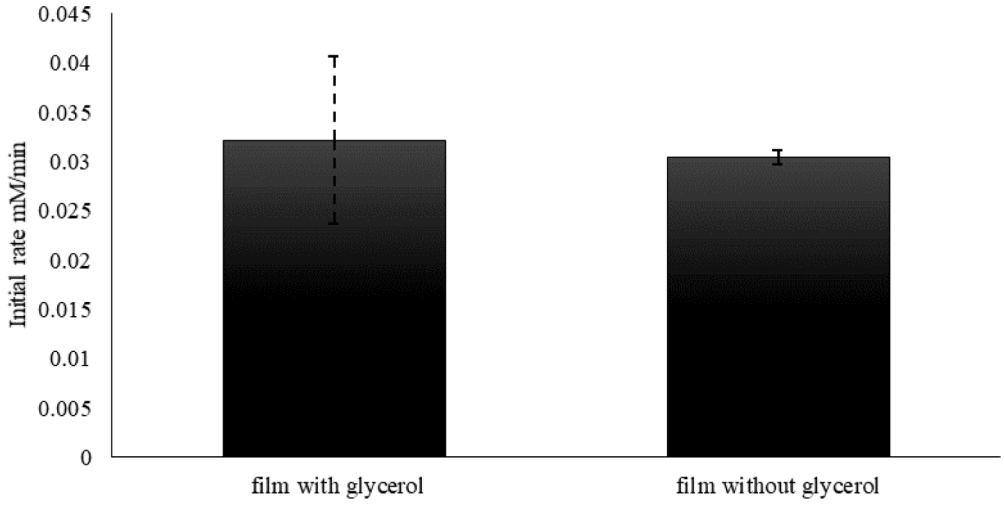

Fig. 2. Synthetic activity of *M. miehei* lipase immobilized on film in the presence and absence of glycerol, as expressed for the esterification of lauric acid with 1-propanol (100 mM each). HPMC:CS = 2:1; 1 mg lipase from *M. miehei* / g of film; Glycerol: 0.5 g / g of film.

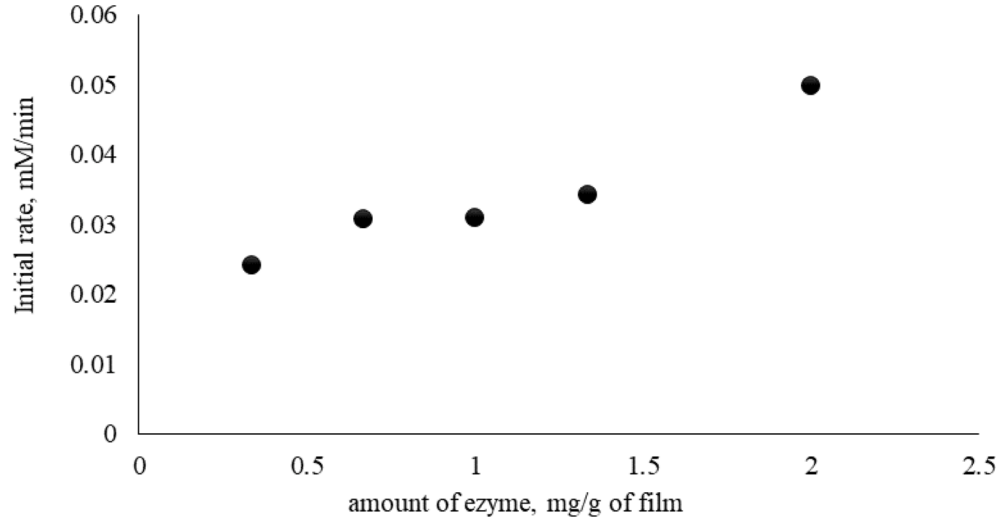

Fig. 3. Effect of the amount of *M. miehei* lipase immobilized on HPMC:CS=2:1 film, calculated as mg of lipase per g of film, on the esterification rate of 1-propanol (100 mM) with lauric acid (100 mM).

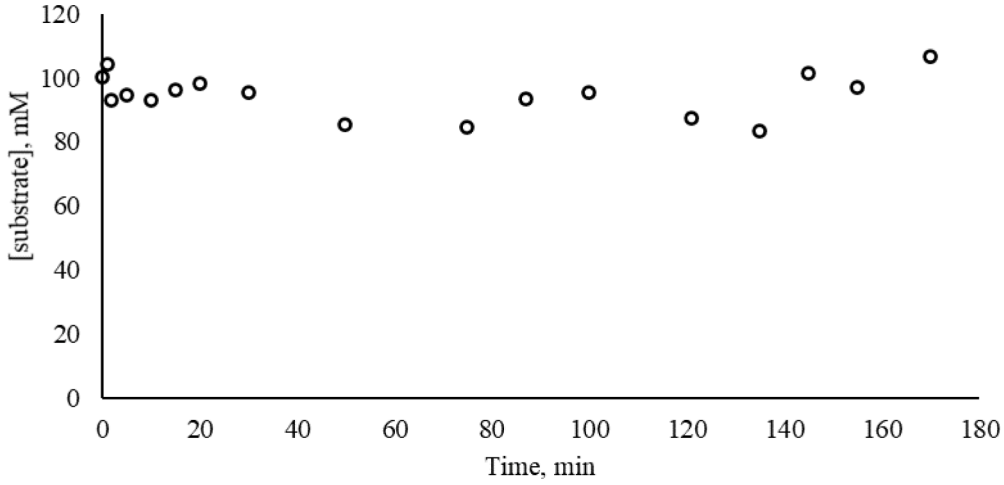

Fig. 4. Concentration of butyl laurate in the external solvent (isooctane), at 25 °C. Initial concentration 100 mM; solvent volume 10 mL. Film with ratio HPMC:CS = 2:1.

this increase is not linear. This lack of linearity can be attributed to mass transfer limitations at lower enzyme amounts, as linearity is consistent with kinetically controlled procedures [38].

3.4. Diffusion of products

During heterogeneous catalysis diffusion of substrates and products into the catalyst plays an important role, as it may be the reaction's limiting step. Since in our case changing the amount of immobilized enzyme does not linearly affect the esterification rate of propyl laurate synthesis (Fig. 3) indicating mass transfer limitations, an effort to clarify this was made by studying the diffusion of the products into the matrix. Therefore, films were prepared in the absence of enzyme and placed in vials with isooctane as an external solvent containing butyl laurate as a reaction product. In defined time intervals, samples were withdrawn and analyzed by GC to study the changes in product concentration in the external solvent.

As shown in Fig. 4, the concentration of butyl ester is constantly changing, causing a dynamic equilibrium between the ester in the film and the ester in the external solution, in which approximately 90% of the total amount of ester is present. Therefore, although mass diffusion limitations are present (Fig. 3), they do not restrict the use of the film as a suitable lipase carrier for esterification reactions.

3.5. Effect of energy input

The use of mechanical agitation can enhance the reaction rate not only by offering energy to the system but also by assisting substrate diffusion, overcoming, thus, diffusing limitations. However, in some cases agitation fails to increase mass transfer [39]. To take a step further, the use of other energy sources such as ultrasound to increase the initial rate of reaction and enhance mass transfer can be considered as an alternative energy-efficient technique [40]. In general, the use of ultrasound reduces energy consumption almost by 25–50% as compared to mechanical agitation [41].

To study the effect of these parameters on the esterification rate, energy was supplied to the reaction via different methods. In the first case reaction took place in controlled temperature, at 45 °C. In the second case mechanical agitation was used by using an orbital shaker at 200 rpm and in the third case energy input took place by using sonication. As a control, a reaction took place at room temperature, without stirring or any energy input. In each case, biocatalysts were formed with HPMC:CS ratio of 2:1, containing lipase from *M. miehei* and were used for propyl laurate synthesis. The results are shown in Fig. 5.

It is clear from Fig. 5 that the use of ultrasound significantly accelerates the catalysis, with the initial rate of the reaction being almost double in the first four hours of observation. These results are in accordance to the findings of relevant studies [42–45], where the use of ultrasound dramatically increases the catalytic activity when compared to mechanical agitation. In particular, Deshmane, et al. [44] reported that the use of ultrasound increases the yield of isopropyl esters from palm fatty acid distillate by 75% in 6 h, whereas with mechanical agitation the equilibrium conversion was at 65% in 7 h. Xiao, et al. [45] reported 98% conversion of glucose to glucose ester with sonication, compared to 48% without sonication, within two hours.

Temperature increase, as shown in Fig. 4, causes a small increase to the reaction rate, up to 7%. In previous studies of our group involving chitosan [5] and HPMC [46] gels, it has been stated that temperature increase leads to increase of the reaction rate, however, higher temperature than 50 °C could cause the loss of lipase activity due to enzyme denaturation [5,46].

Mechanical agitation increased the initial rate of the reaction as expected. The increase was higher than that induced by temperature increase; however, the result was not as pronounced as in the case of sonication. This is not the first time that similar results have been observed. Xiao et al. [45] reported that the reaction yield under ultrasonication in the first 2 h was double that under shaking. Moreover, Brenelli and Fernandes reported that rates of acyl transfer increased up to 10 times using ultrasonication as compared to magnetic stirring [47].

3.6. Effect of incubation temperature

Temperature is a crucial parameter when it comes to biocatalytic reactions. It affects enzyme activity in two different ways. On one hand, the energy provided accelerates the mobility of the substrates. On the other hand, the catalytic rate is confined due to possible enzyme denaturation at high temperatures, which redound to enzyme activity loss. For this purpose, the activity of the biocatalyst was studied by incubation at a range of temperature between 30 and 60 °C.

As can be seen from Fig. 6, the higher initial rate was observed at 40 °C. As stated in Section 3.5, studies have shown [5,46] that even though temperature increase leads to increase of the reaction rate due to the energy input, higher temperature than 50°C could cause the loss of lipase activity. This could be attributed to either enzyme denaturation or destruction of the immobilization matrix. It should be mentioned here that the films studied at all temperatures did not show any

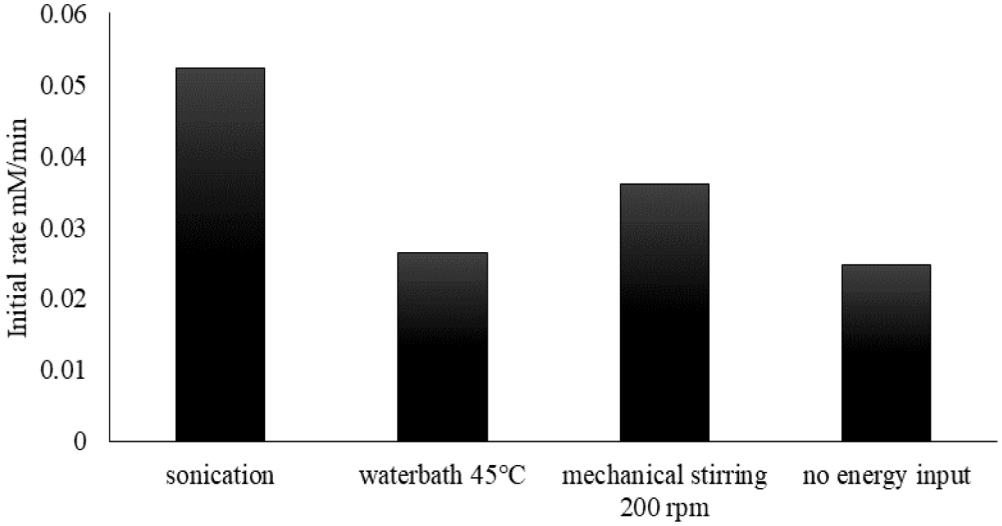

Fig. 5. Influence of energy input on the synthetic activity of M. miehei lipase (1 mg / g of film) immobilized on CS:HPMC =1:2 film, as expressed for the esterification of lauric acid with 1-propanol (100 mM, each).

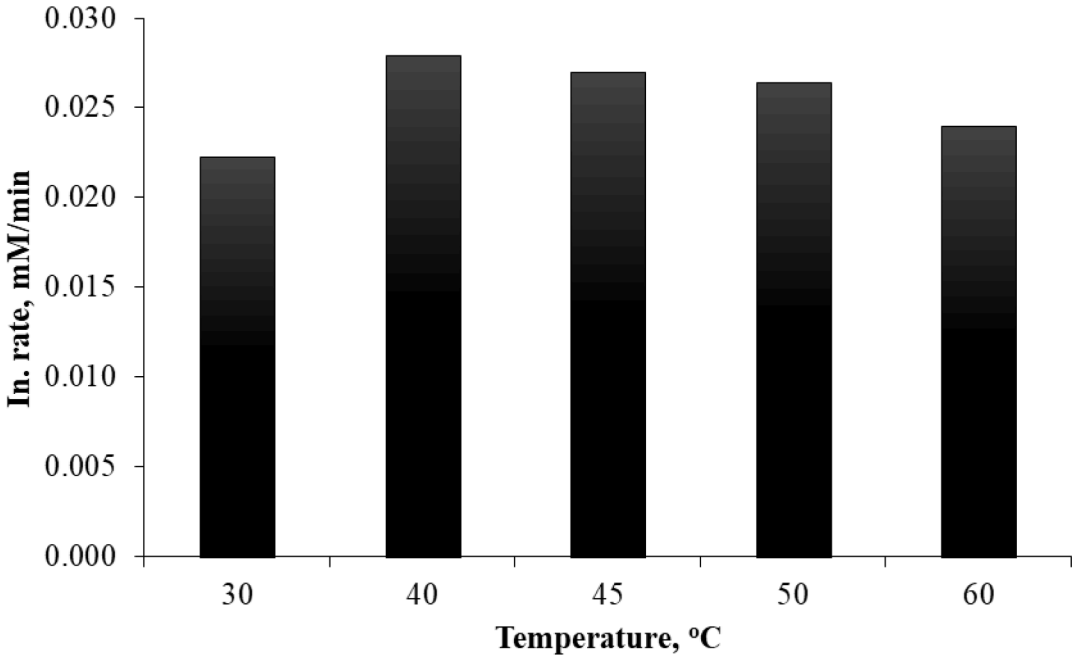

Fig. 6. Influence of temperature on the synthetic activity of *M. miehei* lipase (1 mg / g of film) immobilized on CS:HPMC =1:2 film, as expressed for the esterification of lauric acid with 1-propanol (100 mM, each).

macroscopically noticeable change in their structure, however, in microscale the increased temperature may have caused changes in film structure.

Similar results were found for the same lipase immobilized on chitosan hydrogels where the optimum temperature was found to be 30 °C [5], while for the same lipase immobilized on HPMC organogels this was not the case as increased temperature led to increased reaction rate up to 70 °C [46]. Another study [48] reported a similar temperature profile for *C. rugose* lipase immobilized on chitosan beads towards the hydrolysis of p-nitrophenyl palmitate.

The fact that the reaction rate only slightly changes upon temperature increase (the highest increment is almost 14% for temperature increase from 30 to 40 °C) suggests that the reaction rate is limited by mass transport phenomena and not by the reaction steps. This is in agreement with the results presented in paragraph 3.3 where the addition of enzyme did not affect linearly the reaction rate, leading to the same conclusion.

Moreover, the activation energy was calculated for the range of temperatures shown in Fig. 6. The Arrhenius plot for the synthesis of propyl laurate using the films is shown in Supporting Material (Fig. S1). The apparent activation energy was calculated and found to be 6 kJ/mol. The order of magnitude of the activation energy calculated here is similar to that calculated for the same lipase immobilized on organogels based on either HPMC or agar [46] and to the activation energy measured by Hedström et al. for immobilized *C. antarctica* lipase [49].

3.7. Effect of reaction medium

To study the influence of the reaction solvent on the enzymatic activity, several solvents were tested for the esterification reaction of lauric acid with 1-propanol. The solvents tested were alcohols, hydrocarbons and esters, either branched or non-branched. Fig. 7 presents the initial rate of propyl laurate synthesis in different solvents.

Although the film retained integrity in all solvents used, as can be

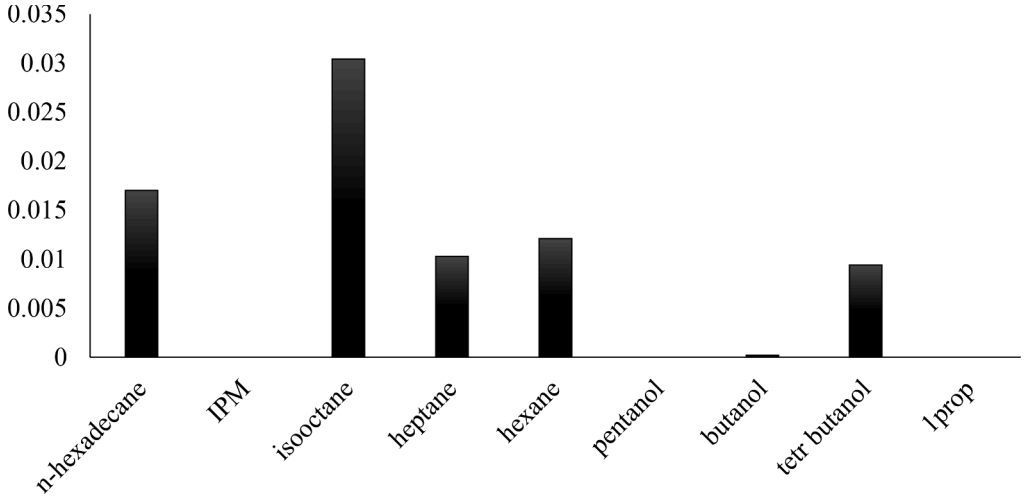

Fig. 7. Effect of the reaction solvent on the esterification rate of propyl laurate synthesis. HPMC:CS= 2:1, lipase from *M. miehei* 0.1 mg / g of gel. (IPM: Isopropyl myristate).

seen from Fig. 7, the nature and the polarity of the organic solvent influence the activity of the immobilized lipase. Thus, as it can be observed, polar solvents such as alcohols seem to create a non-favorable environment for the enzyme. This could occur due to the tendency of polar solvents to replace or remove essential water from the enzyme surface, leading to its inactivation. The highest lipase activity was observed in the less polar solvents, i.e. in hydrocarbons.

The highest reaction rate can be observer in the presence of isooctane and that could be explanted by the branched structure of its molecules that keeps them from packing tightly, offering thus higher diffusion of the substrates [5,46]. Branched hydrocarbons, especially isooctane, have been reported as the optima solvents by many authors in studies of enzymes immobilized on organogels [5,38,50,51].

Under the optimum conditions as determined thus far (room temperature, HPMC:CS = 2:1, isooctane as solvent, and enzyme concentration 1 mg/g of film) the final yield of propyl laurate synthesis in 24 h is 96%. Under these conditions, a kinetic study was conducted for the enzyme upon propyl laurate synthesis. The kinetic study revealed an Ordered Bi Bi mechanism with inhibition by both substrates at concentrations higher than 75 mM. However, the calculation of the kinetic constants was not feasible as significant mass transfer limitations effect the reaction and are more pronounced for low substrate concentrations. The effect of lauric acid concentration on the initial reaction velocity of the esterification for constant 1-propanol concentration can be seen at the Supporting Material (Fig. S2).

3.8. Reusability

For any industrial application of immobilized enzymes, the feasibility of reuse of the biocatalyst is important for the economic viability of a biosynthetic process. Therefore, the ability of the biocatalyst to be reused was tested for repeated cycles of propyl laurate synthesis.

Fig. 8. shows the ability of the biocatalyst to be reused, for the esterification reaction of propyl laurate synthesis. The film appears to have an excellent performance since the enzyme maintained its full activity for 35 uses. After the 35th use, the initial rate of the reaction shows a decrease down to 79% at 36th and rapidly to 60% at 39th use. These results are remarkable, as in other studies where films based on natural polymers have been used as carriers for lipases [52,53], the repeated use of films under optimized reaction conditions, showed the ability to be reused for five times, while the conversion decreases up to 69% at the fourth or fifth reuse. Similarly to these studies, in our case by performing the same test for the glycerol-containing films, we found that the reaction rate decreased to 64% at the 13th use (data not shown).

The decrease of the activity after several uses could be due to leaching of lipase from the support during each use by contact with the solvent, after each use by the contact with the washing solution, or gradual inactivation (i.e. from the stress upon each use or storage in refrigerator after each use) [3,54]. Since the loss of activity for 35 uses is insignificant, we can assume that it is caused by the gradual inactivation of the enzyme and not by leaching or washing it out.

3.9. Morphological analysis of the surface

Atomic Force Microscopy (AFM) is used to obtain images with atomic resolution of up to one tenth of nanometers. This type of microscopy can be effectively applied in the field of polymers to study the surface characteristics of polymer film samples [55]. Furthermore, AFM can offer information on the interaction between the matrix and the immobilized enzyme. Based on these information, catalyst optimization is possible by tuning the surface properties [56]. For the surface examination of the biocatalyst, four samples were analyzed, namely, (A) a HPMC:CS = 2:1 film, (B) a HPMC:CS = 2:1 film with immobilized *M. miehei* lipase, (C) a HPMC:CS = 2:1 glycerol-containing film and (D) a HPMC:CS = 2:1 glycerol-containing film with immobilized *M. miehei* lipase. The AFM height images are reported in Fig. 9 for $10 \times 10\ \mu m^2$ and $1 \times 1\ \mu m^2$. The other scan sizes are not shown.

For sample A corresponding to the biopolymer mixed film, the existence of domains with different heights can be observed. These domains show that the polymer film is nanostructured. The Fourier Tranform of a $60 \times 60\ \mu m^2$ image does not allow defining a characteristic size of these domains. They are polydispersed in size and shape. At a smaller scan size (Fig. S3, Supporting Material), it appears that the light domains exhibit themselves a height variation at a smaller scale and some fibrils seems to be present. The roughness of the film (size 10 μm x10 μm), Rq, is equal to 42.8 nm. When the enzyme is added to the film (sample B), the domains are smaller and the roughness decreases by almost a factor 8 as Rq = 5.55, showing that the film is much smoother. For glycerol containing films (sample C), the domains have disappeared and small nodules are visible (scale of the order of 20 nm). The film roughness is equal to 12.8 nm. The picture of the film containing both glycerol and the enzyme (sample D), is very similar to the previous one and nodules are also visible. The film roughness, Rq, is equal to 8.3 nm.

To summarize, pure biopolymer films exhibit a nanostructuration, with a large size and shape distribution and a roughness of the order of 43 nm. The enzyme levels the film. So does also the glycerol in a smaller extent. Adding the enzyme to the film containing glycerol has only a small additional smoothing effect and does not alter the presence of

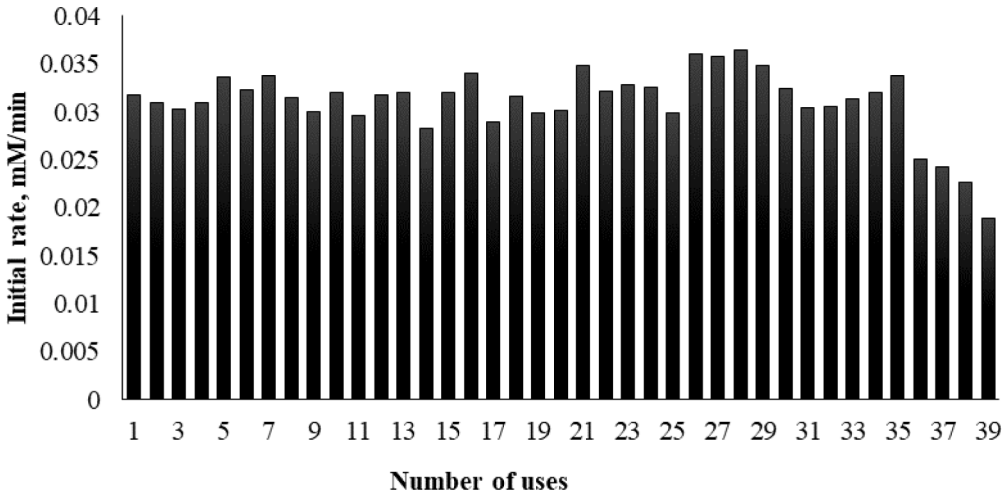

Fig. 8. Reaction rate as a function of number of uses for M. miehei lipase immobilized on the HPMC:CS=2:1 film, in successive batch syntheses of propyl laurate. Solvent: isooctane; lipase from M. miehei 1 mg / g of film; ambient conditions.

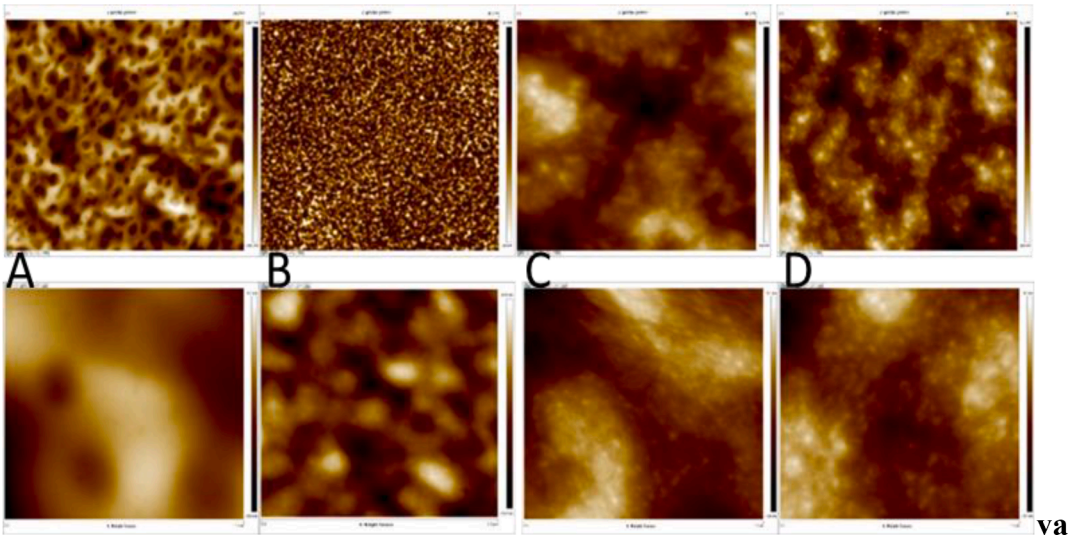

Fig. 9. Height imaging of films with scan size 10 μm; (A) HPMC:CS= 1:2 film; (B) HPMC:CS = 2:1 film with immobilized lipase, (C) a HPMC:CS = 2:1 glycerol-containing film, (D) a HPMC:CS = 2:1 glycerol-containing film with immobilized lipase. Lipase: *M. miehei* 1 mg / g of film; Glycerol: 0.5 g / g of film. First row scan size of 10 × 10 μm^2 and second row scan size of 1 × 1 μm^2. The height scale is not the same for all images.

nodules due to glycerol.

4. Conclusion

Chitosan and cellulose derivative HPMC were combined for the preparation of a film that was used as an enzyme carrier. Lipase from *Mucor miehei* was immobilized on the films and its activity and stability in organic media were studied. The novel catalyst permits easy diffusion of the substrates and products, although mass transfer limitations are present for the lower enzyme concentrations. Several ratios of two polymers were examined to optimize the biocatalyst over the esterification of propyl laurate synthesis, with the ratio of HPMC:CS=2:1 presenting the highest reaction yield. The immobilized lipase maintains its activity in non-polar solvents, showing higher activity in isooctane. Moreover, energy input via ultra-sonication increases enzyme activity more than thermal energy or mechanical agitation. The most remarkable result of the study is the excellent biocatalytic performance that occurred when testing the reusability of the biocatalyst, with the activity of the enzyme remaining up to 60% for 39 uses. Lastly, the films were investigated in terms of surface texture and morphology via Atomic Force Microscopy (AFM). AFM showed a nanostructuration of the polymer blend films. The addition of the enzyme led to a smoother film. Glycerol was also responsible for a smoother film. Moreover, nodules of about 20 nm are visible with glycerol. As it would be interesting to further characterize these nanostructurations using X-ray scattering techniques, the present AFM study can serve as preliminary work to our next steps.

Funding

This research was financially supported by the project "STHENOS-b" (MIS 5002398), which is funded by the Operational Programme "Competitiveness, Entrepreneurship and Innovation" (NSRF 2014–2020) and co-financed by Greece and the EU (European Regional Development Fund). AX thanks the University of Bordeaux, IdEx Visiting Scholars for his stay. EV thanks CRPP, for the accommodation provided to carry out the AFM experiments.

CRediT authorship contribution statement

Evdokia Vassiliadi: Data curation, Formal analysis, Conceptualization, Writing – original draft, Visualization. **Anastasios Aridas:** Data curation, Formal analysis. **Véronique Schmitt:** Data curation, Formal analysis, Writing – review & editing. **Aristotelis Xenakis:** Conceptualization, Writing – review & editing. **Maria Zoumpanioti:** Conceptualization, Data curation, Writing – original draft, Writing – review & editing.

Declaration of Competing Interest

The authors declare that they have no known competing financial interests or personal relationships that could have appeared to influence the work reported in this paper.

Acknowledgments

The authors want to thank Mr. Hassan Saadaoui and Gilles Pecastaings from CRPP for their help on AFM experiments and fruitful discussions.

Supplementary materials

Supplementary material associated with this article can be found, in the online version, at doi:10.1016/j.mcat.2022.112252.

References

[1] A. Mateescu, Y. Wang, J. Dostalek, U. Jonas, Thin hydrogel films for optical biosensor applications, Membranes 2 (1) (2012) 40–69, https://doi.org/10.3390/membranes2010040. Basel.
[2] S. Mondal, S. Das, A.K. Nandi, A review on recent advances in polymer and peptide hydrogels, Soft. Matter. 16 (6) (2020) 1404–1454, https://doi.org/10.1039/c9sm02127b.
[3] K.C. Badgujar, K.P. Dhake, B.M. Bhanage, Immobilization of Candida cylindracea lipase on poly lactic acid, polyvinyl alcohol and chitosan based ternary blend film: Characterization, activity, stability and its application for N-acylation reactions, Process Biochem. 48 (2013) 1335–1347, https://doi.org/10.1016/J.PROCBIO.2013.06.009.
[4] M.H. Kim, S. An, K. Won, H.J. Kim, S.H. Lee, Entrapment of enzymes into cellulose-biopolymer composite hydrogel beads using biocompatible ionic liquid, J. Mol. Catal. B Enzym. 75 (2012) 68–72, https://doi.org/10.1016/j.molcatb.2011.11.011.
[5] E. Vassiliadi, A. Xenakis, M. Zoumpanioti, Chitosan hydrogels: a new and simple matrix for lipase catalysed biosyntheses, Mol. Catal. 445 (2018) 206–212, https://doi.org/10.1016/j.mcat.2017.11.031.
[6] K.A. Batista, F.M. Lopes, F. Yamashita, K.F. Fernandes, Lipase entrapment in PVA/Chitosan biodegradable film for reactor coatings, Mater. Sci. Eng. C Mater. Biol. Appl. 33 (2013) 1696–1701, https://doi.org/10.1016/J.MSEC.2012.12.082.

[7] A.F. Zanette, I. Zampakidi, G.T. Sotiroudis, M. Zoumpanioti, R.O.M.A. Souza, L. Cardozo Filho, A. Xenakis, L. Cardozo Filho, Chemo-enzymatic epoxidation catalyzed by C. antarctica lipase immobilized in microemulsion-based organogels, J. Mol. Catal. B Enzym. 107 (2014) 89–94, https://doi.org/10.1016/j.molcatb.2014.05.013.

[8] C. Blattner, M. Zoumpanioti, J. Kröner, G. Schmeer, A. Xenakis, W. Kunz, Biocatalysis using lipase encapsulated in microemulsion-based organogels in supercritical carbon dioxide, J. Supercrit. Fluids. 36 (3) (2006) 182–193, https://doi.org/10.1016/j.supflu.2005.06.007.

[9] L.N. de Lima, A.A. Mendes, R. Fernandez-Lafuente, P.W. Tardioli, R. de Lima Camargo Giordano, Performance of different immobilized lipases in the syntheses of short- and long-chain carboxylic acid esters by esterification reactions in organic media, Molecules 4 (2018) 766, https://doi.org/10.3390/molecules23040766.

[10] M. Shahedi, M. Yousefi, Z. Habibi, M. Mohammadi, M.A. As'habi, Co-immobilization of Rhizomucor miehei lipase and Candida antarctica lipase B and optimization of biocatalytic biodiesel production from palm oil using response surface methodology, Renew. Energy 141 (2019) 847–857, https://doi.org/10.1016/j.renene.2019.04.042.

[11] X. Yuan, Y. Liu, F. Cao, P. Zhang, J. Ou, K. Tang, Immobilization of lipase onto metal–organic frameworks for enantioselective hydrolysis and transesterification, AIChE J. 66 (9) (2020) e16292, https://doi.org/10.1002/aic.16292.

[12] S. Zeng, J. Liu, S. Anankanbil, M. Chen, Z. Guo, J.P. Adams, R. Snajdrova, Z. Li, Amide Synthesis via aminolysis of ester or acid with an intracellular lipase, ACS Catal. 8 (9) (2018) 8856–8865, https://doi.org/10.1021/acscatal.8b02713.

[13] S. Datta, L.R. Christena, Y.R.S. Rajaram, Enzyme immobilization: an overview on techniques and support materials, 3 Biotech 3 (1) (2012) 1–9, https://doi.org/10.1007/S13205-012-0071-7.

[14] C. Garcia-Galan, Á. Berenguer-Murcia, R. Fernandez-Lafuente, R.C. Rodrigues, Potential of different enzyme immobilization strategies to improve enzyme performance, Adv. Synth. Catal. 353 (16) (2011) 2885–2904, https://doi.org/10.1002/adsc.201100534.

[15] S. Gupta, A. Bhattacharya, C.N. Murthy, Tune to immobilize lipases on polymer membranes: techniques, factors and prospects, Biocatal. Agric. Biotechnol. 2 (3) (2013) 171–190, https://doi.org/10.1016/j.bcab.2013.04.006.

[16] I. Cacciotti, C. Lombardelli, I. Benucci, M. Esti, Clay/chitosan biocomposite systems as novel green carriers for covalent immobilization of food enzymes, J. Mater. Res. Technol. 8 (2019) 3644–3652, https://doi.org/10.1016/J.JMRT.2019.06.002.

[17] M. Marciello, M. Filice, J.M. Palomo, Different strategies to enhance the activity of lipase catalysts, Catal. Sci. Technol. 2 (8) (2012) 1531–1543, https://doi.org/10.1039/c2cy20125a.

[18] R.A. Wahab, N. Elias, F. Abdullah, S.K. Ghoshal, On the taught new tricks of enzymes immobilization: an all-inclusive overview, React. Funct. Polym. 152 (2020), 104613, https://doi.org/10.1016/j.reactfunctpolym.2020.104613.

[19] M. Harguindeguy, C. Antonelli, M.P. Belleville, J. Sanchez-Marcano, C. Pochat-Bohatier, Gelatin supports with immobilized laccase as sustainable biocatalysts for water treatment, J. Appl. Polym. Sci. 138 (2) (2021) 49669, https://doi.org/10.1002/app.49669.

[20] I. Migneault, C. Dartiguenave, M.J. Bertrand, K.C. Waldron, Glutaraldehyde: behavior in aqueous solution, reaction with proteins, and application to enzyme crosslinking, Biotechniques 37 (5) (2004) 790–802, https://doi.org/10.2144/04375rv01.

[21] K.C. Badgujar, B.M. Bhanage, Carbohydrate base co-polymers as an efficient immobilization matrix to enhance lipase activity for potential biocatalytic applications, Carbohydr. Polym. 138 (2) (2015) 49669, https://doi.org/10.1016/j.carbpol.2015.08.036.

[22] P. Laurienzo, M. Malinconico, R. Pizzano, C. Manzo, N. Piciocchi, A. Sorrentino, M. G. Volpe, Natural polysaccharide-based gels for dairy food preservation, J. Dairy Sci. 89 (8) (2006) 2856–2864, https://doi.org/10.3168/jds.S0022-0302(06)72558-9.

[23] E. Vassiliadi, E. Mitsou, S. Avramiotis, C.L. Chochos, F. Pirolt, M. Medebach, O. Glatter, A. Xenakis, M. Zoumpanioti, Structural study of (Hydroxypropyl)methyl cellulose microemulsion-based gels used for biocompatible encapsulations, Nanomaterials 10 (11) (2020) 2204, https://doi.org/10.3390/nano10112204.

[24] X. Shen, J.L. Shamshina, P. Berton, G. Gurau, R.D. Rogers, Hydrogels based on cellulose and chitin: fabrication, properties, and applications, Green Chem. 18 (1) (2015) 53–75, https://doi.org/10.1039/c5gc02396c.

[25] H. Nagahama, H. Maeda, T. Kashiki, R. Jayakumar, T. Furuike, H. Tamura, Preparation and characterization of novel chitosan/gelatin membranes using chitosan hydrogel, Carbohydr. Polym. 76 (2) (2009) 255–260, https://doi.org/10.1016/j.carbpol.2008.10.015.

[26] N.E. Suyatma, L. Tighzert, A. Copinet, V. Coma, Effects of hydrophilic plasticizers on mechanical, thermal, and surface properties of chitosan films, J. Agric. Food Chem. 53 (10) (2005) 3950–3957, 10.1021/jf048790+.

[27] I. Arvanitoyannis, I. Kolokuris, A. Nakayama, N. Yamamoto, S.I. Aiba, Physico-chemical studies of chitosan-poly(vinyl alcohol) blends plasticized with sorbitol and sucrose, Carbohydr. Polym. 34 (1-2) (1997) 9–19, https://doi.org/10.1016/S0144-8617(97)00089-1.

[28] J. Hagen, Industrial Catalysis: A Practical Approach, 3rd ed., Wiley VCH, 2015, p. 5, pageISBN 978-3-527-33165-9.

[29] A. Pawlak, M. Mucha, Thermogravimetric and FTIR studies of chitosan blends, Thermochim. Acta 396 (2003) 153–166, https://doi.org/10.1016/S0040-6031(02)00523-3.

[30] J. Rotta, R.Á. Ozório, A.M. Kehrwald, G.M. de Oliveira Barra, R.D. de Melo Castanho Amboni, P.L.M. Barreto, Parameters of color, transparency, water solubility, wettability and surface free energy of chitosan/hydroxypropylmethylcellulose (HPMC) films plasticized with sorbitol, Mater. Sci. Eng. C 29 (2009) 619–623, https://doi.org/10.1016/J.MSEC.2008.10.032.

[31] R.M. Manzo, R.J. Ceruti, H.L. Bonazza, W.S. Adriano, G.A. Sihufe, E. J. Mammarella, Immobilization of carboxypeptidase a into modified chitosan matrixes by covalent attachment, Appl. Biochem. Biotechnol. 185 (2018) 1029–1043, https://doi.org/10.1007/S12010-018-2708-4.

[32] M. Zappino, I. Cacciotti, I. Benucci, F. Nanni, K. Liburdi, F. Valentini, M. Esti, Bromelain immobilization on microbial and animal source chitosan films, plasticized with glycerol, for application in wine-like medium: microstructural, mechanical and catalytic characterisations, Food Hydrocoll. 45 (2015) 41–47, https://doi.org/10.1016/j.foodhyd.2014.11.001.

[33] M.A. Cerqueira, B.W.S. Souza, J.A. Teixeira, A.A. Vicente, Effect of glycerol and corn oil on physicochemical properties of polysaccharide films-a comparative study, Food Hydrocoll. 27 (1) (2012) 175–184, https://doi.org/10.1016/j.foodhyd.2011.07.007.

[34] P.V.A. Bergo, R.A. Carvalho, P.J.A. Sobral, R.M.C. Dos Santos, F.B.R. Da Silva, J. M. Prison, J. Solorza-Feria, A.M.Q.B. Habitante, Physical properties of edible films based on cassava starch as affected by the plasticizer concentration, Packag. Technol. Sci. 22 (2) (2008) 85–89, https://doi.org/10.1002/pts.781.

[35] N.R. Khan, S.D. Gawas, V.K. Rathod, Enzyme-catalysed production of n-butyl palmitate using ultrasound-assisted esterification of palmitic acid in a solvent-free system, Bioprocess Biosyst. Eng. 41 (11) (2018) 1621–1634, https://doi.org/10.1007/s00449-018-1988-y.

[36] H. Kim, N. Choi, Y. Kim, H.R. Kim, J. Lee, I.H. Kim, Immobilized lipase-catalyzed esterification for synthesis of trimethylolpropane triester as a biolubricant, Renew. Energy 130 (2019) 489–494, https://doi.org/10.1016/j.renene.2018.06.092.

[37] H. Kim, T. Kim, N. Choi, B.H. Kim, S.W. Oh, I.H. Kim, Synthesis of diethylhexyl adipate by Candida antarctica lipase-catalyzed esterification, Process Biochem. 78 (2019) 58–62, https://doi.org/10.1016/j.procbio.2018.12.030.

[38] C. Delimitsou, M. Zoumpanioti, A. Xenakis, H. Stamatis, Activity and stability studies of Mucor miehei lipase immobilized in novel microemulsion-based organogels, Biocatal. Biotransform. 20 (5) (2002) 319–327, https://doi.org/10.1080/10242420290025539.

[39] A. Liese, L. Hilterhaus, Evaluation of immobilized enzymes for industrial applications Motivation and recent developments, Chem. Soc. Rev. Chem. Soc. Rev. 42 (15) (2013) 6236–6249.

[40] V.B. Veljković, J.M. Avramović, O.S. Stamenković, Biodiesel production by ultrasound-assisted transesterification: state of the art and the perspectives, Renew. Sustain. Energy Rev. 16 (2) (2012) 1193–1209, https://doi.org/10.1016/j.rser.2011.11.022.

[41] N. Melais, M. Boukachabia, L. Aribi-Zouioueche, O. Riant, Easy preparation of enantiomerically enriched heteroaromatic alcohols through lipase-catalyzed acylation with succinic anhydride under unconventional activation, Bioprocess Biosyst. Eng. 38 (8) (2015) 1579–1588, https://doi.org/10.1007/s00449-015-1400-0.

[42] K. Zhu, H. Liu, P. Han, P. Wei, Study of ultrasound-promoted, lipase-catalyzed synthesis of fructose ester, Front. Chem. Eng. China 4 (3) (2010) 367–371, https://doi.org/10.1007/s11705-009-0312-4.

[43] S.R. Bansode, V.K. Rathod, Ultrasound assisted lipase catalysed synthesis of isoamyl butyxzfhtgr42134342rate, Process Biochem. 49 (8) (2014) 1297–1303, https://doi.org/10.1016/j.procbio.2014.04.018.

[44] V.G. Deshmane, P.R. Gogate, A.B. Pandit, Ultrasound assisted synthesis of isopropyl esters from palm fatty acid distillate, Ultrason. Sonochem. 16 (3) (2009) 345–350, https://doi.org/10.1016/j.ultsonch.2008.09.004.

[45] Y.M. Xiao, Q. Wu, Y. Cai, X.F. Lin, Ultrasound-accelerated enzymatic synthesis of sugar esters in nonaqueous solvents, Carbohydr. Res. 340 (13) (2005) 2097–2103, https://doi.org/10.1016/j.carres.2005.06.027.

[46] M. Zoumpanioti, P. Parmaklis, P.D. De María, H. Stamatis, J.V. Sinisterra, A. Xenakis, Esterification reactions catalyzed by lipases immobilized in organogels: effect of temperature and substrate diffusion, Biotechnol. Lett. 30 (9) (2008) 1627–1631, https://doi.org/10.1007/s10529-008-9734-1.

[47] E.C.S. Brenelli, J.L.N. Fernandes, Stereoselective acylations of 1,2-azidoalcohols with vinyl acetate, catalyzed by lipase Amano PS, Tetrahedron Asymmetry 14 (10) (2003) 1255–1259, https://doi.org/10.1016/S0957-4166(03)00206-4.

[48] E.B. Pereira, G.M. Zanin, H.F. Castro, Immobilization and catalytic properties of lipase on chitosan for hydrolysis and esterification reactions, Braz. J. Chem. Eng. 20 (2003) 343–355.

[49] G. Hedström, S. Backlund, F. Eriksson, Influence of diffusion on the kinetics of an enzyme-catalyzed reaction in gelatin-based gels, J. Colloid Interface Sci. 239 (2001) 190–195, https://doi.org/10.1006/JCIS.2001.7552.

[50] W.W. Zhang, Y.J. Zhou, H. Ting, X.Q. Yu, Enhancement of activity and stability of lipase by microemulsion-based organogels (MBGs) immobilization and application for synthesis of arylethyl acetate, J. Mol. Catal. B Enzym. 78 (2012) 65–71, https://doi.org/10.1016/j.molcatb.2012.02.005.

[51] T. Raghavendra, D. Sayania, D. Madamwar, Synthesis of the "green apple ester" ethyl valerate in organic solvents by Candida rugosa lipase immobilized in MBGs in organic solvents: effects of immobilization and reaction parameters, J. Mol. Catal. B Enzym. 63 (1-2) (2010) 31–38, https://doi.org/10.1016/j.molcatb.2009.11.015.

[52] V.C. Badgujar, K.C. Badgujar, P.M. Yeole, B.M. Bhanage, Immobilization of Rhizomucor miehei lipase on a polymeric film for synthesis of important fatty acid esters: kinetics and application studies, Bioprocess Biosyst. Eng. 40 (10) (2017) 1463–1478, https://doi.org/10.1007/s00449-017-1804-0.

[53] K.P. Dhake, P.J. Tambade, Z.S. Qureshi, R.S. Singhal, B.M. Bhanage, HPMC-PVA film immobilized rhizopus oryzae lipase as a biocatalyst for transesterification reaction, ACS Catal. 1 (4) (2011) 316–322, https://doi.org/10.1021/cs100162t.

[54] G. Ozyilmaz, E. Gezer, Production of aroma esters by immobilized Candida rugosa and porcine pancreatic lipase into calcium alginate gel, J. Mol. Catal. B. Enzym. 3–4 (2010) 140–145, https://doi.org/10.1016/J.MOLCATB.2009.04.013.
[55] F.M. Ali, F. Maiz, Structural, optical and AFM characterization of PVA:La^{3+} polymer films, Phys. B Condens. Matter. 530 (2018) 19–23, https://doi.org/10.1016/J.PHYSB.2017.10.124.
[56] B. Chen, N. Pernodet, M.H. Rafailovich, A. Bakhtina, R.A. Gross, Protein immobilization on epoxy-activated thin polymer films: effect of surface wettability and enzyme loading, Langmuir 24 (23) (2008) 13457–13464, https://doi.org/10.1021/LA8019952.

gels

MDPI

Article

(Hydroxypropyl)methyl Cellulose-Chitosan Film as a Matrix for Lipase Immobilization—Part II: Structural Studies

Evdokia Vassiliadi [1,2], Marta Tsirigotis-Maniecka [3], Henry E. Symons [4], Pierangelo Gobbo [5], Frédéric Nallet [6], Aristotelis Xenakis [1] and Maria Zoumpanioti [1,*]

1 Institute of Chemical Biology, National Hellenic Research Foundation (NHRF), 48 Vassileos Constantinou Ave., 11635 Athens, Greece
2 Department of Biological Applications and Technology, University of Ioannina, 45110 Ioannina, Greece
3 Faculty of Chemistry, Wrocław University of Science and Technology, 50-370 Wroclaw, Poland
4 School of Chemistry, University of Bristol, Bristol BS8 1TS, UK
5 Department of Chemical and Pharmaceutical Sciences, University of Trieste, 34127 Trieste, Italy
6 Centre de Recherche Paul-Pascal, University Bordeaux, CNRS, UMR 5031, 115 Avenue du Docteur-Schweitzer, 33600 Pessac, France
* Correspondence: mariaz@eie.gr; Tel.: +302-107-273-796

Abstract: The present work reports on the structural study of a film made of a hybrid blend of biopolymers used as an enzyme carrier. A cellulose derivative (HPMC) and chitosan (CS) were combined in order to formulate a film on which *Mucor miehei* lipase was immobilized. The film was successfully used as a biocatalyst; however, little is known about the structure of the system. Therefore, small-angle X-ray scattering, Fourier transform infrared spectroscopy (FTIR), optical microscopy, and scanning electron microscopy (SEM), as well as microindentation measurements, were used to shed light on the structure of the promising biocatalyst. Among the results, intermolecular hydrogen bonds were observed between the amide groups of the two polymers and the lipase. The presence of the enzyme does not seem to affect the mechanical properties of the matrix. The used film after 35 cycles of reaction seemed to be fatigued and had lost part of its humidity, explaining the reduction of the enzyme activity.

Keywords: hydroxypropylmethyl cellulose; characterization; blended polymers; film; enzyme immobilization; lipase

Citation: Vassiliadi, E.; Tsirigotis-Maniecka, M.; Symons, H.E.; Gobbo, P.; Nallet, F.; Xenakis, A.; Zoumpanioti, M. (Hydroxypropyl)methyl Cellulose-Chitosan Film as a Matrix for Lipase Immobilization—Part II: Structural Studies. *Gels* **2022**, *8*, 595. https://doi.org/10.3390/gels8090595

Academic Editors: Christian Demitri, Laura Riva and Lorenzo Bonetti

Received: 14 August 2022
Accepted: 13 September 2022
Published: 17 September 2022

1. Introduction

Natural-polymer-based matrices are widely used for enzyme immobilization [1] due to their practical significance in the design of biocatalytic hydrogels/membranes/vessels for industrial synthesis [2,3]. In addition, compared to free enzymes, immobilized ones are more resistant to environmental changes. Furthermore, with enhanced stability, immobilized enzymes can be easily separated from the reaction mixture and reused, thereby simplifying the separation and recovery processes [4,5].

Enzyme immobilization can take place by physical or chemical methods [6]. Physical methods, where no covalent bonds appear, can be either absorption [7,8] or entrapment [4,9], where enzymes are adsorbed on the surfaces of support carriers or occluded in polymeric networks, respectively. In these cases, no additional coupling agents and modification steps are required for the immobilization, offering thus a low-cost preparation. The performance of the immobilized enzymes depends on the properties of the supporting material used as well as the composition and structure of the immobilization matrix.

Cellulose, chitin, and their derivatives are attractive materials for enzyme immobilization [10]. They are the two most abundant natural polymers. The matrices they produce do not alter under physiological conditions. In addition, their hydrophilic/hydrophobic character can be adjusted according to the needs of the

application [11,12]. While in most cases, the formation of hydrogels that are based on native cellulose or chitin is a two-step process which involves firstly dissolution and afterwards cross-linking (i.e., gelation) [13], there is also a different approach by which only the physical interactions affect the linking of the two polymers. In the latter case, the derivatives of the polymers are most commonly used as they are much easier to fabricate into hydrogels because they are water- or acid-soluble [14]. To add to this, cellulose and cellulose derivatives are the most studied polymers as they are biocompatible, cost-effective, and renewable [15,16].

For film carriers, an understanding of the microstructure of the film is critical since it determines the advantages and disadvantages for their potential application. Several studies offer a detailed analysis of polymer mixtures morphologically and structurally [15,17,18]. The techniques used aim to reveal the structure and the film surface image, as well as to present the interaction between the system's compounds [19,20].

The present study is an attempt to understand the morphology and structure of a well-studied biocompatible film, in an effort to provide insight into the performance of the biocatalyst that has been proven to give good results [21]. Having already studied the optimal conditions in which the film as a biocatalyst could perform on the model reaction of propyl laurate synthesis, the first morphological results were obtained with the use of atomic force microscopy. The results triggered the interest to perform a deeper analysis on this easily reusable biocatalyst [21]. Therefore, the aim of the present study is to structurally characterize a biocatalyst based on the blend of two polymers, namely, (hydroxypropyl)methyl cellulose (HPMC) and chitosan (CS). For this purpose, small-angle X-ray scattering (SAXS) and Fourier transform infrared spectroscopy (FTIR) studies were conducted, whereas morphological analysis was conducted via optical and scanning electron microscopy (SEM). For the physicochemical studies, the electrophoretic zeta potential (ζ) was measured, and the moisture content of the films was determined gravimetrically using a moisture analyzer. Lastly, to investigate the mechanical properties, microindentation measurements were carried out.

2. Results and Discussion

The purpose of the present study is to thoroughly describe the structure of a biocatalyst used successfully in a previous work [21]. In this work, the two polymers (namely, HPMC and chitosan) were combined in order to formulate a film on which *Mucor miehei* lipase was immobilized. To investigate the ability of the matrix to maintain the enzyme's catalytic activity, the biocatalyst was tested towards the model esterification reaction of propyl laurate synthesis, a 6 h profile of which can be seen in Figure 1.

In that perspective, several parameters were studied. The ratio of the polymers used was examined and the ratio HPMC:CS = 2:1 proved to form the most promising matrix. Increasing the amount of the immobilized enzyme appears to improve the reaction yield, indicating, however, mass transfer limitations. The optimum catalytic performance was observed for the biocatalyst with enzyme:polymer ratio = 1/200. The enzyme-loaded film presented a remarkable reusability, since it could be used for up to 35 times without loss of activity [20].

Before small-scale investigation of its properties, several macroscopical observations were made. Each polymer solution mixture, regardless of the HPMC/CS ratio used to prepare it, was macroscopically homogeneous [22]. When only HPMC was used for film preparation, it resulted in a transparent, colorless film, whereas in the presence of chitosan, the films prepared had a slightly yellowish color. This is in accordance with previous reports on films that contained chitosan [17]. Furthermore, the presence of the immobilized enzyme provided an opaque effect on the film.

The aim of the study is to structurally characterize the biocatalyst which will be proposed for the synthesis of high-added-value products of industrial interest.

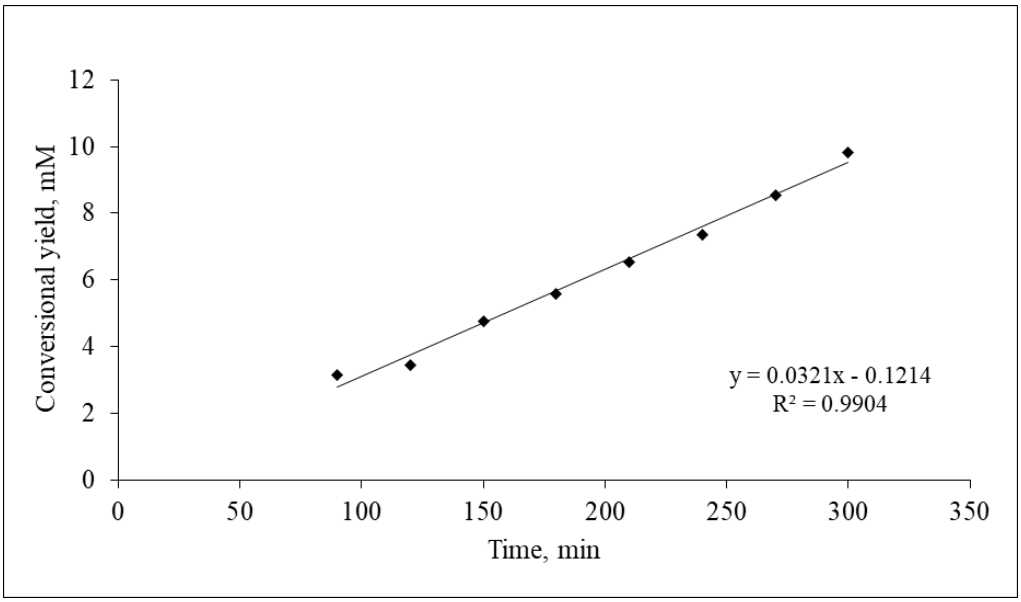

Figure 1. Reaction profile, for up to six hours, of the esterification of 1-propanol with lauric acid (100 mM, each) catalyzed by *M. miehei* lipase immobilized on HPMC:chitosan film (2:1 ratio). Lipase concentration, 0.3 mg/g of film; 10 mL of isooctane as solvent, at room temperature.

2.1. Structural Studies of the Biocatalyst via Spectroscopic Methods

2.1.1. Small-Angle X-ray Scattering (SAXS)

The structural studies of the HPMC–CS films were conducted using two spectroscopic techniques to reveal any alterations of the polysaccharide-based matrix after lipase incorporation. The first approach involved using a small-angle X-ray scattering (SAXS) technique that is an analytical and nondestructive method used to investigate nanostructures in liquids and solids. SAXS is able to probe the length scales of 10–1000 Å and therefore is an appropriate method to determine the size and the structure of gels and films. In the present study, this method was used in order to clarify the possible alterations that may be provoked in the film matrix after the incorporation of the enzyme. Figure 2 represents the intensity profile of the empty (blue curve) or loaded with enzyme (green curve) film.

According to Figure 1, adding the enzyme to the HPMC–CS system has very little structural effect at scales probed by SAXS. The intensity upturn observed for low q values (below *circa* 2.5×10^{-2} $Å^{-1}$), with a scaling $1/q^4$, as commonly observed in locally heterogeneous systems such as gels, is less pronounced for the enzyme-free film. Supramolecular objects in the reference HPMC–CS, as well as for enzyme-loaded HPMC–CS films, look similar to elongated cylinders, as suggested by the (not fully developed) intermediate regime scaling such as $1/q$ with very similar diameters, since the large-q crossover from the intermediate regime to the asymptotic regime (also known as Porod's law) occurs in the same scattering wave vector range, about 15 $Å^{-1}$ [20].

2.1.2. Fourier Transform Infrared (FTIR)

Fourier transform infrared (FTIR) spectroscopy is a nondestructive technique which can be used to monitor discrete changes related to the interactions between specific functional groups of the constituents of the HPMC–CS films. Several absorption bands typical for polysaccharides and lipase were observed in the spectra (Figure 3). The wide band observed in the 3600–3200 cm^{-1} corresponds to overlapped signals from inter- or intramolecular stretching vibrations of the OH and –NH groups [16], and symmetrical and asymmetrical vibrations of the NH_2 groups [23]. The signals visible around the 2900 cm^{-1} shift are assigned to the stretching vibrations of the C–H bonds in the propyl group of HPMC. The band located around shift 1650 cm^{-1} (the most pronounced for the HPMC:CS = 2:1 used film) can be ascribed to amide I [24]. Signals visible in region I (~1545 cm^{-1}) (Figure 3B),

assigned to the amide II band, which is a combination of $–NH_2$ in plane bending and C–N stretching vibrations, are the most pronounced for the lipase-loaded film. Additionally, the presence of these signals confirms the formation of intermolecular hydrogen bonds between the amide groups of CS and lipase and hydroxyl groups of HPMC [24]. The signals in region II (~1410 cm^{-1}) (Figure 3B), assigned to the in-phase combination of the vibration of N–H deformation with C–N in amides III with a contribution of symmetric deformation from $–COO^-$ [3,25], are visible for films with or without lipase. The signals visible in region III (Figure 3B) in the range of ~1060–1020 cm^{-1} can be ascribed to the stretching skeletal vibrations of the C–O–C bridge of the pyranose ring in HPMC, and asymmetric deformation of $–COO^-$ [24] are the weakest for the unloaded film, while the signal from –COOH (1738 cm^{-1}) is visible only in the spectrum of the film used. When comparing the spectroscopic behavior of the unloaded film and the enzyme-loaded film, it can be confirmed that there are some weak electrostatic interactions between the polysaccharides and the lipase.

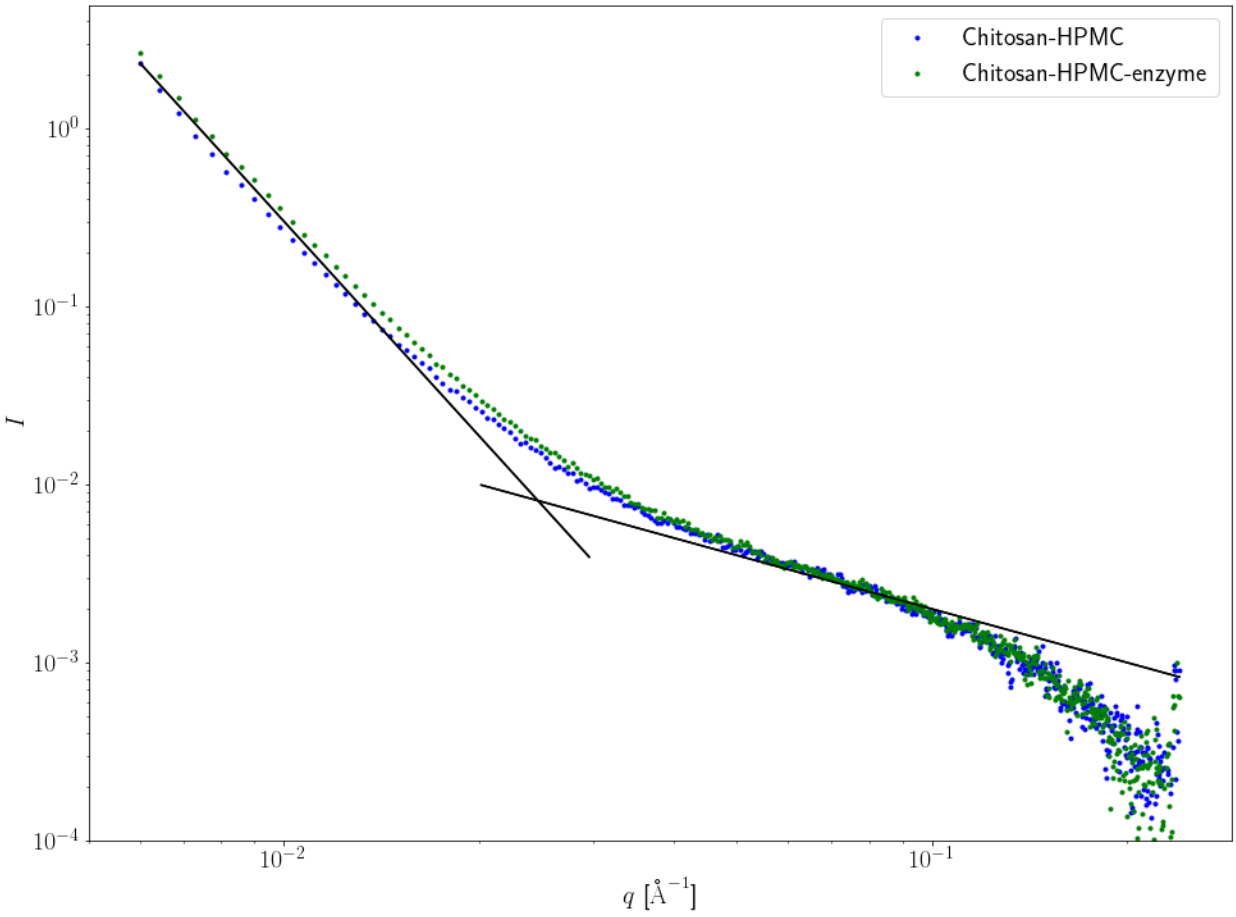

Figure 2. Processed (background-subtracted) data; double logarithmic scale; SAXS spectra for HPMC:CS films. Blue curve: empty film; green curve: enzyme-loaded film. HPMC:CS = 2:1. Enzyme: *M. miehei* lipase, 1 mg/g of film. The two superimposed black lines correspond to power-law decays, as $1/q^4$ and $1/q$, respectively.

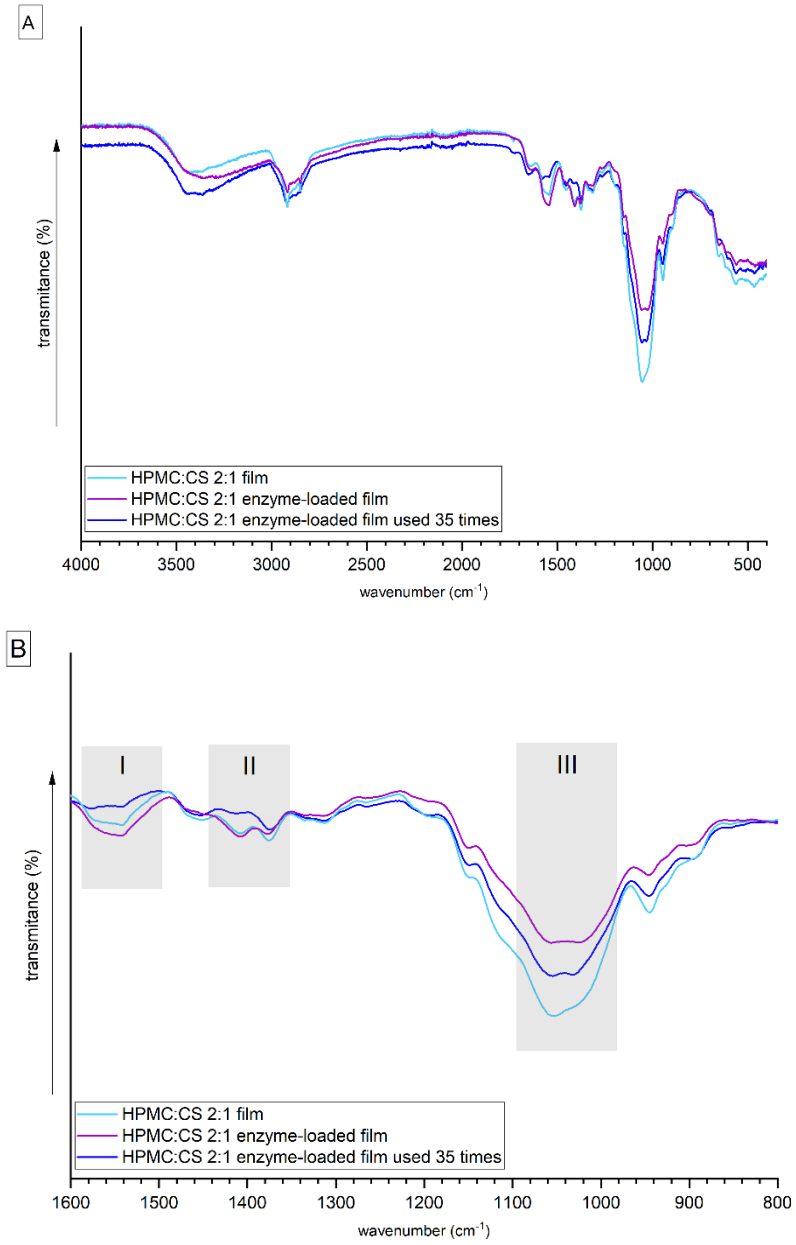

Figure 3. (**A**) Full FTIR spectra for HPMC–CS film. Light blue curve: unloaded film; purple curve: enzyme–loaded film; blue curve: enzyme–loaded film after 35–times usage cycles. (**B**) Focused FTIR spectra from 800 to 1600 cm^{-1}. HPMC:CS = 2:1.

2.2. Physicochemical Studies of the Biocatalyst

The electrostatic interaction between the enzyme and the polysaccharides is also confirmed by measurements of the zeta potential of aqueous solutions of polysaccharides and the enzyme. The ζ values of 2% solutions of HPMC and CS were as expected, typical for these polysaccharides [26], -1.94 ± 3.82 and 33.35 ± 4.53, respectively. The ζ value of polyelectrolytes solutions is the result of a surface charge that strongly depends on the pH of the environment due to the presence of ionizable functional groups within their structure, i.e., amine in CS and carboxylic in HPMC [27]. The mixing of HPMC and CS solution caused an increase in the pH of the solution from ~2.0 (for CS) to ~5.0 (for HPMC:CS = 2:1); thus, the amine groups were still partially protonated, while carboxylic groups were already partially deprotonated. The attractive electrostatic interactions between COO and NH_3^+ (2:1) caused a significant neutralization of the surface charge of polyelectrolytes, which greatly reduced the number of positive charges and affected the zeta potential value to

$\zeta = 18.95 \pm 6.22$. Adding the enzyme to the HPMC–CS mixture caused an increase of ζ value to 21.90 ± 5.10, which may suggest that the amine groups present in lipase also exploit carboxylic groups of HPMC, further neutralizing the surface charge.

The aqueous environment is beneficial for enzymes, including lipases, and thus enzyme immobilization in hydrophilic polymeric structures, i.e., matrices, helps to maintain their catalytic activity. Although the fabricated biocatalyst is designed to work in organic media, the presence of residual water molecules may be desirable for the enzyme and may be important to keep the polysaccharide-based matrix physically intact. The dehydration of the hydrophilic matrix may lead to weakening of its structure and reduced resistance to mechanical disturbance. Loading the films with enzyme caused more water molecules to remain trapped within the matrix, as the unloaded film had 1.4% moisture content, while the moisture content increased for the loaded film to 2.7%. Water molecules trapped in the film structure provide the conditions for the enzyme to remain active, but when the moisture content was reduced to 0.9% for the HPMC–CS enzyme-loaded film after 35 uses, not only did the enzyme activity drop significantly [21], but those nonpolar and unfavorable for polysaccharides conditions also influenced the morphology of the film. Thus, the results suggest that extensive usage of the film indirectly causes changes in the chemical structure of the enzyme (chemical degradation or precipitation) as a result of the progression of dehydration of the polysaccharide-based film. This is undoubtedly reflected in the alteration of the structure of the polysaccharide-based matrix.

2.3. Morphological Studies of the Biocatalyst via Optical Microscopy

Initial morphological studies showed that the HPMC, CS, and unloaded HPMC–CS films were transparent (Figures 4 and 5). Lipase loading reduced the transparency of the film, as it became slightly opaque with areas of white color and turbidity affecting light transmission. This is probably an effect of crystallization of lipase and/or buffer salts in the film after drying.

The composition of the matrix, as well as immobilization of the enzyme, clearly influences the appearance of the film (Figure 4). The HPMC film is rather patchy, with numerous bumps and many crystals (approximately 20 μm in diameter), both on the entire surface and inside the film. The CS film is rather smooth, mostly homogeneous, with only a few lumps. It was observed that the higher the film's CS content, the smoother its surface became (Figure 4B–D). This is probably a result of lower viscosity of the HPMC/CS mixture than that of the HPMC solution. In addition, the film consisting of HPMC and CS is less porous. The polyelectrolyte complexes formed between CS and HPMC cause a change in the degree of dispersion of polymer chains and phase structure, and a change in intermolecular interactions at the interface of the film. Furthermore, it was observed that when the enzyme is incorporated into the film, fewer crystals are visible. A similar result was observed via AFM in our previous study, where the enzyme seemed to level the roughness of the film [21]. To add to this, long, narrow channels appear across most of the surface of the film (Figure 5). This may suggest that immobilization of lipase affects the continuity and mechanical properties of the film's surface. The film, after repeated use in organic media, seems fatigued, as it has even more longitude marks. The resulting electrostatic complexes are not very stable; therefore, the use of the film under the conditions of an organic solvent may cause structural changes in the film, especially since the biopolymers used are not compatible with isooctane (which was used as a medium for the catalytic reaction).

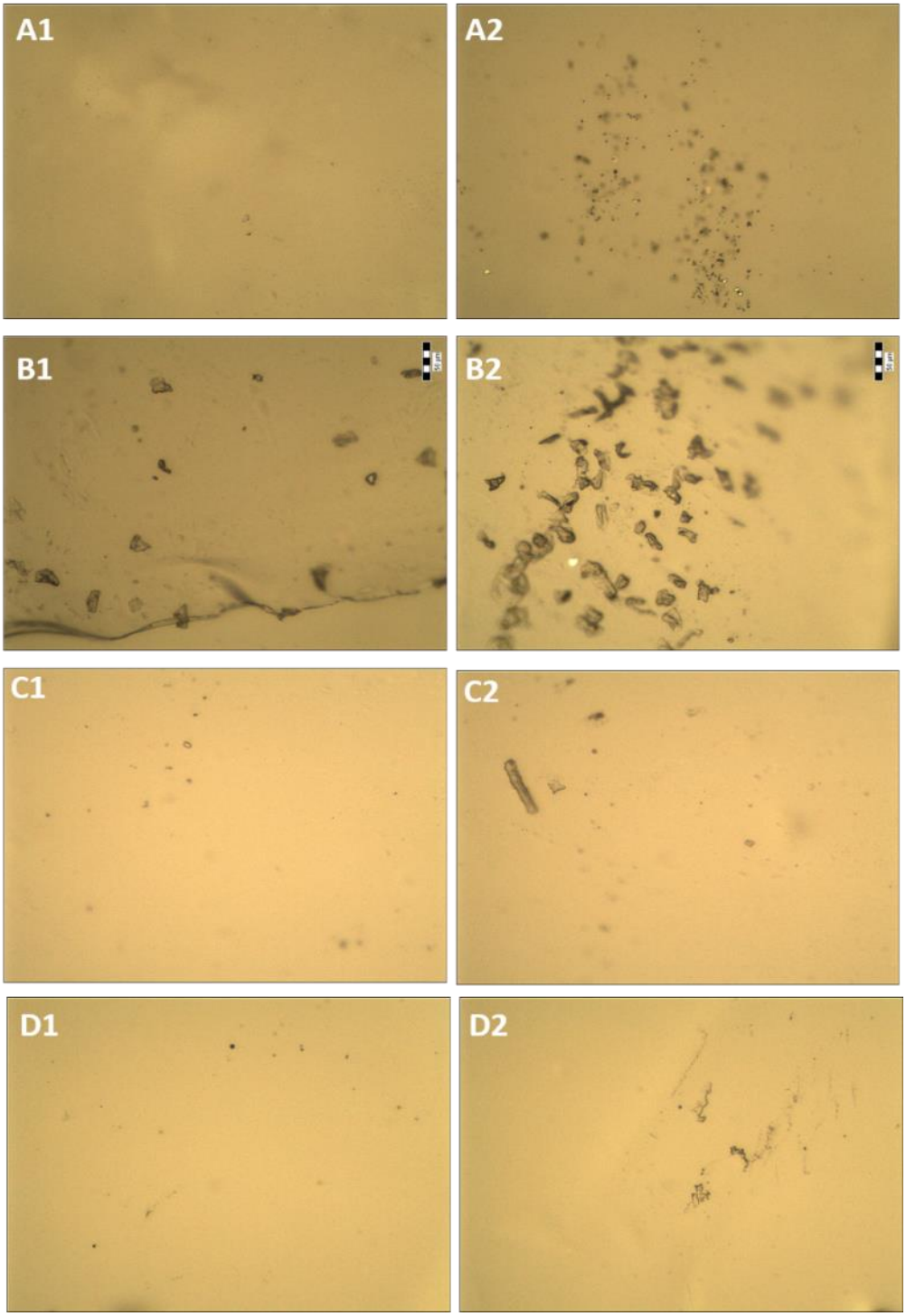

Figure 4. Optical images of unloaded films: (**A1**) and (**A2**) different surface sections of CS film; (**B1**) and (**B2**) different surface sections of HPMC film; (**C1**) and (**C2**) different surface sections of HPMC:CS = 1:1 film; (**D1**) and (**D2**) different surface sections of HPMC:CS = 2:1 film. The scale bar represents 50 μm.

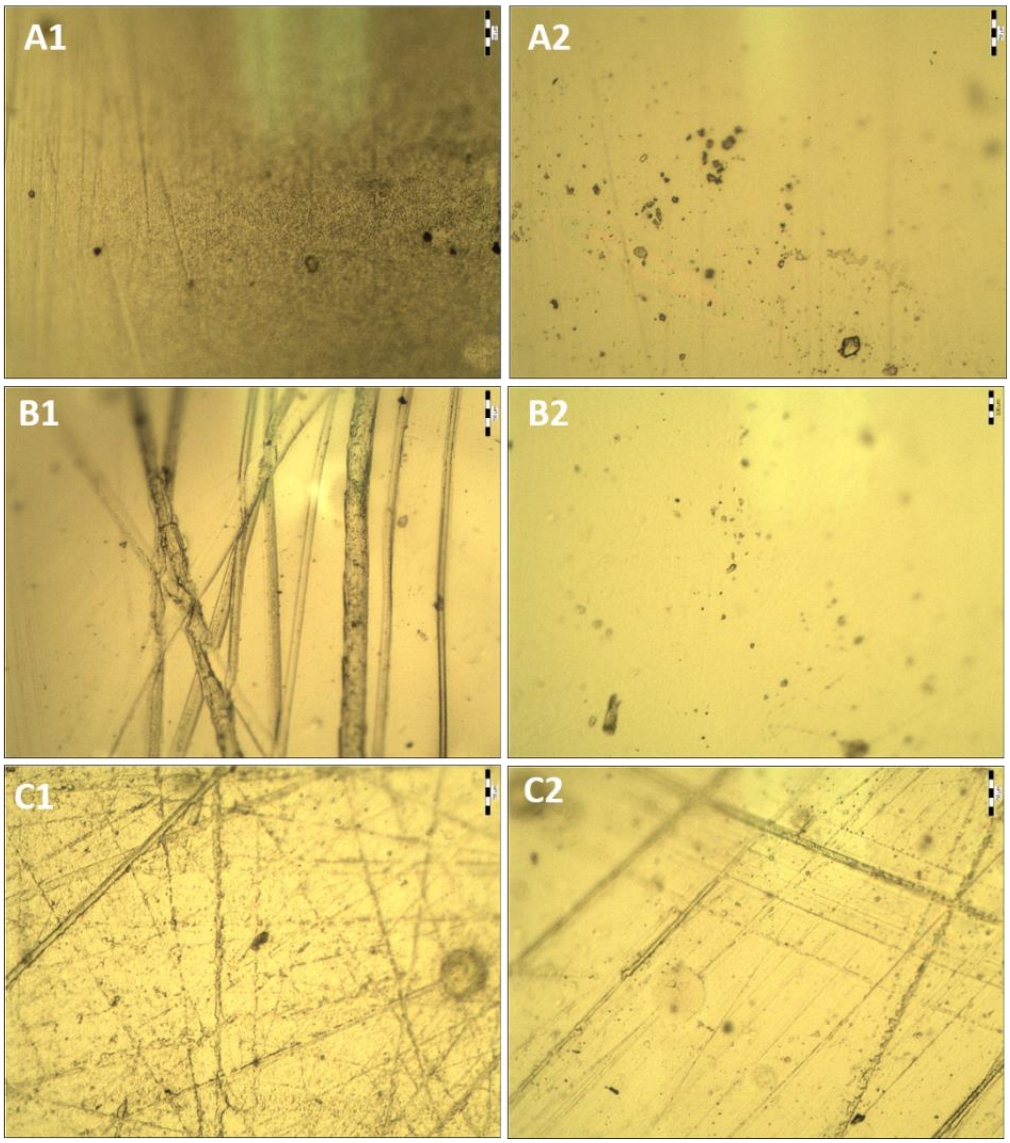

Figure 5. Optical images of HPMC–CS (2:1) unloaded film (**A1**); different surface section of unloaded film (**A2**); enzyme–loaded film (**B1**); different section of enzyme-loaded film (**B2**); enzyme-loaded film after 35 usage cycles (**C1**); different surface section of enzyme-loaded film after 35 usage cycles (**C2**). The scale bar represents 50 μm.

2.4. Microstructural Studies of the Biocatalyst via Scanning Electron Microscopy

Scanning electron microscopy (SEM) was used to investigate valuable details of the microstructural changes in the morphology of films in the absence and presence of the enzyme, as well as the effect of repeatedly using the biocatalyst 35 times in organic solvent. SEM images show that the structure of the films differs along with its composition (Figure 6). The surface of all unloaded films, regardless of their composition, was rather smooth, continuous, and even. When the enzyme was loaded, some fine lines appeared. Furthermore, on the surface of the film used, some slight clumps and irregularities occurred (Figure 6C). It is most likely that the lines on the surface of lipase-loaded films were caused by the higher force needed to detach the films from the glass plates, as enzyme addition causes slightly greater stiffness to the film [28].

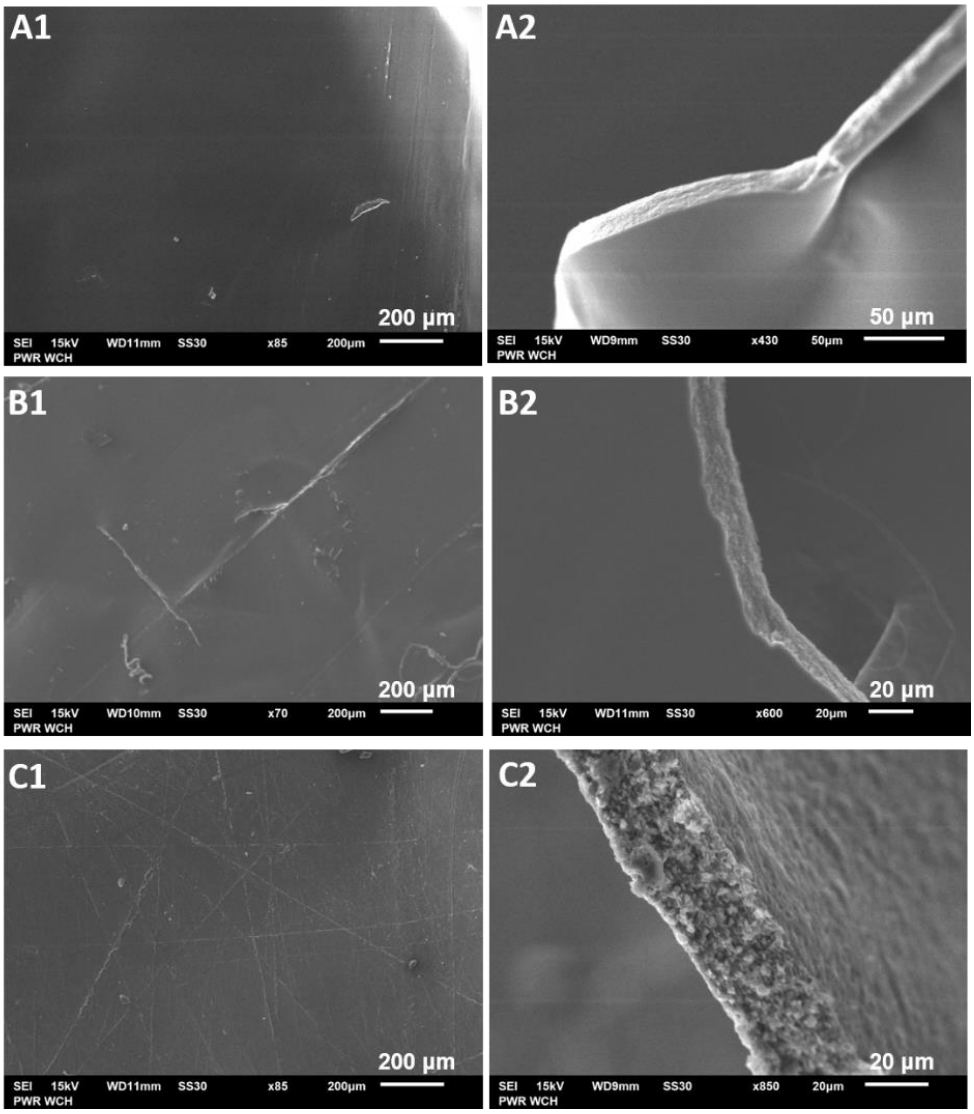

Figure 6. SEM images of (**A1**) unloaded film; (**A2**) cross section of unloaded film; (**B1**) enzyme-loaded film; (**B2**) cross section of enzyme-loaded film (**C1**) enzyme-loaded film after 35 usage cycles. HPMC:CS = 2:1; (**C2**) cross section of enzyme-loaded film after 35 usage cycles.

The cross sections of the films revealed that immobilization of the enzyme slightly changes the structure of the film (Figure 6B2). The film, prior to enzyme loading, due to the structural compatibility between CS and HPMC, was slightly elastic, smooth, compact, and without phase separation. After loading the enzyme, the film became brittle and uneven (lumpy), with a tendency to fracture, but was still nonporous. This indicated that the enzyme was evenly distributed, which is in accordance with results reported in other studies [22,29–31]. The film, after repeated use in organic media, became softer and more susceptible to mechanical stress, while multiple shallow pores and granular structures seem to appear inside the enzyme-loaded film after 35 usage cycles. This is clearly visible in the intersection pictures and is probably caused by dehydration of the film, since, when water evaporated during multiple usage cycles, polymer chains and lipase were locally accumulated in the form of granules.

2.5. Mechanical and Topographical Characterization

To clarify these points, strength analysis took place via mechanical and topographical characterization. The thickness of HPMC–CS film was measured by optical microscopy and profilometry measurements, shown in Figure 7. Optical micrographs of the edge of a film

revealed a mean thickness of approximately 16 µm. Profilometry measurements yielded a mean height of 22 µm; however, these measurements also revealed notable fluctuations in height from 19–26 µm across a section of film investigated. Both values appear to be in good agreement with the SEM analysis presented in Section 2.4.

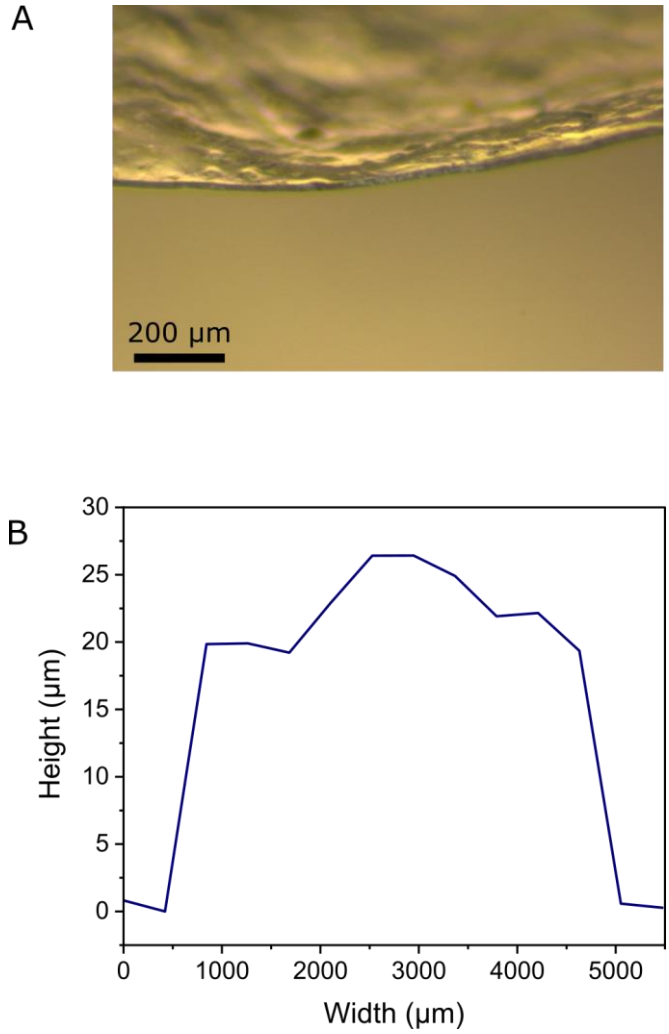

Figure 7. (**A**) Optical micrograph of the edge of an HPMC–CS film. (**B**) Height profile of a section of HPMC–CS film.

The Young's moduli of HPMC–CS films and their spatial relationships were investigated using microindentation measurements. In this method, a microscale (50 µm diameter) spherical probe was indented into films (folded threefold to ensure minimal influence of the underlying substrate), and force was measured as a function of probe displacement. All materials displayed rate-independent hysteresis between loading and unloading data, typical of an elastoplastic material response, and are therefore best modeled by the Oliver–Pharr approach [32]. In this analysis method, only unloading data are fit (as described in the Methods section), based on the assumption that both plastic and elastic deformation occur during the loading phase, whereas only an elastic response is present during unloading [33]. Arrays of indentation measurements (15 × 15 locations) across a 3 × 3 mm area were made for HPMC–CS and HPMC–CS enzyme-loaded films, prior to use, and after 5 and 10 usage cycles. Young's moduli maps obtained from these individual tests (along with accompanying microscopy images) are presented in Figures S2 and S3, and are summarized in Figure 8.

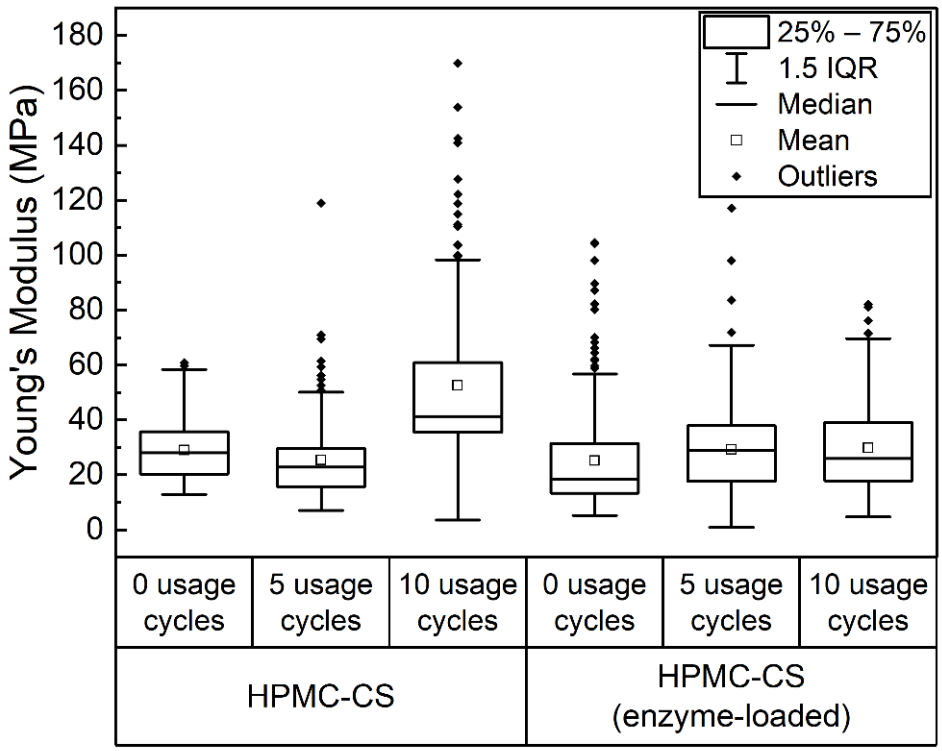

Figure 8. Box plot displaying Young's modulus values obtained from HPMC–CS films (with and without enzyme loading) before usages, and after 5 and 10 usage cycles. Each plot indicates the distribution of 225 datapoints collected from measurements across a 3 × 3 mm area of film.

The distributions of mechanical properties in Figure 8 are notably broad, with individual measurements (Figures S2 and S3 revealing a high degree of spatial heterogeneity in the stiffness of all films with localized regions of substantially higher Young's moduli. These broadly distributed mechanical properties could be due to inhomogeneity in film composition from the drying process, or simply a result of the aforementioned variation in film thickness. Importantly, however, no significant differences in the mechanical properties are evident between the two film types, with values of 29.9 ± 10.6 MPa (mean ± SD) and 25.2 ± 19.0 MPa for new films without and with enzyme loading, respectively. Furthermore, statistical analysis showed no substantial changes in the mechanical properties of both types of films after usage, which maintained mean Young's modulus values between 25 and 30 MPa. The only exception was the HPMC–CS film tested after 10 usage cycles, which, due to the high inhomogeneity of the sample, displayed a much wider distribution of Young's modulus values and, consequently, a statistically higher mean Young's modulus of 52.5 ± 26.7 MPa. However, in general, the stability of the Young's modulus of these films is in good agreement with previous findings that films could undergo up to 35 usage cycles [21].

3. Conclusions

Hydroxypropyl)methyl cellulose and chitosan were combined to form a film which was used to immobilize lipase from *Mucor miehei*. The main aim of the present work was to structurally investigate the empty and enzyme-loaded film. Enzyme loading onto the matrix appears to have very little effect on the structure of the film. Mixing the original HPMC and CS solutions resulted in an increase of the solution's pH, and adding the enzyme resulted in an even more neutral surface charge. The presence of a combination of $–NH_2$ in plane bending and C–N stretching vibrations showed the formation of intermolecular hydrogen bonds between the amide groups of two polymers with the lipase. Weak electrostatic interactions between the polysaccharides and the lipase were observed. Regarding

the reuse of the biocatalyst, it can be stated that the texture became quite fatigued, and in the intersection some granules could be observed. This could be due to the moisture reduction of the matrix after repeated use. Furthermore, no significant differences in the mechanical properties were evident between the loaded and unloaded films. The two polymers seem to have good interaction, and taking into account the drying and loading with enzyme process, which does not undergo any smoothing steps, the film offers a stable environment with enough water for the enzyme to perform multiple times.

4. Materials and Methods

4.1. Materials

The films prepared within this study were based on two natural polymers (hydroxypropyl)methyl cellulose (HPMC) (3600–5500 mPa.s), which was obtained from Sigma, Darmstadt, Germany, and chitosan (CS) from shrimp and other crustacean shells (viscosity 200–600 mPa.s, 0.5% in 0.5% acetic acid, 20 °C; deacetylation value: 80%, molecular mass 1526.464 g/mol), which was purchased from TCI, Belgium. Lauric acid was obtained from Sigma, Darmstadt, Germany. Acetic acid was obtained from LachNer, Neratovice, Czech Republic. All other materials were at least reagent grade. Millipore Milli-Q water was used for the preparation of gels and buffer solutions. Lipase from *Mucor miehei* (*M. miehei*) was supplied by Fluka, Basel, Switzerland, and had a specific activity of 1.19 U/mg of protein (1 U corresponds to the amount of enzyme which liberates 1 μmol butyric acid per min at pH 8.0 and 40 °C using tributyrin as substrate).

4.2. Methods

4.2.1. Film Preparation

Films based on HPMC–CS were prepared by diluting HPMC in distilled water and CS in 1% acetic acid, resulting in a solution of 2% *w*/*w*, each. The two solutions were left overnight until fully transparent and homogeneous. Then, a mixture of them was prepared in the right ratio, for each experiment, and placed on a Petri dish to dry overnight. In the case of single-polymer film, only one of the two polymers' solutions was placed on a Petri dish. After drying, approximately 0.3 g of films were produced. After the two solutions were mixed, no phase separation could be observed regardless of the composition, showing the fine biopolymers' compatibility. The procedure is illustrated in Supplementary Materials Figure S1.

4.2.2. Enzyme-Loaded Films Preparation

To prepare the biocatalyst (HPMC–CS film loaded with lipase (2:1)), the appropriate amount of Tris/HCl buffer, pH 7.5 containing lipase, was added to the polymers' solution, prior to drying. In a typical experiment, 1 g of CS solution 2% *w*/*w* was mixed with 2 g of HPMC solution 2% *w*/*w*, followed by the addition of 30 μL of buffer containing 0.3 mg lipase and stirred gently at room temperature. The final mixture was left overnight on a Petri dish to dry, thus formulating a film in which the enzyme was immobilized. After peeling the film from the Petri dish, it was washed three times with 5 mL of isooctane to remove any enzyme molecules that may not be effectively immobilized on the network and leak to the reaction solvent. The final biocatalyst produced contained 1 mg lipase/g of film.

4.2.3. Reuse of Film

In the case of reused films, the biocatalyst (HPMC:CS film loaded with lipase (2:1)) was used for the repeated catalysis of propyl laurate synthesis. For this purpose, approximately 0.3 g of a film containing 1 mg lipase/g of film was placed in a screw-cap bottle with 10 mL of the appropriate organic solvent containing lauric acid and 1-propanol (100 mM each). Each day, the film was placed in a new bottle with fresh solvent and substrates, and after several uses, part of the film was cut and studied.

4.2.4. Small-Angle X-ray Scattering (SAXS) Measurements

SAXS experiments for films in the presence and absence of the immobilized enzyme or in the presence or absence of glycerol were performed on an XEUSS 2.0 (XENOCS, Grenoble, France) with a GeniX 3D source delivering a 8 keV beam coupled to an FOX 3D single reflection optical mirror centered on the Cu Kα radiation (λ = 1.54 Å). The beam was further collimated and defined by a set of two motorized scatterless slits. The samples were placed in capillaries for solid samples and were folded twice to obtain a stronger signal. The samples, under vacuum as the whole flight path from the FOX3D mirror to the detector window, were exposed for 3 hours. The data were collected by a two-dimensional PILATUS-300k detector (DECTRIS, Baden-Dättwill, Switzerland) placed perpendicular to the direct beam at a distance of 1634 mm, calibrated with a Silver behenate standard. Rectangular images with shape (487, 619—horizontal, vertical) were obtained and further processed with the FOXTROT 3.4.9-3471 software (collaboration between XENOCS (Grenoble, FRANCE) and the SOLEIL synchrotron (Gif-sur-Yvette, FRANCE) SWING beamline team), giving access to a range of scattering wave vectors q from typically 0.007 $Å^{-1}$ to 0.24 $Å^{-1}$.

4.2.5. Fourier Transform Infrared Spectroscopy (FTIR)

Fourier transform infrared (FTIR) spectroscopy was used to investigate the functional groups of the polymers that made up the film to determine the possible interactions between their functional groups and the enzyme in the composite systems. The samples were analyzed between 4000 to 400 cm^{-1} with a resolution of 2 cm^{-1} using a Bruker VERTEX 70 V vacuum spectrometer (Bruker Optik GmbH, Birrika, MA, USA) equipped with a diamond attenuated total reflectance (ATR) accessory and Opus software (Bruker Optik GmbH, Ettlingen, Germany) for the spectra analysis.

4.2.6. Microscopic Studies

The film morphology and microstructure were examined via optical microscopy and scanning electron microscopy (SEM). Newly prepared and 35-times repeatedly used enzyme-loaded films, as well as unloaded films, were deposited on a glass slide and subjected to microscopic observations via an optical microscope 41-CX (Olympus, Japan) (with 10× magnification) equipped with a 500MI digital camera (Ataray, Turkey). Quick-photo 2.2 software was used to capture and analyze pictures. Films were also attached to a double-sided carbon tape, sputtered with carbon, and examined using a JSM-6601LV scanning electron microscope (JEOL, Akishima, Japan) (operating voltage 15 kV).

4.2.7. Physiochemical Studies

The moisture content of the HPMC–CS films was determined gravimetrically using the moisture analyzer MB27 (Ohaus, Nänikon, Switzerland), and the moisture content was estimated as a percentage of weight loss after 30 min at 100 °C. The experiment was performed three times for each type of film studied. The electrophoretic zeta potential (ζ) of polyelectrolyte solutions was measured with a Zetasizer Nano ZS (ZEN3600) from Malvern Instruments (UK) at 25 °C equipped with a HeNe laser (632.8 nm) and using a noninvasive backscatter (NIBS) technology. For these measurements, the following solutions were prepared: 2% CS, 2% HPMC, HPMC–CS 2:1 w/w, and HPMC–CS 2:1 w/w with enzyme. The measurements were performed thrice for each solution.

4.2.8. Mechanical and Topographical Studies

The mechanical properties and topography of the HPMC–CS films were determined using an FT-MTA03 (FemtoTools AG, Buchs, Switzerland) equipped with an FT-S2000 microforce sensing probe (range: ±2000 μN, resolution: 0.005 μN) capped with a 50 μm borosilicate glass sphere (BSGMS-2.2 from Cospheric).

For profilometry tests, a single layer of film (approximately 0.5 cm wide) was held taut over a glass slide. Indentation measurements were made from a fixed height across

the width of the film segment and surrounding glass slide. A stick-slip actuator (29 mm vertical range, 1 nm positional resolution) was used, operating in a stepped mode (with 0.5 µm steps and a 0.02 s delay), at a speed of 50 µm/s, until a force of 1500 µN was reached. Data were analyzed by determining the vertical position at which a force of 1000 µN was reached, and calculating the corresponding material height compared to the glass slide.

For mechanical tests, films were first folded into a 3-layer structure, then compressed between two glass slides prior to measurement. Samples were then placed on a glass slide, whilst a light pressure was applied to the edges of the sample with additional glass slides to maintain sample flatness throughout measurement. Measurements were conducted using a piezoscanner (50 µm vertical range, 0.1 nm positional resolution) in a continuous actuation mode to indent the probe into the sample. The film surface was found by applying a force threshold of 3 µN, then retracting the probe 1 µm from the surface to allow the acquisition of baseline data. Measurements were then carried out at a speed of 1 µm s^{-1}, to a maximum force of 30 µN (corresponding to a maximum indentation depth of approximately 0.5 µm), with data collected at a frequency of 200 Hz. Data were collected throughout the approach and indentation into the material (loading) and retraction back to the initial probe position (unloading).

Data were analyzed using a custom Python-based application. For each set of force–displacement data, a contact point was firstly determined by the location of a maximum in the second derivative of force as a function of displacement. Unloading data beyond the contact point were then analyzed using the method described by Oliver and Pharr outlined below [33,34]. A total of 50% of the data with greatest indentation depth were fitted to a power law of the form:

$$P = \alpha\left(h - h_f\right)^m \tag{1}$$

where P is the load at displacement h, m is an exponent set to 1.5 for a spherical indentation probe, and α and h_f are fitting parameters. From these parameters, stiffness ($S = dP/dh$) at peak load (P_{max}) is determined. SP_{max} are then used to calculate the contact depth (h_c) and contact area (A_c) using:

$$h_c = h_{max} - 0.75 \times \frac{P_{max}}{S} \tag{2}$$

$$A_c = \pi\left(2Rh_c - {h_c}^2\right) \tag{3}$$

where h_{max} is the maximum displacement. The reduced modulus (E_R) is then given by:

$$E_R = \frac{S\sqrt{\pi}}{S\sqrt{A_c}} \tag{4}$$

Finally, the Young's modulus of the sample (E_S) is given by:

$$\frac{1}{E_R} = \frac{1 - {\nu_S}^2}{E_S} + \frac{1 - {\nu_P}^2}{E_P} \tag{5}$$

where E_P and ν_P are the Young's modulus and Poisson's ratio of the probe (values for borosilicate glass of 63 Gpa and 0.2 were used), and ν_S is the sample Poisson's ratio, for which a value of 0.4 was used and is typical for biopolymer materials [35].

Supplementary Materials: The following supporting information can be downloaded at: https://www.mdpi.com/article/10.3390/gels8090595/s1, Figure S1: Step-by-step procedure for the formation of the loaded film with enzyme. (A) Powders of the two polymers, HPMC and chitosan; (B) dilution of the two polymers in distilled water and acidic water (1%) for HPMC and chitosan, respectively; (C) overnight solution of the two polymers; (D) mix of the two solutions on the Petri dish (2:1 ratio HPMC:chitosan); (E) addition of the enzyme buffer; (F) gentle stirring with spatula to homogenize the liquid; (G) after overnight drying, we peeled off the dried film from the Petri dish; Figure S2: Mechanical characterization of HPMC–CS films: Optical micrographs of the films used for mechanical testing before usage (A), after 5 usage cycles (C), and after 10 usage cycles (E), with testing

area and coordinates shown. Young's modulus maps from areas depicted in optical micrographs for films before usage (B), after 5 usage cycles (D), and after 10 usage cycles (F). Colormap maintained for comparison between samples; Figure S3: Mechanical characterization of enzyme-loaded HPMC–CS films: Optical micrographs of the films used for mechanical testing before usage (A), after 5 usage cycles (C), and after 10 usage cycles (E), with testing area and coordinates shown. Young's modulus maps from areas depicted in optical micrographs for films before usage (B), after 5 usage cycles (D), and after 10 usage cycles (F). Colormap maintained for comparison between samples.

Author Contributions: E.V., methodology, investigation, visualization, data curation, writing—original draft, writing—review and editing; M.T.-M., methodology, investigation, data curation, writing—original draft; H.E.S., methodology, investigation, data curation, writing—original draft; P.G., data curation; F.N., data curation; A.X., conceptualization, writing—review and editing; M.Z., conceptualization, visualization, methodology, data curation, writing—original draft, writing—review and editing. All authors have read and agreed to the published version of the manuscript.

Funding: This work was supported by a statutory subsidy from the Ministry of Higher Education for Wrocław University of Science and Technology. Mechanical characterization was carried out using equipment supported by an UKRI EPSRC New Investigator Award with grant reference EP/T01508X/1.

Institutional Review Board Statement: Not applicable.

Informed Consent Statement: Not applicable.

Data Availability Statement: SAXS data available upon request at Centre de recherche Paul-Pascal, Pessac, France.

Acknowledgments: We acknowledge Ahmed Bentaleb, Univ. Bordeaux, Centre de recherche Paul-Pascal, France, for his contribution on the execution of the SAXS experiments. A.X. thanks the University of Bordeaux, IdEx Visiting Scholars for his stay. E.V. thanks CRPP for the accommodation provided to carry out the SAXS experiments.

Conflicts of Interest: The authors declare no conflict of interest.

References

1. Blattner, C.; Zoumpanioti, M.; Kröner, J.; Schmeer, G.; Xenakis, A.; Kunz, W. Biocatalysis using lipase encapsulated in microemulsion-based organogels in supercritical carbon dioxide. *J. Supercrit. Fluids* **2006**, *36*, 182–193. [CrossRef]
2. Badgujar, V.C.; Badgujar, K.C.; Yeole, P.M.; Bhanage, B.M. Immobilization of Rhizomucor miehei lipase on a polymeric film for synthesis of important fatty acid esters: Kinetics and application studies. *Bioprocess Biosyst. Eng.* **2017**, *40*, 1463–1478. [CrossRef] [PubMed]
3. dos Santos Carvalho, J.D.; Rabelo, R.S.; Hubinger, M.D. Thermo-rheological properties of chitosan hydrogels with hydroxypropyl methylcellulose and methylcellulose. *Int. J. Biol. Macromol.* **2022**, *209*, 367–375. [CrossRef] [PubMed]
4. Bilal, M.; Iqbal, H.M.N.; Hu, H.; Wang, W.; Zhang, X. Enhanced bio-catalytic performance and dye degradation potential of chitosan-encapsulated horseradish peroxidase in a packed bed reactor system. *Sci. Total Environ.* **2017**, *575*, 1352–1360. [CrossRef]
5. Zoumpanioti, M.; Parmaklis, P.; de María, P.D.; Stamatis, H.; Sinisterra, J.V.; Xenakis, A. Esterification reactions catalyzed by lipases immobilized in organogels: Effect of temperature and substrate diffusion. *Biotechnol. Lett.* **2008**, *30*, 1627–1631. [CrossRef]
6. Liu, D.M.; Chen, J.; Shi, Y.P. Advances on methods and easy separated support materials for enzymes immobilization. *TrAC Trends Anal. Chem.* **2018**, *102*, 332–342. [CrossRef]
7. Malcata, F.X.; Hill, C.G.; Amundson, C.H. Use of a lipase immobilized in a membrane reactor to hydrolyze the glycerides of butteroil. *Biotechnol. Bioeng.* **1991**, *38*, 853–868. [CrossRef]
8. Junior, J.C.Q.; Ferrarezi, A.L.; Borges, J.P.; Brito, R.R.; Gomes, E.; da Silva, R.; Guisán, J.M.; Boscolo, M. Hydrophobic adsorption in ionic medium improves the catalytic properties of lipases applied in the triacylglycerol hydrolysis by synergism. *Bioprocess Biosyst. Eng.* **2016**, *39*, 1933–1943. [CrossRef] [PubMed]
9. Stamatis, H.; Xenakis, A.; Kolisis, F.N. Bioorganic reactions in microemulsions: The case of lipases. *Biotechnol. Adv.* **1999**, *17*, 293–318. [CrossRef]
10. Vassiliadi, E.; Mitsou, E.; Avramiotis, S.; Chochos, C.L.; Pirolt, F.; Medebach, M.; Glatter, O.; Xenakis, A.; Zoumpanioti, M. Structural study of (Hydroxypropyl)methyl cellulose microemulsion-based gels used for biocompatible encapsulations. *Nanomaterials* **2020**, *10*, 2204. [CrossRef]
11. Kosaka, P.M.; Kawano, Y.; el Seoud, O.A.; Petri, D.F.S. Catalytic activity of lipase immobilized onto ultrathin films of cellulose esters. *Langmuir* **2007**, *23*, 12167–12173. [CrossRef] [PubMed]
12. Malmiri, H.J.; Jahanian, M.A.G.; Berenjian, A. Potential Applications of Chitosan Nanoparticles as Novel Support in Enzyme Immobilization. *Am. J. Biochem. Biotechnol.* **2012**, *8*, 203–219.

13. Ali, H.U.; Iqbal, D.N.; Iqbal, M.; Ezzine, S.; Arshad, A.; Zeeshan, R.; Chaudhry, A.A.; Alshawwa, S.Z.; Nazir, A.; Khan, A.F. HPMC crosslinked chitosan/hydroxyapatite scaffolds containing Lemongrass oil for potential bone tissue engineering applications. *Arab. J. Chem.* **2022**, *15*, 103850. [CrossRef]
14. Shen, X.; Shamshina, J.L.; Berton, P.; Gurau, G.; Rogers, R.D. Hydrogels based on cellulose and chitin: Fabrication, properties, and applications. *Green Chem.* **2016**, *18*, 53–75. [CrossRef]
15. Misenan, M.S.M.; Isa, M.I.N.; Khiar, A.S.A. Electrical and structural studies of polymer electrolyte based on chitosan/methyl cellulose blend doped with BMIMTFSI. *Mater. Res. Express* **2018**, *5*, 055304. [CrossRef]
16. Jiang, S.; Zhang, M.; Jiang, S.; Tuo, Y.; Qian, F.; Mu, G. Transglutaminase and hydroxypropyl methyl cellulose enhance mechanical properties of whey protein concentrate film. *Int. J. Food Sci. Technol.* **2022**, *57*, 5472–5478. [CrossRef]
17. Pinotti, A.; García, M.A.; Martino, M.N.; Zaritzky, N.E. Study on microstructure and physical properties of composite films based on chitosan and methylcellulose. *Food Hydrocoll.* **2007**, *21*, 66–72. [CrossRef]
18. Zhao, D.; Zhu, Y.; Cheng, W.; Chen, W.; Wu, Y.; Yu, H. Cellulose-Based Flexible Functional Materials for Emerging Intelligent Electronics. *Adv. Mater.* **2021**, *33*, 2000619. [CrossRef]
19. Gökmen, F.Ö.; Bayramgil, N.P. Preparation and Characterization of Bio-Nanocomposite Films of Some Cellulose Derivatives. *SSRN* **2022**, *25*, 4151872.
20. Wang, Y.; Wang, J.; Sun, Q.; Xu, X.; Li, M.; Xie, F. Hydroxypropyl methylcellulose hydrocolloid systems: Effect of hydroxypropy group content on the phase structure, rheological properties and film characteristics. *Food Chem.* **2022**, *379*, 132075. [CrossRef]
21. Vassiliadi, E.; Aridas, A.; Schmitt, V.; Xenakis, A.; Zoumpanioti, M. (Hydroxypropyl)methyl cellulose-chitosan film as a matrix for lipase immobilization: Operational and morphological study. *Mol. Catal.* **2022**, *522*, 112252. [CrossRef]
22. Barros, S.C.; da Silva, A.A.; Costa, D.B.; Costa, C.M.; Lanceros-Méndez, S.; Maciavello, M.N.T.; Ribelles, J.L.G.; Sentanin, F.; Pawlicka, A.; Silva, M.M. Thermal–mechanical behaviour of chitosan–cellulose derivative thermoreversible hydrogel films. *Cellulose* **2015**, *22*, 1911–1929. [CrossRef]
23. Song, J.; Feng, H.; Wu, M.; Chen, L.; Xia, W.; Zhang, W. Development of a bioactive chitosan HPMC-based membrane with tea polyphenols encapsulated in β-cyclodextrin as an effective enhancement. *Mater. Today Commun.* **2021**, *27*, 102324. [CrossRef]
24. Ding, C.; Zhang, M.; Li, G. Preparation and characterization of collagen/hydroxypropyl methylcellulose (HPMC) blend film. *Carbohydr. Polym.* **2015**, *119*, 194–201. [CrossRef]
25. Calvo, N.L.; Svetaz, L.A.; Alvarez, V.A.; Quiroga, A.D.; Lamas, M.C.; Leonardi, D. Chitosan-hydroxypropyl methylcellulose tioconazole films: A promising alternative dosage form for the treatment of vaginal candidiasis. *Int. J. Pharm.* **2019**, *556*, 181–191. [CrossRef] [PubMed]
26. Choi, A.J.; Kim, C.J.; Cho, Y.J.; Hwang, J.K.; Kim, C.T. Characterization of Capsaicin-Loaded Nanoemulsions Stabilized with Alginate and Chitosan by Self-assembly. *Food Bioprocess Technol.* **2011**, *4*, 1119–1126. [CrossRef]
27. Tsirigotis-Maniecka, M.; Szyk-Warszyńska, L.; Michna, A.; Warszyński, P.; Wilk, K.A. Colloidal characteristics and functionality of rationally designed esculin-loaded hydrogel microcapsules. *J. Colloid Interface Sci.* **2018**, *530*, 444–458. [CrossRef] [PubMed]
28. Imran, M.; Klouj, A.; Revol-Junelles, A.M.; Desobry, S. Controlled release of nisin from HPMC, sodium caseinate, poly-lactic acid and chitosan for active packaging applications. *J. Food Eng.* **2014**, *143*, 178–185. [CrossRef]
29. Barros, S.C.; da Silva, A.A.; Costa, D.B.; Cesarino, I.; Costa, C.M.; Lanceros-Méndez, S.; Pawlicka, A.; Silva, M.M. Thermo-sensitive chitosan–cellulose derivative hydrogels: Swelling behaviour and morphologic studies. *Cellulose* **2014**, *21*, 4531–4544. [CrossRef]
30. Larsson, M.; Hjärtstam, J.; Larsson, A. Novel nanostructured microfibrillated cellulose–hydroxypropyl methylcellulose films with large one-dimensional swelling and tunable permeability. *Carbohydr. Polym.* **2012**, *88*, 763–771. [CrossRef]
31. Bigi, F.; Haghighi, H.; Siesler, H.W.; Licciardello, F.; Pulvirenti, A. Characterization of chitosan-hydroxypropyl methylcellulose blend films enriched with nettle or sage leaf extract for active food packaging applications. *Food Hydrocoll.* **2021**, *120*, 106979. [CrossRef]
32. Oyen, M.L.; Cook, R.F. A practical guide for analysis of nanoindentation data. *J. Mech. Behav. Biomed. Mater.* **2009**, *2*, 396–407. [CrossRef] [PubMed]
33. Oliver, W.C.; Pharr, G.M. An improved technique for determining hardness and elastic modulus using load and displacement sensing indentation experiments. *J. Mater. Res.* **1992**, *7*, 1564–1583. [CrossRef]
34. Kontomaris, S.V.; Malamou, A. Hertz model or Oliver & Pharr analysis? Tutorial regarding AFM nanoindentation experiments on biological samples. *Mater. Res. Express* **2020**, *7*, 033001.
35. Pawłowski, Ł.; Bartmański, M.; Strugała, G.; Mielewczyk-Gryń, A.; Jazdzewska, M.; Zieliński, A. Electrophoretic Deposition and Characterization of Chitosan/Eudragit E 100 Coatings on Titanium Substrate. *Coatings* **2020**, *10*, 607. [CrossRef]